IC/82/237

INTERNATIONAL CENTRE FOR THEORETICAL PHYSICS

REPORT ON NON-CONVENTIONAL ENERGY ACTIVITIES

No.1

INTERNATIONAL ATOMIC ENERGY AGENCY

UNITED NATIONS EDUCATIONAL, SCIENTIFIC AND CULTURAL ORGANIZATION

1982 MIRAMARE-TRIESTE

International Atomic Energy Agency
and
United Nations Educational Scientific and Cultural Organization

INTERNATIONAL CENTRE FOR THEORETICAL PHYSICS

REPORT ON NON-CONVENTIONAL ENERGY ACTIVITIES

No.1

A collection of contributed papers to the
Second International Symposium
on
Non-Conventional Energy
(14 July - 6 August 1981)

MIRAMARE - TRIESTE
December 1982

EDITORIAL NOTE

The editorial board will publish articles and contributions which show originality and scientific achievements whether local or international. The bulletin will appear, hopefully, twice a year and publish articles about alternative energy and allied subjects. Each article is to be properly referred and edited prior to publication. The I.C.T.P. is the home of this bulletin and Professor Furlan, I.C.T.P., Professor Mancini, University of Catania, Professor Ali Sayigh, Kuwait Institute for Scientific Research and Professor B.O. Seraphin, University of Arizona, are the founding editors.

The editors encourage and urge all scientists and engineers from developing countries, who participate in the ICTP activities, to submit their contributions.

PREFACE

With this bi-annual Bulletin the International Centre for Theoretical Physics introduces a series of publications intended to communicate solar research and development in Third World countries. The papers will be based on reports presented at the International Symposia and Workshops on Non-Conventional Energy Sources sponsored each summer by the Centre.

Alternately held in Trieste and in a country other than Italy, the annual meeting unites for three/four weeks researchers from industrial countries with their colleagues in the Third World.

Until now there has been no regular attempt to publish the reports presented at the Workshops. In an endeavour to fulfill an existing need, this series of Bulletins intends to give the contributions submitted by participants from developing countries the visibility they deserve.

Energy conversion from non-conventional sources is frequently of greater importance to developing than to industrial countries. Many of their principal needs - residential uses, irrigation, desalination, agricultural applications, to name just a few - can easily be matched to the decentralized, low temperature character of these sources. It will be among developing societies that the corresponding technologies will first find their testing ground and eventually prove their economic feasibility.

Frame, scope and orientation of the reports are original and specific with respect to needs and resources of their home countries. A highly visible communication may influence efforts on a global scale, since the work was performed under boundary conditions much better matched to the aim of the technology than research in an industrial setting.

The Bulletin has been initiated by a consensus of Third World scientists during the 1981 meeting. It is hoped that their community will give substance and viability to their initiative. Given their lively and competent support, the series of Bulletins could then develop into a means of scientific communications as widely distributed as the principal scientific journals but bearing its own distinctive character.

The Editorial Board

LIST OF CONTENTS

Solar Materials Research in the Third World

Marvin Cohen*

International Centre for Theoretical Physics
Trieste, Italy

This Bulletin is the first in a regular series published for the purpose of reporting solar research and development in Third World countries. The author of this lead-off article has worked in energy always in the economically-comfortable setting of industrialized countries. However, during the last ten years he has had ample opportunity, on lecture tours and in collaboration with developing countries, under the sponsorship of the International Centre for Theoretical Physics, Trieste, to compare the frame of his own work with the needs and conditions of the host countries. In this introduction, some general thoughts will be sketched that have resulted from this frequent comparison of aims and scope, problems and promises, directions and conditions, here and there.

Optical solid-state physicist turned solar materials researcher, the author is most familiar with the materials science aspects of solar technology, and will consequently touch briefly on two aspects. We shall first ask: Why materials research in a field that so long has been dominated by the engineer? We shall secondly address the role that materials science can and should play in the solar efforts of developing countries.

A. Materials Research in Solar Technology

a. The principle issues in the utilization of solar energy are neither scientific proofs nor feasibility demonstrations on the engineering level. Solar energy has heated and cooled residential space, boiled water for comfort and desalination, irrigated land and dried crops, fuelled thermal processes in industry, and, to a limited extent generated electricity.

---

* On sabbatical leave from the Optical Sciences Center, University of Arizona, Tucson, Arizona 85721, U.S.A. during the academic year 1982/83.

As a consequence, public expectations have been high for the successful development and early commercialization of solar energy conversion. Technological feasibility taken for granted, the remaining economic difficulties are supposed to be reduced by developments on the engineering level, and, in particular, by sufficiently large mass production. Consequently, insufficient attention is paid to the necessary effort and investment in basic and applied research.

The gap between public expectation and technological reality has been of particular consequence for the potential role of materials science in the development of solar energy. An effort to improve the performance of existing devices, and to lower their cost, encounters problems that involve materials and manufacturing processes. In its search for better solutions, solar energy technology must engage the various aspects of materials science more effectively. This may involve parts of the field which are at present outside the mainstream of solar research, and do not use recognized solutions or approaches.

The direction of research will continue to be dictated by economic considerations, even though the basic question of the feasibility of solar energy conversion has been resolved. Most problems have more than one technologically-satisfactory solution. A large number of them however, were developed in the financially liberal context of the space programmes, and are highly unsatisfactory once economic considerations are important.

Existing technologies must be re-opened at a level where they touch on fundamental research. Economic gains derived from large-scale production are limited, and efforts must not be restricted simply to produce more cheaply what is already available.

b. The remaining problems can be classified into the categories of acceptable performance, adequate service life, and its cost low enough to enable widespread use.

Acceptable performance is the criterion most easily established. It is often tied to the demand for a threshold performance that must be met, or the overall systems costs rise beyond economic feasibility. To give an example, for large-scale terrestial conversion, a solar cell with a 5% conversion efficiency could not be profitably installed, supported, interconnected and serviced, even if it would be given away for free.

The demand for sufficient service life results from the fact that

solar systems, although they require no fuel, are characterized by high initial costs. Life times in the order of decades are required to amortize this high initial cost. Of importance are durability in the face of adverse environmental conditions and cyclic thermal load.

Last but not least, cost reduction is an essential element in the materials research programme. Of major concern are materials cost and availability, the development and demonstration of mass production processes that are inexpensive and of low energy consumption.

c. To meet the requirements for performance, life and cost, materials science engages different disciplines. The selection of candidate materials for a given function requires the knowledge of the basic mechanisms that solid-state physics provides. To improve and tailor performance and durability according to demands, questions of composition and microstructure must be answered. The supporting disciplines of metallurgy, ceramics, polymers, surface science and chemical engineering will come into play.

d. Decades of effort on the engineering level have developed solar technology to the point where most applications are now clearly materials-limited. Fortunately, the science of materials has made large strides in the past two decades. Modern semiconductor electronics with an abundance of novel effects in man-made materials, thin-film technology expanding the range of properties of materials by systematic variations of their composition and microstructure, the availability of novel materials in alloys and multi-phase systems - these are accomplishments of very recent origin. They are not available in the previous phases of solar popularity such as the early nineteen fifties. Success or failure of the present, more urgent effort to push solar technology through to economic feasibility will largely depend on the willingness of the materials researcher to utilize the advances that his speciality has made during the recent past.

B. Solar Materials Research in Developing Countries

a. On the professional level, the emphasis attached to materials research in the first chapter applies to developing and industrialized countries alike. In justifying this emphasis, however, one may encounter the often-asked questions: Should developing countries with

limited resources, personally as well as materially, engage in research at all. Aren't their basic needs such that research offers little to fill them? Shouldn't they rather satisfy their technological demands in the big "Supermarket of Technology" which is continuously being stocked by work in the industrialized countries?

The pros and cons of this question have been widely discussed. Nobel Laureate Professor Abdus Salam, Director of the International Centre for Theoretical Physics, firmly rejects this solution. As its main mission, the Centre, founded nearly twenty years ago, exposes every year hundreds of young scientists from developing countries to current research. If the "Supermarket of Technology" approach works at all Salam states, it will do so only if the customers can discriminate. He argues that the discriminating attitude and talent that can properly select according to individual needs comes most easily through frequent and intimate contacts on the research level.

b. Still proceeding in the same general vein it is this author's long-standing experience that research is most effectively-communicated among the members of the "Club" that consists of the active contributors to a given field. The members that add to the state-of-the-art, even on a small scale and in a fringe area, will benefit tremendously from being in touch through reports on their own work. The inactive spectator will find himself cut off from timely communication of research that may lead to technology of significant use to his country. It follows that even the country with severely-limited resources should devote a small portion of them to the support of research, although its immediate use is not always evident.

c. In materials research, the need for active familiarity goes beyond the capability to properly discriminate what is offered by others. Once materials research approaches the industrial pilot-plant stage, the transfer of results requires "in-house research capability" at the receiving end. The difficulties of transferring under license, say, the processes of integrated-circuit technology, are notorious. Most other developments resulting from materials research share the difficulty of teaching technology "by the cook book". It takes the insight of the active researcher to effectively handle such a transfer in his field. The savings in time and cost are often many times the expenditures devoted previously to related research.

d. Although complex and not easily transferred to the outside, materials research does not require expensive equipment on the scale of nuclear physics. Some contribution can always be made to most

aspects of solar materials research with an initial layout of in between 10^4 and 10^5 US-$, most of it invested into small pieces of general use. There is no threshold investment into one big machine, unless one wants to go into sophisticated materials characterization.

e. The promise of solar materials research for the developing country rests with the novelty of the work. Not counting valuable but rare exceptions, systematic materials studies addressed to the needs of solar technology originated during the last decade. Progress is rapid, but not covering every aspect. The imaginative and well-informed researcher in a developing country will find numerous opportunities to make original and significant contributions. Even in areas already well worked over, he can apply a new direction that follows from the needs and conditions of his society. He will often be able to develop a simpler approach, avoiding the complexity of design and processing that his colleagues in an industrialized country can afford. Local conditions will often open new approaches. A series of papers from a group in Indonesia recently published in Solar Energy Materials, makes the point: They reported a process for the production of silane gas from by-products of rice processing, going all the way to the fabrication of solar-grade silicon. There was little precedent or competition from other than rice-producing countries, and the value of the work for their region was evident.

The series of Bulletins, composed of articles from developing countries, will give this type of valuable contributions the visibility they deserve. Their communication to, and their acceptance by, the scientific community will further encourage prospective authors. Some of them may feel that their capacity to contribute is limited, and that most scientific journals shield off access by excessive demands. This Bulletin will help as a vehicle of communication for work acceptable not only for its quality, but mainly for its significance to the further development of research in the Third World countries.

THE ESTIMATION OF DIFFUSE RADIATION IN YUGOSLAVIA

P. Kulisic
Faculty of Electrical Engineering
Zagreb
Yugoslavia

ABSTRACT:

There are various methods for estimating the diffuse from total radiation but it seems that no single form of equation is applicable to all atmospheric environments and their applicability should be tested for a particular region. In this paper Liu-Jordan and Page correlations between monthly average daily diffuse and global irradiation were discussed and their applicability for diffuse radiation estimation in Yugoslavia was investigated. It was shown that they should be modified in order to fit measured data. Regional correlations based on long term measured data for three Yugoslav sites were developed and specific correlations valid for this climatic region was recommended.

INTRODUCTION

Calculations of annual performance for solar energy systems require monthly average of global irradiation on a tilted collector surface. The only measurements for which long term records are available for quite a number of stations are measurements of global insolation on a horizontal surface. In order to calculate irradiation on inclined (collector) surface besides the global irradiation, one needs to know the diffuse irradiation on horizontal surface too. However, the diffuse radiation is measured at only a few stations which has led to the development of various methods for estimating the diffuse from global radiation.

Liu and Jordan[2] and Page [3] have found that the percentage of diffuse radiation in horizontally collected monthly average daily global irradiation on a horizontal surface is a function of clearness index. (Clearness index is the ratio of the measured monthly average global to the monthly average daily extraterrestrial irradiation on a horizontal surface). Page's correlation is expressed in a simple linear form while Liu-Jordan one is somewhat more complicated third order parabolic function. These empirical correlations are based on measured data from various U.S. stations and it was hoped that they are valid in wide variety of climatic regions. However, the question has been raised lately about general validity of these correlations. Several investigators[4,6,7,8] have shown that no single form of the equation is applicable to all climatic regions and that these correlations should be tested in a wide

variety of atmospheric environments in order to find the best one or in order to determine the specific regional correlation applicable in a particular region.

The purpose of this work was to extend the study of this method to the Yugoslav region, to examine how Liu-Jordan's and Page's correlations fit the experimental data from the Yugoslav stations and to find specific regional correlation for Yugoslavia.

RESULTS AND DISCUSSIONS

A simple method for estimating the average daily radiation on tilted collector surface facing towards the south has been developed by Liu and Jordan[1,5]. Monthly average global daily irradiation H can be expressed:

$$(1) \qquad \bar{H} = \bar{R}\,\bar{H} = \left(1 - \frac{\bar{H}_d}{\bar{H}}\right)\bar{R}_b + \left(\frac{1+\cos\beta}{2}\right)\frac{\bar{H}_d}{\bar{H}} + \bar{H}\rho\left(\frac{1-\cos\beta}{2}\right)$$

where $\bar{H}_d$ is the monthly average daily diffuse irradiation, $\bar{R}_b$ is the ratio of the average beam radiation on the tilted surface to that on a horizontal surface for each month, β is the tilt of the surface from horizontal and ρ is ground albedo. An expression for calculation of the direct beam factor $\bar{R}_b$ can be found in the literature[5].

In order to evaluate irradiation on a tilted surface one should know monthly average daily global irradiation $\bar{H}$ and diffuse irradiation $\bar{H}_d$. If data for diffuse radiation are not known they can be evaluated from the global irradiation by using empirical correlations such as the ones developed by Liu-Jordan[2] and Page[3].

Liu and Jordan developed empirical correlation between the diffuse ratio $\bar{H}_d/\bar{H}$ and the clearness indes $\bar{K}_T = \bar{H}/\bar{H}_o$. Klein[5] developed the following mathematical expression for that correlation:

$$(2) \qquad \bar{H}_d/\bar{H} = 1.39 - 4.027\,\bar{K}_T + 5.531\,\bar{K}_T^{\,2} - 3.108\,\bar{K}_T^{\,3}.$$

Page[3] developed correlation between monthly average global irradiation and its diffused component in the linear form:

$$(3) \qquad \frac{\bar{H}_d}{\bar{H}} = 1.00 - 1.096\,\bar{K}_T$$

Global solar radiation is measured on 18 meteorological stations in Yugoslavia and for another 100 locations it could be calculated from the data of sunshine recorders. However, long term diffuse radiation data are available only at three stations (Bar, Beograd and Zagreb). Trying to estimate diffuse irradiation at other locations, for which there is no measured data, we tried to use Liu-Jordan correlation[2] but noticed that the values for diffuse irradiations obtained by equation (2) are too low, so we decided to investigate its applicability for this climatic region.

If the diffuse ratio $\bar{H}_d/\bar{H}$ for the Yugoslav sites[9,10,11] is compared with that for the U.S. sites at the same latitude (Fig. 1), one can notice that in Yugoslav climate region the percentage of diffuse radiation is higher: it is about 30-60%, while in the region for which the Liu-Jordan formula was developed, it is about 20-40%.

The fraction of diffuse radiation $\bar{H}_d/\bar{H}$ as a function of the clearness index $\bar{K}_T$ is plotted on Fig. 2, for three Yugoslav sites and then compared to the Liu-Jordan and Page correlation. It can be noticed that Liu-Jordan correlation does not correspond closely with the measured data and that it cannot be used for diffuse data calculation in this region while Page correlation would give better results. However, both correlations should be modified in order to fit the measured data.

Least-square technique was used to fit the experimental data and the following fits were obtained:

$$(2a) \qquad \frac{\bar{H}_d}{\bar{H}} = 1.60 - 4.17\,\bar{K}_T + 5.29\,\bar{K}_T^{\,2} - 2.86\,K_T^{\,3}$$

and

$$(3a) \qquad \frac{\bar{H}_d}{H} = 1.05 - 1.125\,\bar{K}_T$$

Solar water heating simulation study using developed correlation (2a) was carried out for Zagreb and it gave results closest to those obtained by using measured horizontal diffused data. Modified Page correlation (3a) comes next in accuracy, then follows equation (3) while original Liu-Jordan correlation (2) gives the highest fraction and is not suitable for this region.

This study showed that for the three stations examined, equation (3a) gives the best results and it is recommended to use it in order to estimate diffused radiation in Yugoslavia.

CONCLUSION:

Because the percentage of diffused radiation in global in the region where Yugoslavia is situated is somewhat higher than in the part of the world for which empirical correlations for diffused radiation were developed, Liu-Jordan and similar correlations cannot be used without modification. The regional correlation evaluated in this work can be used to calculate diffused irradiation for each place in Yugoslavia where global irradiation is known and therefore it could be useful in design procedure for solar energy systems. The developed correlations could also be useful in solar radiation investigation in other countries in this geographical region.

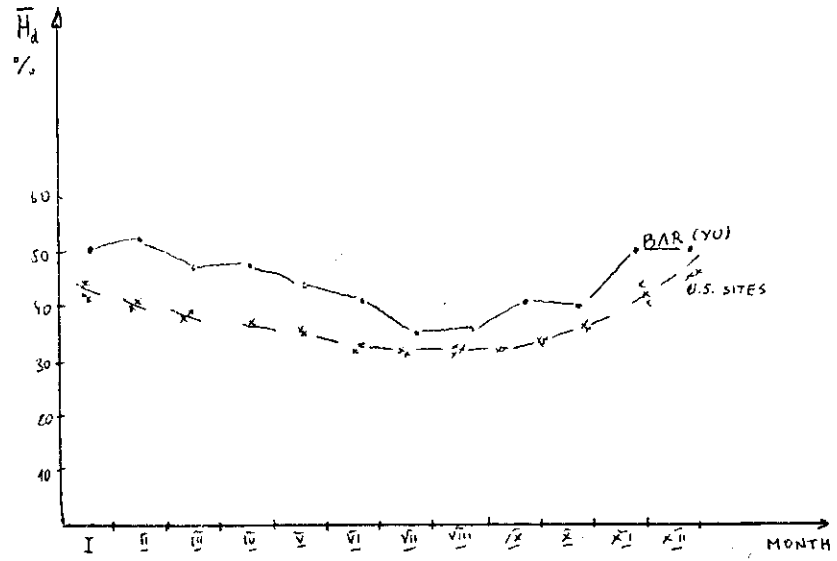

Fig. 1.

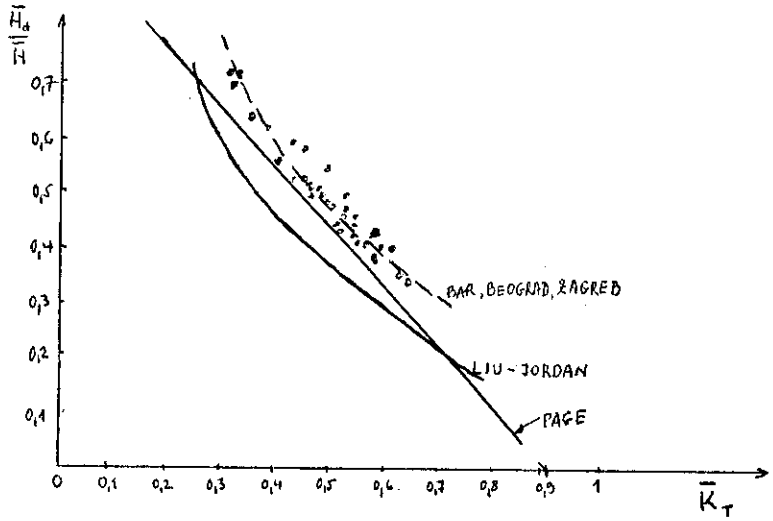

Fig. 2.

REFERENCES:

1. B.Y.H. Liu and R.C. Jordan, "Daily Insolation on Surface Tilted towards the Equator", trans. ASHRAE, pp. 526-541, (1962).

2. B.H.Y. Liu and R.C. Jordan, "The Interrelationship and Characteristic Distribution of Direct, Diffuse and Total Solar Radiation", Solar Energy 4 (1960) no. 3, p.1-19.

3. J.K. Page, "The Estimation of Monthly Mean Values of Daily Total Short-Wave Radiation on Vertical and Inclined Surface from Sunshine Records for Latitude 40°N - 40°S", Proc. UN Conf. on New Sources of Energy, Paper no. 35/5/98 (1961).

4. S.E. Tuller, "The Relationship between Diffuse, Total and Extra-terrestrial Solar Radiation", Solar Energy 18 (1976) 259-263.

5. S.A. Klein, "Calculation of Monthly Average Insolation on Tilted Surface", Solar Energy 19 (1977) 325-329.

6. M. Igbal, "A Study of Canadian Diffuse and Total Solar Radiation", Solar Energy 22 (1979) 81-90.

7. M. Collares-Pereira and A. Rabl, "The Average Distribution of Solar Radiation - Correlation between Diffuse and Hemispherical and between Daily and Hourly Insolation Values", Solar Energy 22 (1979) 81-86.

8. F. Newwirth, "The Estimation of Global and Sky Radiation in Austria" Solar Energy 24 (1980) 421-426.

9. F. Gamser, Rospodela komponenata Suncevog zracenja u Jugoslaviji, Savetovanje, "Sunceva Energija u Jugoslaviji", Beograd, 1977.

10. V. Gburcik; Z. Krajinovic, Dnevne i godisnje varijacije globalnog Suncevog zracenja, Solar '80, Beograd, 1980.

11. A. Bratanic, Private Communication.

AN ANALYSIS OF SOLAR RADIATION EXPERIENCED IN ZONGULDAK

Prof. Suavi Eyice
Yildiz University, Mechanical Engineering Faculty
Istanbul, Turkey

Dr. Hasan Kulunk
Yildiz University, Kocaeli Engineering Faculty
Izmit, Turkey

ABSTRACT:

The precise evaluation of the daily duration of sunshine supported with the daily insolation for a certain location is accepted as a threshold for further development in solar energy applications. These may include, solar: heating, cooling, agricultural irrigation, distillation and generation of electricity via thermal conversions, photovoltaics and ponds.

From this point of view, the measurements on the daily duration of sunshine and insolation have been carried out for the City of Zonguldak with latitude of $41^{o}27'N$. The main reason in the selection of Zonguldak for this study was just due to the fact that the Academy which we belong to was situated in this City. However, the method and the techniques which are employed here can be applied adequately to any other location provided that its latitude, duration of sunshine and insolation datum are known.

In the present work, Campbell-Stokes type of recorder is used in the measurement of the yearly distribution of the daily duration of sunshine and bimetallic actinograph of Fuess Berlin Steglitz type in the daily radiation.

The datum obtained for the daily duration of sunshine and insolation are compared with the predictions of the following equations:

$$w_s = (2/15) \arccos(-\tan\phi.\tan\delta) \quad \ldots.(1)$$

$$Q_{TT} = Q_o((2w_1/15).\sin\phi.\sin\delta + (24/\pi).\cos\phi.\cos\delta.\sin w_1) \quad ....(2)$$

and the declination angle is calculated from the relation given below:

$$\delta = 23{,}45 \{\sin (360(284+n)/365) \} \quad ....(3)$$

Results are offered on Fig. 1 and Fig. 2. Fig. 1 reveals that of the comparison between the theoretical and experimental values of the daily duration of sunshine and Fig.2 that of the daily insolation.

Both figures predict similar behaviour for the yearly distribution considered. The gap between the theoretical and experimental curves can be attributed to the effects of the climatic conditions. The ratio of the average daily duration of sunshine and the ratio of the average daily insolation for Zonguldak, in 1978, are found to be 46 and 36 per cent respectively. Hence it is concluded that the solar energy experienced at Zonguldak was below the average. Since Turkey is situated between the latitudes of 36-42°N, this implies that these two ratios represent the lower limits for Turkey, because the intensity of solar radiation is expected to increase by a factor of nearly 1.5 in the south as compared with the north.

It is concluded that both instruments which are employed here in Turkey, like in many other countries, possess a few drawbacks (i.e. humidity and temperature dependency, etc.) which severely affect the reliability and the sensitivity of these devices.

On the other hand, various versions of the insolation maps of Turkey which are published in the literature (two of these maps are presented on Fig.3 and Fig.4) are presumably partly originated from the use of these old fashioned and insensitive instruments. The replacement of these instruments by contemporary counterparts is urgently required. In order to succeed in the prospective solar energy projects, some more study combined with reliable insolation datum covering the whole country is needed. This has not been managed yet.

NOMENCLATURE:

w_s	:	daily duration of sunshine (hour).
w_1	:	daily duration of sunshine (°).
ϕ	:	latitude angle (°).
δ	:	declination angle (°).
n	:	day of the year (n = 1 implies January 1).
Q_o	:	solar constant (=116,4 cal/cm^2.h).
Q_{TT}	:	daily solar insolation (cal/cm^2.day).

FIGURE LEGENDS:

Figure 1 : Comparison between the theoretical and experimental values of the daily duration of sunshine, Zonguldak 1978 (1).

Figure 2 : Comparison between the theoretical and experimental values of the daily solar insolation, Zonguldak 1978 (1).

Figure 3 : A map of distribution of the duration of sunshine over Turkey (in arbitrary units) (2).

Figure 4 : Annual mean of daily total solar insolation incident on a horizontal surface for various stations in Turkey (langleys/day), (3).

REFERENCES

1. Bilunk, H. The assessment of solar energy and the investigation of a suitable heat transfer material for solar power plants, Ph.D. Thesis, Z.D.M.M.A. 1981.

2. Akyurt, M. Isitek Yayini No. 36, MAG-TBTAK, p.77, Ankara 1978.

3. Ogelman, H. Distribution of total solar radiation in Turkey, Cukurova University, F-1-79.

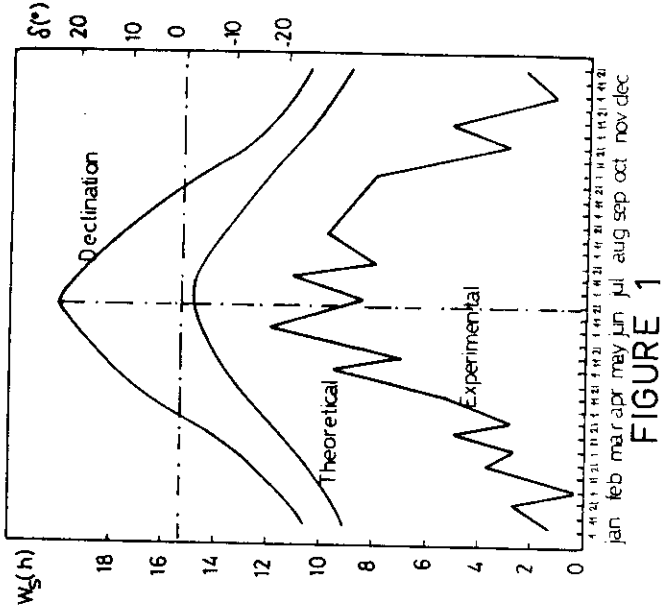

FIGURE 1

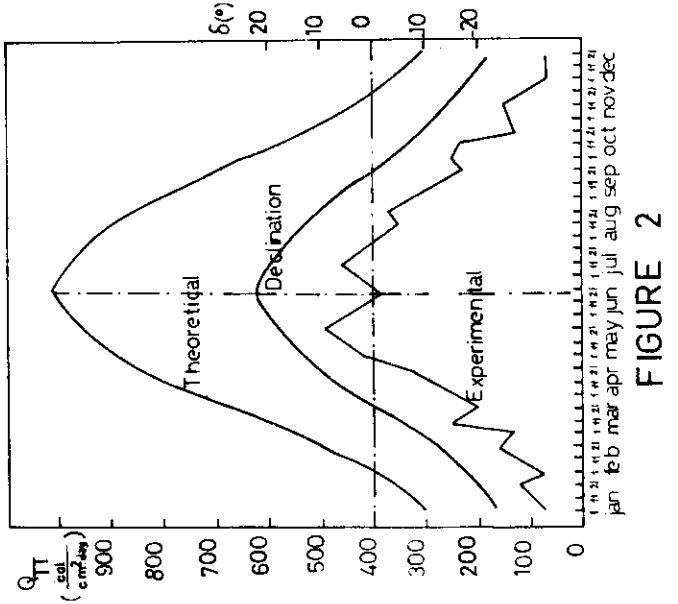

FIGURE 2

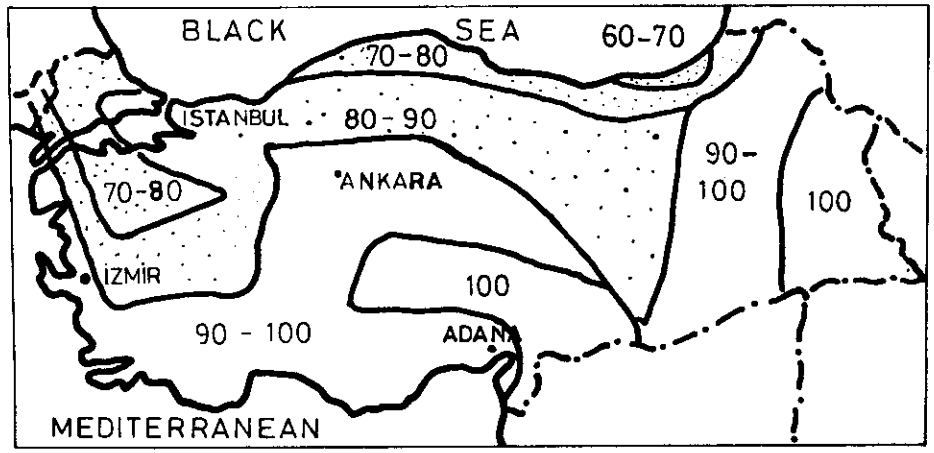

FIGURE 3

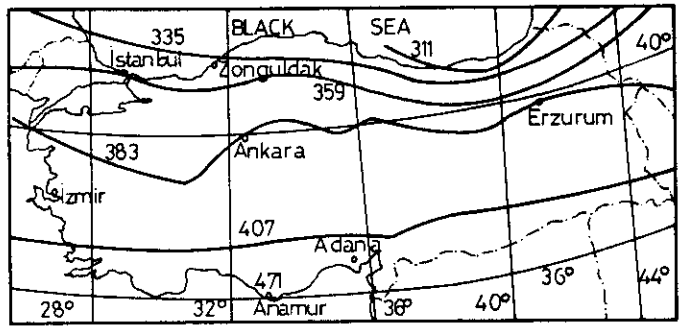

FIGURE 4

A METHOD OF ESTIMATION OF TOTAL SOLAR RADIATION FOR SRI LANKA

T.D.M.A. Samuel and R. Srikanthan
Faculty of Engineering,
University of Peradeniya,
Sri Lanka.

INTRODUCTION:

For the proper planning of the utilisation of Solar Energy in Sri Lanka it is necessary to know the total radiation falling on any part of the country at any time. The Meteorological Department has climatological data on parameters like relative humidity, maximum, minimum temperature, rainfall, sunshine hours, etc. from many of its stations for several years, but only one station in Colombo the capital, has measured values of total radiation. Over the last few years, the Agriculture Department has set up its own meteorological stations which take radiation measurements, but these have been for relatively short periods from few stations. This shortage of data warrants a search for total radiation estimation methods for Sri Lanka.

Many of the available total radiation estimation formulae are examined empirically, and a procedure is suggested for the estimation of total radiation for Sri Lanka. It is found that the formula due to Angstrom (1) subsequently modified by Page (3) is best suited for Sri Lanka with the constants in the formula to be determined by a modification of the method due to Fre're et al (2).

SRI LANKA:

It is an island which lies between $5^{o}55'$ and $9^{o}50'$ North latitude in the Indian Ocean. The longest diameter is from North to South and is about 434km and its area is 65,630km^2. The island consists of a central mass of mountains surrounded by broad coastal plains. In the north, the coastal plain is almost flat; elsewhere its surface is somewhat irregular.

Fig. 1 is a map giving the topography of the country.

Fig. 2 and Fig. 3 give the isotherm for the annual average temperature and the annual maximum temperature respectively. The central hills have the lowest average temperature around $15^{o}C$. The highest average temperatures around $28^{o}C$ occur in the coastal regions.

Fig.4 gives the isohyets of annual average rainfall in mm. The figure shows that the island as a whole has a high rainfall, the highest being concentrated in the south-western lowlands and the edges of the hill country, on each side of which it steadily decreases. The rains are associated with two monsoons, the North-East and the South-West. The island has no well-defined seasons, but the North-East and South-West monsoons which bring the rains interrupt the normal equatorial conditions.

The air is nearly always moist throughout the country because of its size and the surrounding sea. The annual mean relative humidity is 77% with a standard deviation of 2.5. Great accumulation of clouds occur in the middle part of the day, rains during the monsoons are frequent in the late afternoon, and the nights are uncommonly clear.

DATA:

For the purpose of comparing the different solar radiation estimation formulae, we have used data only from the meteorological stations of the Agriculture Department. Satisfactory climatological data including solar radiation measurements are available from only four stations for about four to eight years. Data from only these stations (test stations), Alutharama, Batalagoda, Mahailluppallama and Peradeniya, are used to compare the radiation estimation formulae.

COMPARISON OF THE DIFFERENT SOLAR RADIATION ESTIMATION FORMULAE:

We consider the following formulae:

Formula 1: $H = H_o (a + b\, S/Z)$.

a, b are constants, H_o the average monthly radiation at the top of the atmosphere, Z the length of the day calculated from

$$Z = (2/15) \cos^{-1}(-\tan \phi \tan \delta)$$

where δ is the declination and ϕ the latitude of the place. This formula was first introduced by Angstrom (1) and subsequently modified by Page (3).

Formula 2.1: $H = (A + B \log n)\, S$.

Formula 2.2: $H = (A' + B' \log n)\, Z$.

These were suggested by Sabbagh et al (4). n takes the values 1,2,3,4,5, 6,6,4,3,2,1 for the months January to December, A, B, A', B' are constants.

Swartman & Ogunlade (7) used the formulae:

$H = 490\, D^{0.357}\, R^{-0.262}$,

$H = 460 \exp (0.607\, (D-R))$.

$H = 464 + 265\, D - 248\, R$,

where

$D = S/12$ and H is in cal $cm^{-2}\, d^{-1}$.

These we have written in the general form:

Formula 3.1: $H = a\, D^{a_1}\, R^{a_2}$,

Formula 3.2: $H = b_o \exp (b_1 D + b_2 R)$,

Formula 3.3: $H = c_o + c_1 D + c_2 R)$,

where

a_1, a_2, b_o, b_1, b_2, c_o, c_1, c_2 are constants to be determined.

In these formulae H is in M J $m^{-2}\, d^{-1}$.

The two formulae due to Sabbagh et al (5) are:

$$H = 1.53\, K \exp \left\{ \phi \left(D - \frac{R^{3/2}}{100} - \frac{1}{T_{max}}\right) \right\}$$

$$H = 1.53\, K \exp \left\{ \phi \left(D' - \frac{R^{1/3}}{100} - \frac{1}{T_{max}}\right) \right\},$$

where ϕ is the latitude in radians, K the latitude factor in g cal $cm^{-2}\, d^{-1}$ and $D' = S/Z$. The second formula, with values of K as obtained by Sayigh (6), was used to estimate solar radiation for the four test stations. The estimations were considerably higher than those recorded in these stations. Therefore the following general forms of the second formula are considered:

Formula 4.1: $H = CK \left\{ \exp \phi \left(D' - \left(\frac{R}{100}\right)^{1/3} - \frac{T_{av}}{T_{max}}\right) \right\}$.

Formula 4.2: $H = C_1 K \exp C_2 \phi \left(D' - \left(\frac{R}{100}\right)^{1/3} - \frac{T_{av}}{T_{max}}\right) \right\}$.

C, C_1, C_2 are constants.

The constants in all the formulae 1, 2.1, 2.2, 3.1, 3.2, 3.3, are determined using the Least-Squares Approximation method with monthly mean values of the solar radiation and the other climatological data from the four test stations. The error ε given by

$$\varepsilon = \left(\frac{H_E - H_R}{H_R}\right) \times 100,$$

where H_E and H_R are respectively the estimated and recorded values of the monthly mean solar radiation, are computed for all the formulae as applied to each test station for all the twelve months. Table 1 gives the range of the errors. It is seen that with the same values of a, b for all the months, Formula 1 estimates solar radiation satisfactorily. Table 2 give the a and b values for the test stations. Thus it appears to be possible to include the influence of the maximum temperature and relative humidity in the solar radiation estimation into the constants of the Angstrom-Page formula. This conforms with the observations we

have made of the relative humidity and maximum temperature of the country. These remain almost constant in all parts of the island throughout the year.

THE ANGSTROM - PAGE FORMULA:

If this formula is to be used to estimate the solar radiation in all parts of the country, the constants a, b should be known for all stations having monthly mean sunshine hour records but having no radiation measurements. As we have noted earlier, the Meteorological Department has long periods of sunshine records from different parts of the island. Therefore to determine a and b we follow a method due to Fre're et al (2). They have two curves as shown in Fig. 5 relating a and b to the average annual values of (S/Z), but the four sets of values of (a,b) computed for the four test stations do not fall on Fre're's curves. Moreover, (a+b) for Fre're's curves are higher than the average values obtained for (a+b) from the test stations. Since $(a+b) = t^m$ where t is the transmission coefficient and m the air mass, it is reasonable to expect a small value for (a+b) because of the high relative humidity and heavy cloud cover. Therefore, we modify Fre're's curves in such a way that the four sets of values of a & b fall on the modified curves and also (a+b) = 0.60, the value obtained from the test stations. With these modified curves, a, b is determined for all the stations having sunshine hour records. When this is known, solar radiation can be estimated and with these estimates the annual and the monthly isoradiation maps can be drawn.

DISCUSSION AND CONCLUSIONS:

The annual isoradiation map in Fig. 6 shows the existence of three distinct regions:

(i) a low radiation region around Nuwara Eliya ($6^{o}58'N$ & $80^{o}46'E$).
(ii) another low radiation region around Matale ($7^{o}27'N$ & $80^{o}39'E$).
(iii) the other regions of the country other than (i) and (ii) having a fairly constant radiation of 15 to 17 MJ m^{-2} d^{-1}.

The maps corresponding to each of the other months can be considered as a variation of the annual isoradiation map, for the equatorial condition expected in the island is interrupted by the two monsoons, and the variations in the monthly isoradiation maps are as a result of the rains associated with the monsoons. For instance, as shown in Figs. 7 and 8 giving the monthly mean daily radiation for the months of May and November, there is a tendency to produce high radiation regions. In May, the rains are associated with the South-West monsoon, and in November they are associated with North-East monsoon. These are the months with the heaviest rainfall. This observation confirms a relation one can expect between the intensity of radiation and the monsoon rains.

We conclude, therefore, that the following is a reasonable procedure to estimate total radiation for Sri Lanka with the present available data:

(i) modify Fre're curves using the values of a and b from the four test stations and the fact that a + b = 0.60. It is not possible to compare these a and b values with those obtained in neighbouring countries because of the peculiar climatic conditions over Sri Lanka.
(ii) compute annual average (S/Z) for each station having monthly mean sunshine hour data.
(iii) using the annual average (S/Z) determine a and b for each station from the modified Fre're curves.
(iv) use these values of a and b to estimate monthly mean and annual daily total radiation from Angstrom - Page formula.

REFERENCES:

1. Angstrom, A. Solar and Terrestrial Radiation. Q.J.R. Meteorological Society 50, 121-126 (1924).

2. Fre're, M, Rijks, J.Q. and Rea, J. Estudio Agroclimatologico de la Zone Ondina, Informe Tecnico, FAO/UNESCO/OMM, Rome (1975).

3. Page, J.K. The estimation of mean values of daily total shortwave radiation on vertical and inclined surfaces from sunshine records for latitudes 40°N - 40°S. Proc. of U.N. Conference on New Sources of Energy, Rome 1961 Conference. Paper No. 35/5/98 (1961).

4. Sabbagh, Sayigh, A.A.M. and El-Salam. "Correlation of Solar Radiation and sunshine duration in Riyadh, Saudi Arabia", Pakistan J. Sci. Ind. Res. 16 (6), (1973).

5. Sabbagh, Sayigh, A.A.M. & El-Salam. "Estimation of the total solar radiation from meteorological data". ISES Conference, Los Angeles (1975).

6. Sayigh, A.A.M. "Solar Energy Engineering", 1st Edition, Academic Press, (1977).

7. Swartman, R.K. & Ogunlade, O. "Solar Radiation estimates from common parameters", Solar Energy, 11 (1). (1967).

ACKNOWLEDGEMENT:

The authors wish to thank the Departments of Agriculture and Meteorology for providing us with valuable data and the Computing Centre in the Faculty of Engineering for the computing facilities.

TABLE 1

The range of errors in the estimation using all the formulae

Formula	Alutharama	Batalagoda	Mahailluppallama	Peradeniya
1	(- 7, 8)	(- 7, 11)	(- 6, 7)	(-16, 12)
2.1	(- 7, 15)	(- 6, 23)	(-11, 22)	(-14, 14)
2.2	(-15, 17)	(-14, 18)	(-14, 15)	(-12, 12)
3.1	(- 9, 7)	(-11, 12)	(-10, 11)	(-25, 44)
3.2.	(-10, 8)	(-11, 12)	(-11, 12)	(-25, 44)
3.3	(- 8, 7)	(- 9, 14)	(-10, 11)	(-24, 48)
4.1	(-18, 36)	(-23, 18)	(-29, 22)	(- 8, 93)
4.2	(-20, 43)	(-23, 20)	(-29, 23)	(- 9, 92)

TABLE 2

Computed values of a and b for Angstrom - Page Formula.

Stations	Latitude ° ' N	Period of observation	Number of months of observation	a	b
Alutharama	7 24	1976 - 79	38	0.224	0.350
Batalagoda	7 33	1972 - 79	74	0.339	0.293
Mahailluppallama	8 07	1972 - 77	50	0.247	0.314
Peradeniya	7 16	1972 - 79	74	0.198	0.377

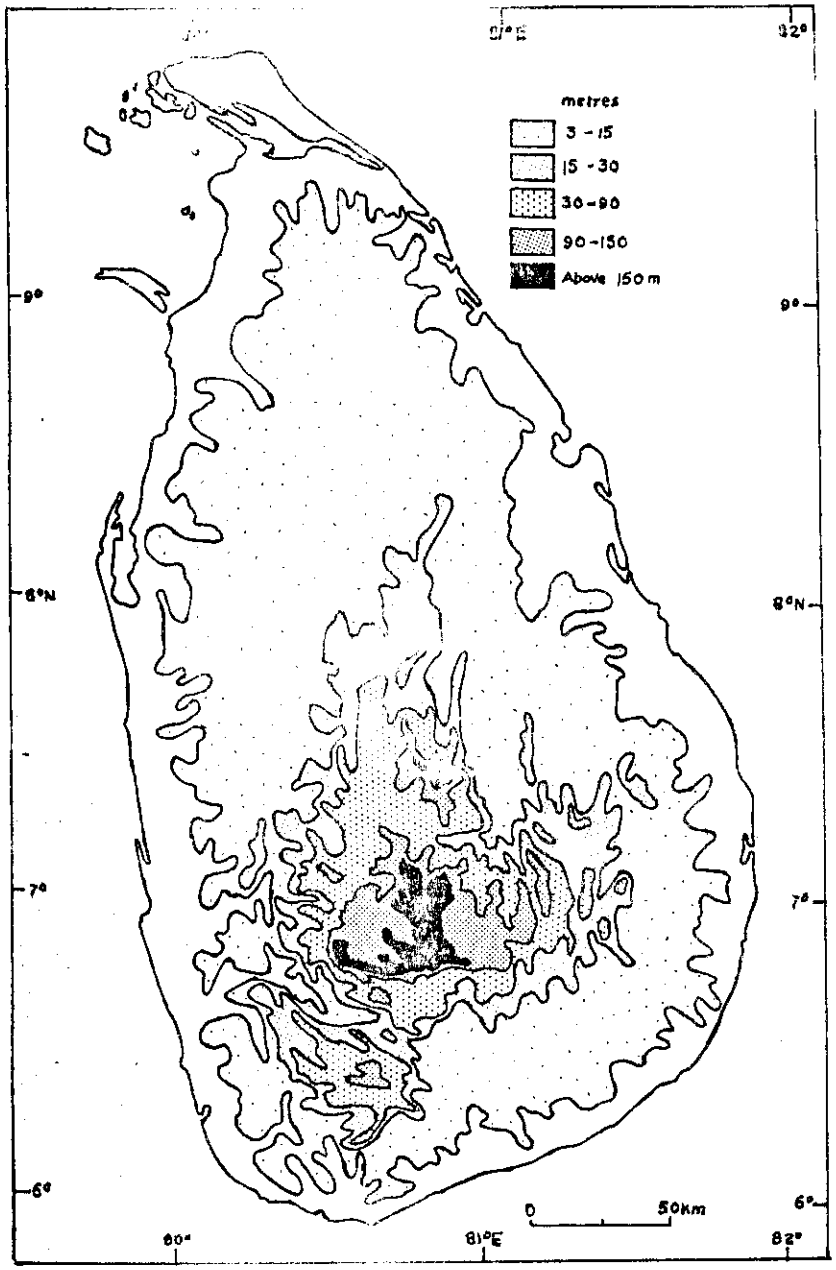
metres
3 - 15
15 - 30
30 - 90
90 - 150
Above 150 m
0
50Km
80°
81°E
82°
9°
8°N
7°
6°

Fig.1

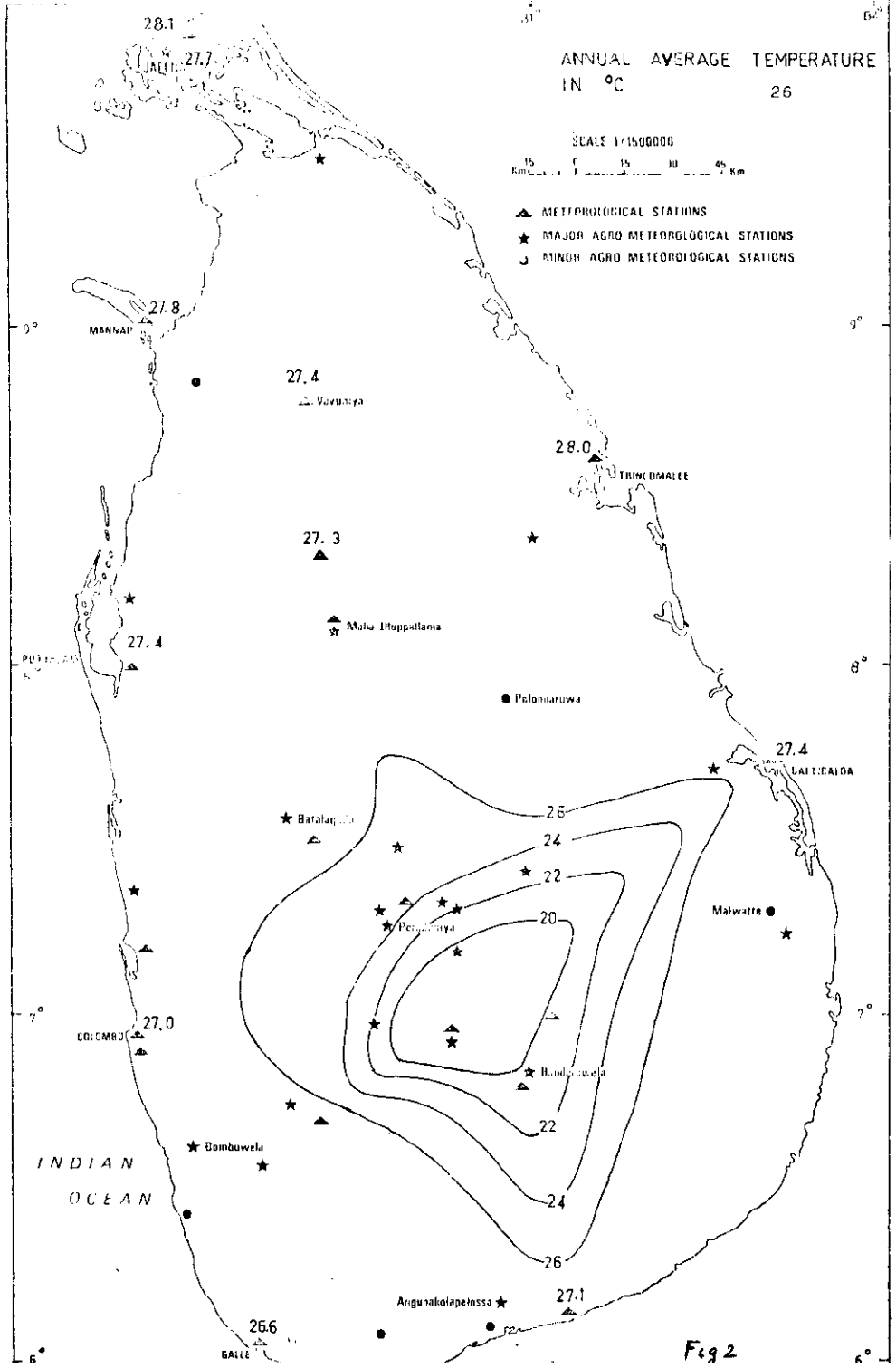
ANNUAL AVERAGE TEMPERATURE
IN °C
26
SCALE 1/1500000
METEOROLOGICAL STATIONS
MAJOR AGRO METEOROLOGICAL STATIONS
MINOR AGRO METEOROLOGICAL STATIONS
28.1
27.7
27.8
MANNAR
27.4
Vavuniya
28.0
TRINCOMALEE
27.3
Mahailuppallama
27.4
Polonnaruwa
27.4
BATTICALOA
Batalagoda
Maduruoya
Malwatte
27.0
COLOMBO
Bombuwela
INDIAN
OCEAN
Angunakolapelessa
27.1
26.6
GALLE
26
24
22
20
22
24
26
9°
8°
7°
6°

Fig 2

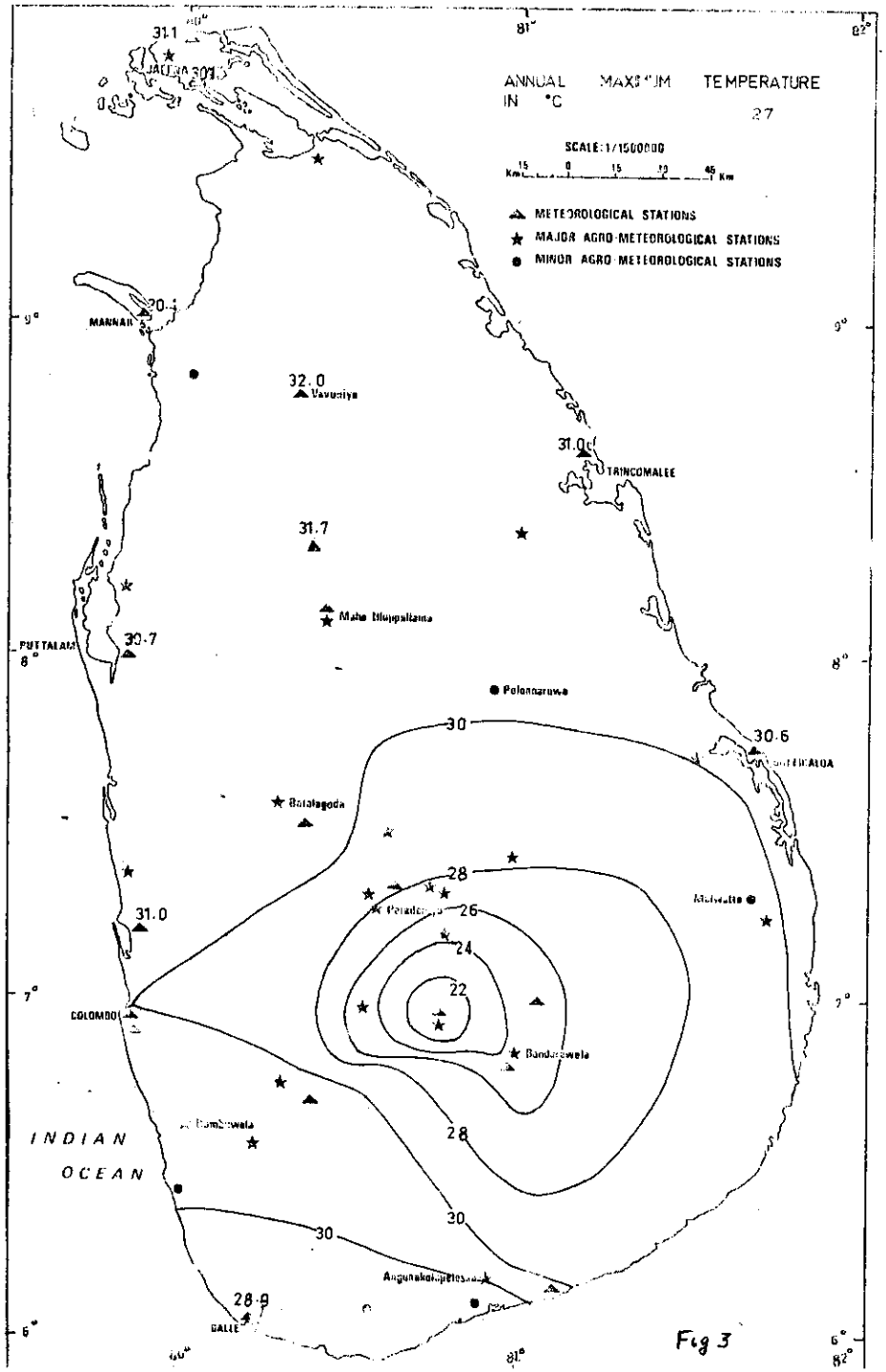
ANNUAL MAXIMUM TEMPERATURE
IN °C
27
SCALE: 1/1500000
METEOROLOGICAL STATIONS
MAJOR AGRO-METEOROLOGICAL STATIONS
MINOR AGRO-METEOROLOGICAL STATIONS
31.1
JAFFNA
MANNAR
32.0
Vavuniya
31.0
TRINCOMALEE
31.7
Maha Illuppallama
PUTTALAM
30.7
Polonnaruwa
30
30.6
BATTICALOA
Batalagoda
28
26
24
22
31.0
Peradeniya
Malwatte
COLOMBO
Bandarawela
Bombuwela
INDIAN
OCEAN
28
30
30
Angunakolapelessa
28.9
GALLE
Fig 3

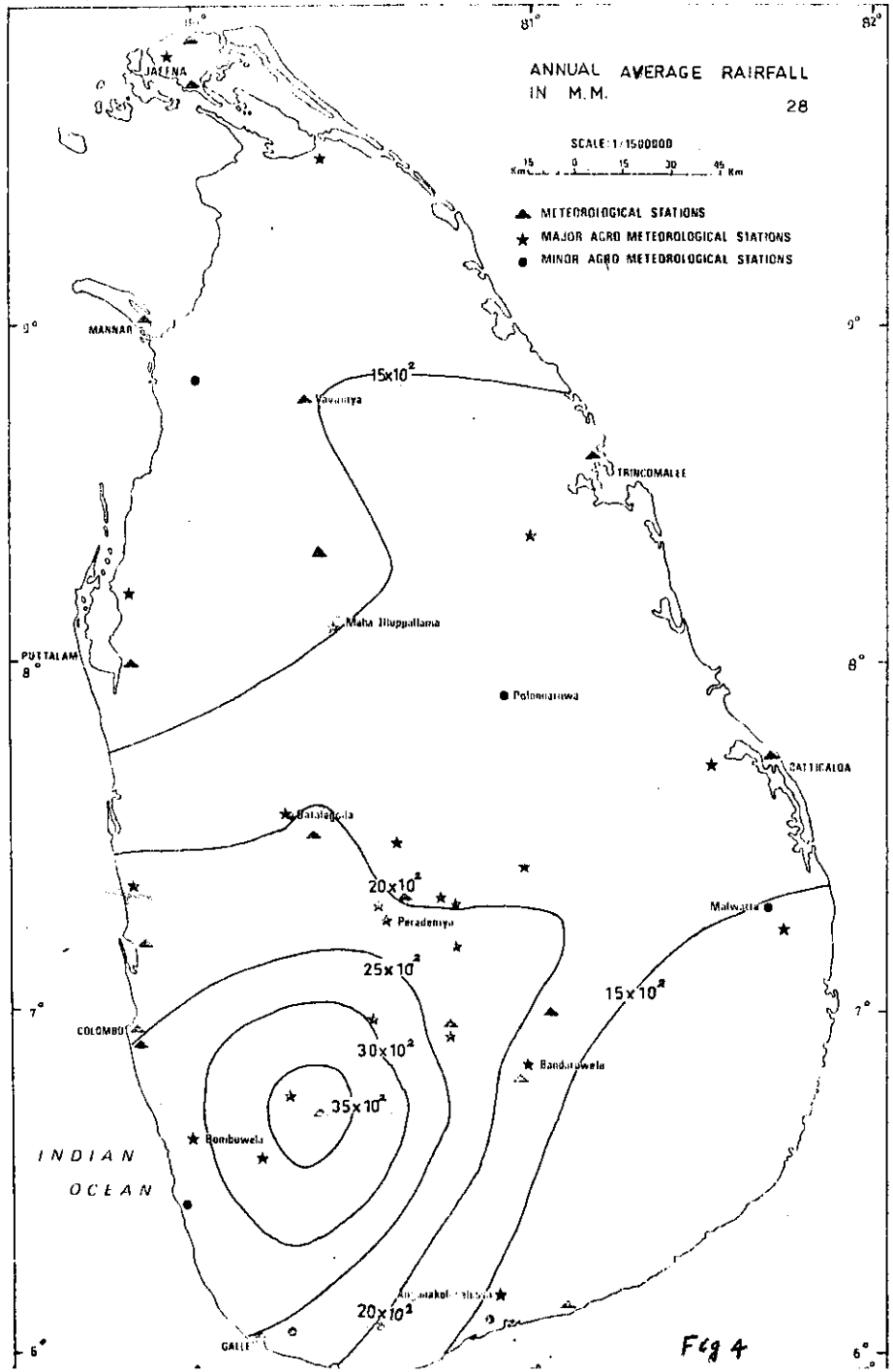
ANNUAL AVERAGE RAINFALL
IN M.M.
28
SCALE: 1/1500000
METEOROLOGICAL STATIONS
MAJOR AGRO METEOROLOGICAL STATIONS
MINOR AGRO METEOROLOGICAL STATIONS
JAFFNA
MANNAR
15x10²
Vavuniya
TRINCOMALEE
Maha Illuppallama
PUTTALAM
Polonnaruwa
BATTICALOA
Batalagoda
20x10²
Peradeniya
Malwatte
25x10²
15x10²
COLOMBO
30x10²
Bandarawela
35x10²
Bombuwela
INDIAN
OCEAN
20x10²
GALLE
Fig 4

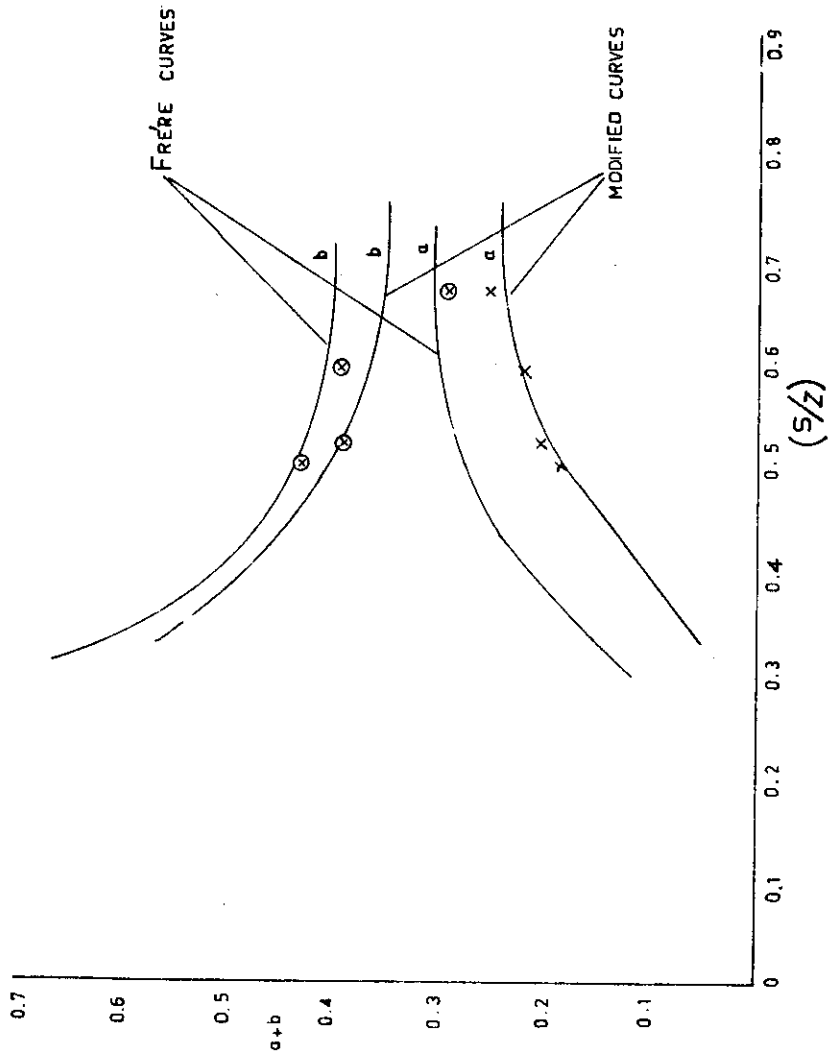
FRERE CURVES
MODIFIED CURVES
a
b
a+b
(S/Z)
0.7
0.6
0.5
0.4
0.3
0.2
0.1
0
0.9
0.8
0.7
0.6
0.5
0.4
0.3
0.2
0.1

Fig 5

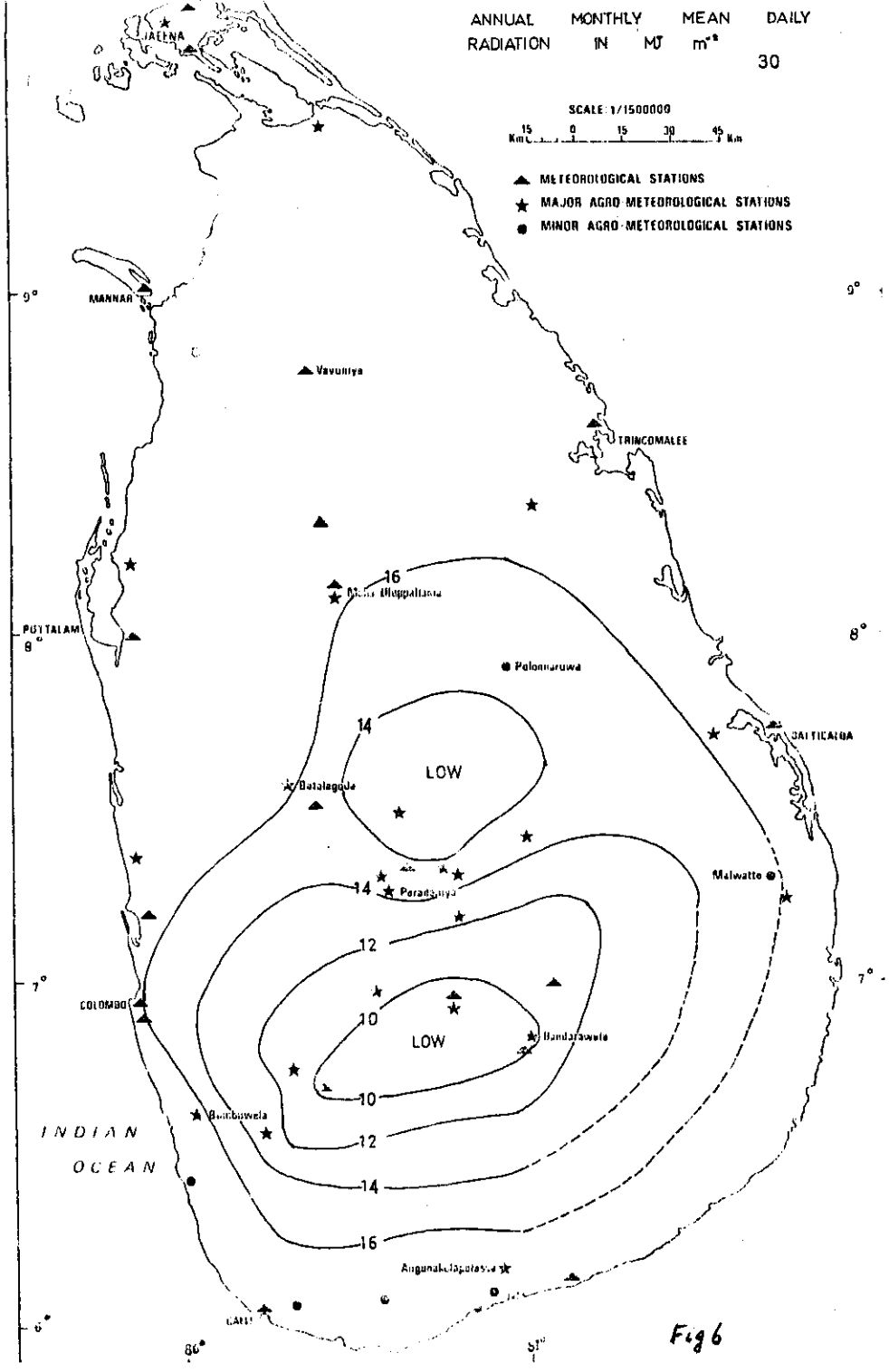
ANNUAL MONTHLY MEAN DAILY
RADIATION IN MJ m⁻²
30
SCALE: 1/1500000
15 0 15 30 45 Km
METEOROLOGICAL STATIONS
MAJOR AGRO METEOROLOGICAL STATIONS
MINOR AGRO METEOROLOGICAL STATIONS
JAFFNA
MANNAR
Vavuniya
TRINCOMALEE
PUTTALAM
Polonnaruwa
BATTICALOA
Batalagoda
Maha Illuppallama
Peradeniya
Malwatte
COLOMBO
Bandarawela
Ratnapura
Angunakolapelessa
GALLE
INDIAN
OCEAN
16
14
12
10
LOW
LOW
9°
8°
7°
6°
80°
81°

Fig 6

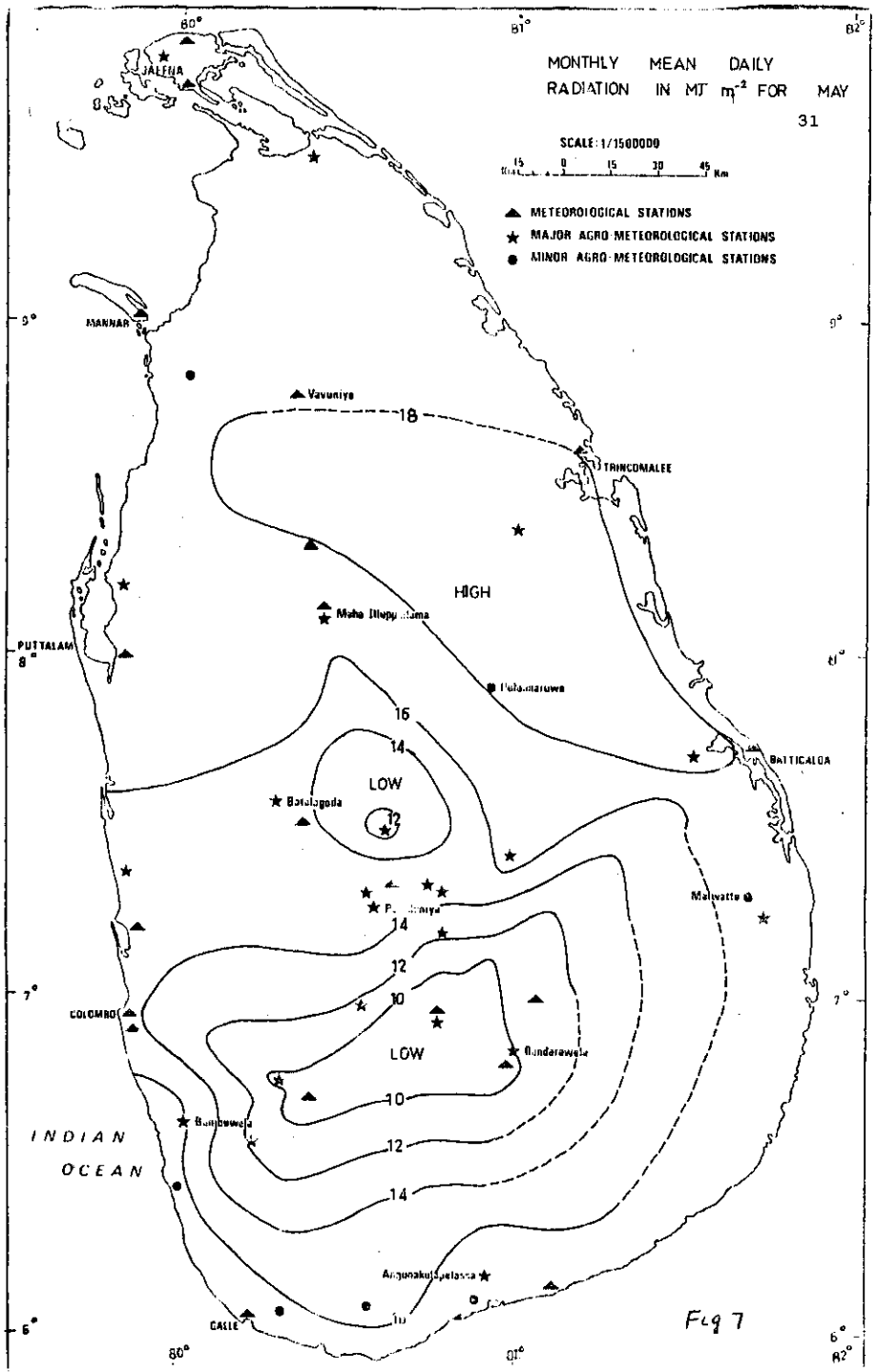
MONTHLY MEAN DAILY RADIATION IN MJ m⁻² FOR MAY
31
SCALE: 1/1500000
METEOROLOGICAL STATIONS
MAJOR AGRO-METEOROLOGICAL STATIONS
MINOR AGRO-METEOROLOGICAL STATIONS
JAFFNA
MANNAR
Vavuniya
TRINCOMALEE
Maha Illuppallama
PUTTALAM
Polonnaruwa
BATTICALOA
Batalagoda
Peradeniya
Maliwatte
COLOMBO
Bandarawela
Bambawela
Angunakulapelessa
GALLE
HIGH
LOW
LOW
INDIAN OCEAN
18
16
14
12
10
14
12
10
12
14
16
10

Fig 7

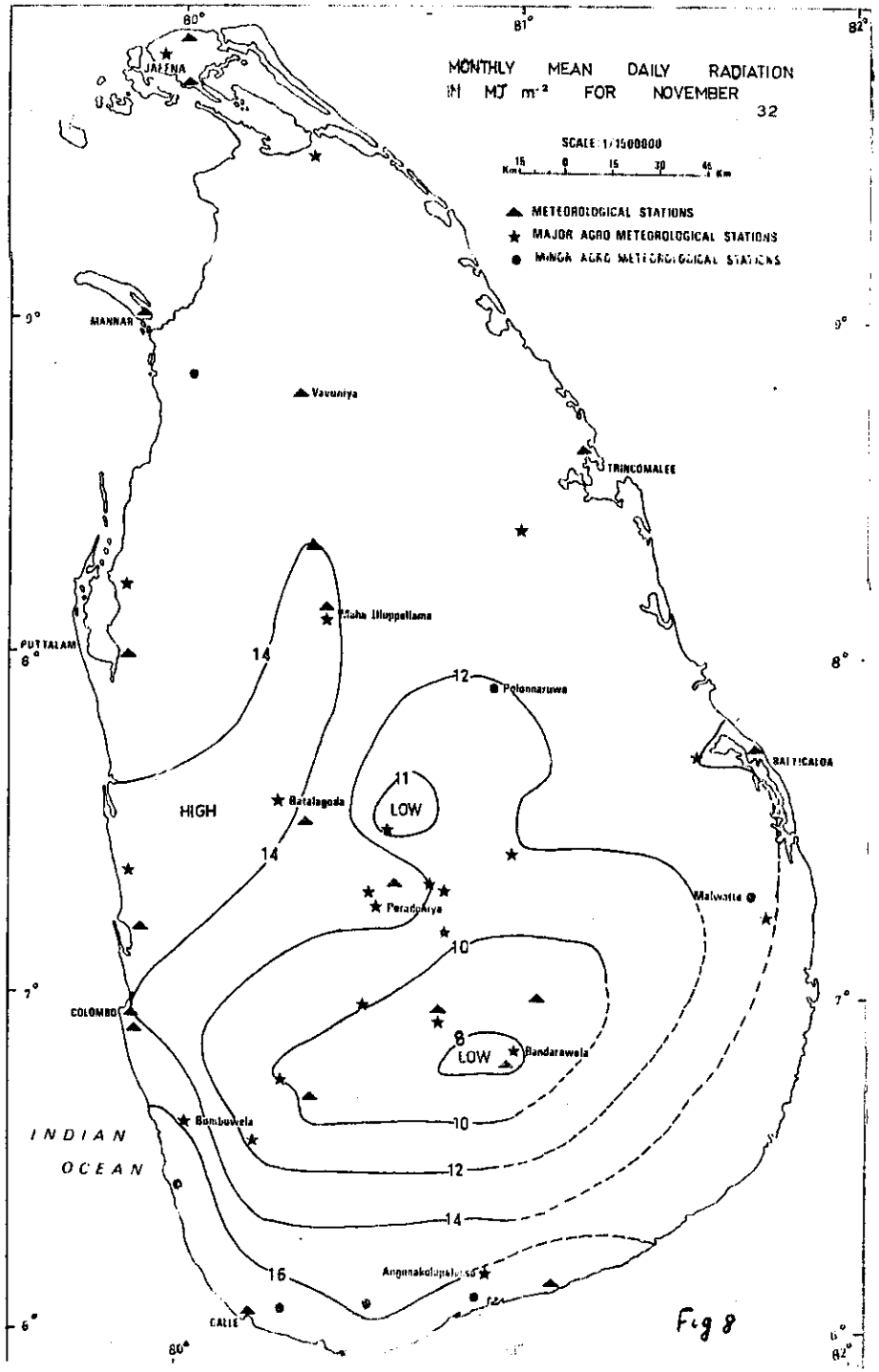
MONTHLY MEAN DAILY RADIATION IN MJ m⁻² FOR NOVEMBER
32
SCALE: 1/1500000
METEOROLOGICAL STATIONS
MAJOR AGRO METEOROLOGICAL STATIONS
MINOR AGRO METEOROLOGICAL STATIONS
JAFFNA
MANNAR
Vavuniya
TRINCOMALEE
Maha Illuppallama
PUTTALAM
Polonnaruwa
BATTICALOA
Batalagoda
Peradeniya
Maliwatte
COLOMBO
Bandarawela
Bambawela
Angunakulapelessa
GALLE
HIGH
LOW
LOW
INDIAN OCEAN
14
12
11
14
10
8
10
12
14
16

Fig 8

A METHOD FOR CALCULATING INTERNAL TEMPERATURES FOR PASSIVE SOLAR BUILDINGS IN AN URBAN SETTING

Martin Evans
Alejandro Ceppi*

* Rawson 2643, 1640 Martinez (S. Isidro)
Prov. de Buenos Aires, Argentina

ABSTRACT:

A method has been developed for calculating the approximate internal temperature, with an average daily value, and the maximum temperature variation above and below this level. The Admittance Method developed by the Building Research Establishment, England, has been used as a base, but to simplify the application, a series of graphs have been prepared so that the designer can understand the relationship between the variables more easily. A new method of calculating the solar radiation intensity has been added so that the designer can readily evaluate the impact of design decisions related to the orientation of glazed openings and collectors, and the proportion of space between buildings on the internal conditions. In the explanation of the method that follows, each figure has been repeated twice; in the second figure a worked example is shown to facilitate the understanding of each graph. Each is interrelated to obtain the final result.

INTRODUCTION:

Many of the existing methods for analysing the thermal performance of buildings with passive solar systems have a series of disadvantages which limit their use in Argentina, and other developing countries. For example, the methods of LASL (1) and the 'f' chart method (2) assume auxiliary heating with thermostats to maintain a minimum temperature, and the result is often expressed as the saving of conventional energy obtained by the use of solar systems. These and other methods assume an ideal orientation towards the equator, without any obstructions in front of the collector or direct gain window. The calculations are often complex and some depend on the availability of computers.

The proportion of conventional energy saved, the solar fraction, is a useful guide in the United States with a tradition of wall heated buildings, where solar heating must be 'competitive' and provide internal conditions equivalent to or better than systems using conventional energy, but in a developing country, the improvement in the standard of comfort may be as important as the saving in fuel (3).

The method explained in this paper has been simplified from the method outlined in the research report presented to SECYT (The Secretary of State for Science and Technology) Buenos Aires, who provided a subsidy for this research project. The research was initiated in the Institute of Planning of the Faculty of Architecture and Urban Design, University of Belgrano during 1980. The research was completed independently by the authors during 1981.

SOLAR RADIATION AVAILABLE:

Figure 1 shows the maximum solar radiation available on a horizontal surface, assuming no atmospheric absorption, according to the month and the latitude. In this and following figures, the month refers to the fifteenth of the month and the latitude ranges from $20^{o}S$ to $56^{o}S$ to cover the continental land area of Argentina and all other parts of the southern hemisphere where passive solar heating is feasible. The radiation intensity in figure 1 is expressed as an average daily flow in Watts per square metre, based on a graph developed by Duffie and Beckman, with values recalculated for this study (4).

Figure 2 shows the actual average intensity of solar radiation received on a horizontal surface. The figure shows the daily values of radiation intensity arranged in ascending order for the month of July (winter in the southern hemisphere) for a location in central Argentina. From this graph, it is possible to select 'design values' representative of days with low and high radiation intensity values. The third day from each extreme of the graph provides such a value, avoiding extremes and values

which may include recording errors. In the example shown, the minimum value is 30 Watts/m^2, while the maximum is 150 Watts/m^2. Figure 1 shows that the maximum intensity for the same latitude (32°S) is approximately 220 W/m^2, so that the design values vary between 13.6% (minimum) and 68.2% (maximum) of the theoretical maximum value.

Figure 3 shows the probable proportion of direct radiation, diffuse radiation from a clear sky, and diffuse radiation from an overcast sky, according to the percentage of the theoretical maximum radiation which is actually received on a horizontal surface. Using the percentages from the example above, a day with minimum radiation intensity (13.6%) will experience diffuse radiation from an overcast sky, while a day with maximum radiation intensity will experience mainly direct radiation with a smaller proportion of diffuse radiation, mainly from a clear sky.

Using these figures, it is possible to estimate the value of radiation intensity according to the type of radiation (diffuse or direct) for 'design days' for the critical months in each location.

DIRECT RADIATION TRANSMITTED THROUGH A VERTICAL GLAZED OPENING:

The large majority of passive solar applications use vertical glazing. The radiation received on a unit area of horizontal surface must therefore be modified to find the radiation passing through a vertical glazed opening. In the examples that follow, single glazing is assumed and a correction should be applied if double glazing is used.

Figure 4 shows the factor by which the average direct radiation intensity should be multiplied to find the average direct radiation intensity which passes through a vertical glazed opening orientated towards the equator (due north in the southern hemisphere) without obstructions facing the opening. In winter this is optimum orientation, assuming that the radiation distribution is symetrical about solar noon. This figure has a similar form to the Boes Relation (5) based on actual measurements of

direct and diffuse radiation combined. Since there is no readily available data giving direct radiation intensity on vertical and horizontal surfaces, figure 4 has been based on theoretical values using a programmable calculator to calculate average daily values. A simplified relationship between the angle of incidence and the transmission of single glazing was developed to speed the calculation.

The assumption that all solar buildings are orientated due north (or due south in the northern hemisphere) and that there are no obstructions facing the glazed opening, is not always valid. To permit the calculation of average daily direct intensities, a further graph has been developed. This graph, figure 5, shows the factor by which the optimum orientation value must be multiplied to allow for variations in orientation to the east or west of north, and for different heights of buildings facing the glazed opening. To simplify the calculation only one case has been considered, that of a continuous building parallel to the plane of the opening. The height of the building is indicated as the vertical angle formed between the horizontal and a line from the opening to the extreme edge of the building in front (in a plane perpendicular to plane of the glass).

In the example given earlier, the average daily radiation intensity was 150 Watts/m^2 on a horizontal surface. Using figure 3, the direct component is found to be (∿) 40% of the theoretical maximum or 88 Watts/m^2 (220 x 0.4). This value is not absolutely correct. Many values have been replaced for an approximate one to simplify the example. The correct figures should be used for an accurate result. Figure 4 shows that the average daily direct radiation intensity passing through a north facing glazed opening, is 1.07 (or 107%) of the intensity on a horizontal surface. This slight increase is due to the favourable angle of incidence resulting from the lower angle winter sun. In latitudes further from the equator, the proportion is even more favourable, but it should be remembered that the intensity of direct radiation on a horizontal surface is much lower for higher latitudes

in winter. In the example the average daily intensity of direct radiation passing through a north facing glazed opening is 94 watts/m^2 (88 x 1.07).

If the opening is orientated 25° to the west of north, with a building subtending a vertical angle of 20° facing the opening, figure 5 shows the reduction in direct radiation intensity that would result. The percentage indicated is 70% giving a direct component of 66 watts/m^2 (94 x 0.7).

Figure 5 also shows the hour of maximum radiation intensity according to the orientation of the opening and the height of a building facing the opening. This information is required later in the calculation. The thinner series of curved lines show the hour of maximum radiation intensity when the orientation of the opening is to the east of north. The corresponding hour for the orientations to the west of north can be easily calculated as the equivalent difference in hours after noon solar time, 1500 hours (west) corresponds with 9.00 hours (east).

DIFFUSE RADIATION TRANSMITTED THROUGH A VERTICAL GLAZED OPENING:

The intensity of diffuse radiation passing through a window or received by a vertical collector must be calculated and added to the direct intensity to find the total average daily solar gain. The direct radiation is highly directional and figure 5 shows that small changes in orientation and in the height of buildings facing the opening can result in significant changes in the radiation received during a day. The diffuse radiation is more evenly distributed, and for the application of this method the orientation of the vertical glazed opening can be ignored in the calculation of the average daily diffuse radiation gain. This will lead to an overestimate of the diffuse gain for south facing windows (in the southern hemisphere). However, the vertical distribution of diffuse radiation can be taken into account to find the proportion that is obstructed by a building facing the opening, according to the angular height.

The vertical distribution of diffuse radiation depends on the atmospheric conditions. In this study, two opposing situations are considered; a clear sky and an overcast sky. In the case of clear sky conditions, the altitude of the sun should also be taken into account. Figure 6 shows the average daily altitude of the sun, according to the month and the latitude. It shows that the average altitude for latitude 32°S in the month of July is 23°.

The diffuse component of the average daily solar intensity on a horizontal surface was found to be 30 watts/m^2 for the minimum design condition and 62 watts/m^2 for the maximum design condition (150 - 88 = 62). In the former case the diffuse radiation comes from an overcast sky, while in the latter it is predominantly from a clear sky. To simplify the calculation, it is often possible to assume diffuse radiation coming entirely from a clear or an overcast sky, since the vertical distribution does not vary greatly.

Figure 7 shows the diffuse radiation transmitted through a vertical glazed opening, as a proportion of the diffuse radiation on a horizontal surface. This proportion can be assumed to be independent of the orientation of the opening and can be applied to the average daily values or maximum diffuse intensities. The different curves show the proportion of diffuse radiation transmitted, according to the angular altitude of the building facing the opening and the conditions of diffuse radiation. The lower solid line shows the proportion of diffuse radiation from an overcast sky (received on a horizontal surface) that is transmitted through a unit area of vertical glazing. If the building facing the opening has an angular altitude of 20°, then 16.5% of the diffuse radiation from an overcast sky will be transmitted. The average daily solar gain for the minimum design conditions is, therefore, 5 watts/m^2 (30 x 0.165).

The dotted lines on the same figure show the proportion of diffuse radiation intensity under clear sky conditions, with different average

solar altitude: 0^{o}, 20^{o} and 60^{o}. For altitudes between these values, the proportion can be found by interpolation. For a solar altitude of approximately 20^{o} and angular building height of 20^{o}, the figure indicates a proportion of 18%. The transmitted diffuse intensity is, therefore, 11 watts/m^2 (62 x .18).

It should be noted that a large proportion of the diffuse component of solar radiation is received from those portions of the sky with an angular altitude less than 20^{o}. This is particularly marked for diffuse radiation from a clear sky with a low angle sun. Under these conditions, the direct radiation will also be received from a low angular altitude.

The curve was calculated using data of the distribution of illumination over the sky (6), and the distribution of diffuse radiation has been assumed to be equal to the distribution of diffuse illumination, originally intended for daylighting calculations.

TOTAL RATE OF HEAT GAIN:

The total rate of heat gain is the total heat received divided by the time during which the heat is received in the room or dwelling under consideration, and is expressed in Watts. The solar gain is the sum of the average daily diffuse and direct solar heat gain, multiplied by the effective glazed area of the opening. The effective area of glazing is the area of the opening less the area of the frame, glazing bars and other obstructions which reduce the area of glass exposed to solar radiation.

If the effective glazed area is $4m^2$, the total solar gain in the example given will be 20 w/m^2 for the minimum radiation conditions (5 x 4), and 308 w/m^2 (4 x (11 + 66)) for the maximum radiation conditions. Using this method the reduction in the radiation received due to the building facing the opening (height 20^{o}) is found to be 36% in the case of maximum radiation conditions with direct radiation and clear skies.

This section of the method provides a guide to the evaluation of the spaces between buildings in relation to the solar radiation received.

The incidental internal heat gains must be added to the solar gains to find the total gain. These internal gains include the metabolic heat produced by the occupants, and the heat produced by installations such as lighting, electrical equipment, ovens, auxiliary heating, etc. These internal heat gains should be expressed as the daily average (24 hours) gain; the total heat produced or received in the space during a day in joules, divided by 86,400 (seconds per day), or alternatively the weighted average gain in watts.

If the room is used by 2 adults for 12 hours per day and electric lighting (200 watts) is used 3 hours per day, the average daily gain would be:-

Inhabitants	2 x 100 x 12 ÷ 24	=	100	
Incidental gains	200 x 3 ÷ 24	=	25	
Solar gains		=	308 (max)	20 (min)
Total Watts			433	145

THE RATE OF HEAT LOSS:

The rate of heat loss of the room or dwelling should next be calculated according to the thermal properties of the external envelope of the building and the ventilation rate, per unit difference between the internal and external air temperature. This calculation is explained in all the basic texts on thermal design, so only a brief summary is given here (7, 8, 9).

The 'U' value or air to air transmittance of each exterior surface of the room or dwelling should be calculated and multiplied by the corresponding surface area. The windows which act as solar collectors should be included as these surfaces can lose heat by conduction and

convection at the same time as they gain heat by radiation. If curtains or night insulation is used a time weighted average of the day and night 'U' values should be used. The total of the products thus obtained indicate the rate of heat loss from the space per unit difference in temperature between the interior and the exterior.

The rate of heat loss due to ventilation must now be added. If the ventilation rate is 2 air changes per hour or less, then the rate of ventilation heat loss is found as the product of the air changes per hour, the volume of the space and a constant 0.33, which relates to the thermal capacity of the air.

If the number of air changes exceeds 2 per hour the mean ventilation heat transfer rate is given by the following formula:

$$Q = \frac{1}{\left(\frac{1}{(ACH.V.0.33)} + \frac{0.21}{S}\right)}$$

At high ventilation rates, the rate of heat transferred from the internal surface of the walls and ceiling must be added to the heat transfer due to the thermal capacity of the air.

THE AVERAGE INTERNAL TEMPERATURE:

The rate of heat gain divided by the rate of heat loss per unit difference in temperature between the interior and the exterior, results in the average temperature difference that is maintained between the interior and the exterior. If the rate of heat loss is 50 watts/^{o}C, and the total gain is 433 watts, then the temperature difference that can be maintained is 8.7^{o}C (433 ÷ 50). This difference must be added to the external design temperature to obtain the average internal temperature for maximum radiation conditions.

To simplify the calculation a nomogram has been prepared, figure 8. The upper left-hand section 'A' is used to multiply the average daily radiation intensity (shown on the vertical scale) by the effective area of glazing (the diagonal lines) to find the total solar gain on the lower horizontal scale. For example, if the total solar gain per square metre is 77 watts and the effective surface area is 4m^{2}, then the gain should be found on the vertical scale, and followed horizontally across to the diagonal line corresponding to the area. The total solar gain is then found vertically below the intersection on the horizontal scale.

The incidental gains should now be added to the solar gains and the corresponding point found on the horizontal scale on the lower left-hand section 'B'. The rate of heat loss per unit difference in temperature should be calculated and the corresponding diagonal found, if necessary interpolating between the lines shown. The temperature difference that can be maintained is found on the vertical scale, horizontally across from the point of intersection between the vertical line of the total gain and the diagonal of rate of heat loss.

The final section of the nomogram 'C' in the lower right-hand corner shows the average internal temperature. The average external temperature is indicated on the horizontal scale, while the temperature difference has already been found on the vertical scale. The diagonal scale corresponding with the intersection of the two scales indicates the average internal temperature.

THE MAXIMUM RADIATION INTENSITY ON A HORIZONTAL SURFACE:

The maximum solar gain must be calculated in order to find the internal temperature variation. A nomogram has been prepared to convert the average daily radiation intensities to maximum intensities. The lower half of the figure indicates the length of the day in hours according to the month and the latitude. Vertically above, and using the same scale

is a graph for finding the hourly intensity as a proportion of the daily average intensity. The upper half of the figure is based on Liu and Jordan's relationship (10).

Figure 5 shows the time of maximum direct radiation intensity on a vertical surface according to the orientation. This will coincide with the time of the maximum global radiation intensity on the same surface. For an orientation 25^{o} to the east of north and a building facing the glazed opening with an angular altitude of 20^{o} (latitude 32^{o}S in July), the maximum direct radiation intensity in that surface will occur at 10 o'clock solar time.

Figure 9 shows that for the same latitude and month, the length of the day is slightly less than 10 hours. The upper half of the figure indicates that for a day of 10 hours at 10 o'clock (two hours before solar noon, interpolating between 9.30 and 10.30), the direct and diffuse maximum radiation on a horizontal surface is 3.12 times the average radiation, while the maximum diffuse radiation is 3 times the average diffuse radiation.

Using the value of 150 watts/m^2 calculated earlier as the average daily intensity of global (direct and diffuse) radiation on a horizontal surface, the maximum intensity is found to be 468 watts/m^2 (150 x 3.12). The diffuse component of the average intensity was earlier calculated to be 62 watts/m^2 on a horizontal surface, so the maximum diffuse intensity on a horizontal surface is therefore 186 watts/m^2 (62 x 3). The direct component is therefore 282 watts/m^2 (468 - 186). These radiation intensities on a horizontal surface must be modified to find the maximum radiation transmitted through a vertical glazed opening.

MAXIMUM DIRECT RADIATION INTENSITY PASSING THROUGH VERTICAL GLAZING.

In this section a method is described to find the intensity of direct radiation that is transmitted through a vertical glazed opening. Firstly,

the altitude and azimuth of the sun must be determined from a sunpath diagram, figure 10. For a location with a latitude 34^{o}S in July at 10 o'clock solar time, the azimuth is 34^{o} (to the east of north) and the altitude is 29.3^{o}. Since the orientation of the opening considered in the example is 25^{o} to the east of north, the projection of the angle of incidence in the horizontal plane is 9^{o} (34 - 25). Figure 11 can be used to find the true angle of incidence for a vertical plane. The vertical scale indicates the solar altitude and the horizontal scale shows the angular difference between the solar azimuth and the orientation of the vertical plane (the projection of the angle of incidence on the horizontal plane). The curved lines show the true angle of incidence. In the example given this is found to be 31^{o}.

The nomogram, figure 12, can now be used to find the maximum direct radiation intensity passing through vertical glazing (11). The first section of the nomogram 'A' is in the lower right hand corner, where the solar altitude is indicated on the vertical scale. The intensity of radiation normal to the surface is found vertically above the intersection of the horizontal line (solar altitude) and the altitude band (0, 1000 or 3000 metres above sea level). Each radiation band ranges from dry to humid so that the effect of water vapour is considered. The vertical line indicating normal radiation should be continued to enter section 'B' in the upper right hand section. The radiating diagonal lines indicate the reduction in radiation due to different levels of pollution, ranging from 0.00 (without pollution) to 0.40 (polluted). On the vertical scale horizontal across from the corresponding intersection, the corrected direct normal radiation intensity can be found.

The final section on the nomogram 'C' indicates the additional reduction in solar radiation intensity according to the angle of incidence.

Two cases are considered; the dotted lines show the radiation incident on a plane surface, while the dotted lines show the direct radiation transmitted through single glazing. The horizontal scale vertically below the intersection of the normal radiation line and the appropriate angle of incidence diagonal line indicates the direct radiation intensity.

The direct intensity has been calculated using the following values:

Latitude	32°S	Month	July
Solar time	10.00 hours		
Solar altitude	29.3	Azimuth	34.0
Altitude above S.L.	0 metres	Humidity	humid
Pollution	0.30		
Angle of incidence	60.3°	On a horizontal surface (90 - 29.3)	
	31°	On a vertical surface, orientation 25°	

Result	690 watts/m^2	normal intensity
	340 watts/m^2	Horizontal surface
	530 watts/m^2	Vertical surface through glazing

The result for the intensity on a horizontal surface is 20% greater than that calculated in the previous section. This former result assumes average monthly cloudiness, based on data from the U.S.A. while the result shown on this page corresponds to clear sky conditions.

A final check should be made to confirm that the direct solar radiation is not obstructed by the building facing the opening at the hour and date considered. This is highly unlikely if the figure 5 has been used to find the time of maximum radiation intensity, but if the figure 12 is used to find the radiation intensity at other times, this factor may be important.

THE MAXIMUM DIFFUSE INTENSITY TRANSMITTED THROUGH VERTICAL GLAZING:

The maximum diffuse intensity on a horizontal surface was found to be 186 watts/m^2. Figure 13 can be used to find the proportion of diffuse radiation on an unobstructed horizontal surface that is transmitted through a vertical glazed opening, according to the solar altitude and the difference between the azimuth of the sun and the orientation of the vertical surface. This graph is based on a relationship developed by Parmlee quoted by Page (12).

The proportion of diffuse radiation which is transmitted through the single glazing must be reduced if there is a building facing the opening. Figure 7 can be used to find the proportion of diffuse radiation passing through a vertical glazed opening with and without an obstruction. The former divided by the latter indicates the proportion of unobstructed diffuse radiation that will be transmitted according to the height of the building facing the opening.

The diffuse intensity passing through a vertical glazed opening can be calculated as follows:

Maximum diffuse intensity on a horizontal surface	186 watts/m^2
Solar altitude	29.3°
Difference between azimuth and orientation	9°
Proportion of diffuse intensity passing through vertical glazing, from figure 13.	0.73
Unobstructed diffuse radiation passing through vertical glazing (0.73 x 186).	135.8 watts/m^2
Proportion of horizontal intensity from an unobstructed sky, from figure 7.	42%
Proportion of horizontal intensity from a 20% obstructed sky, from figure 7.	18%
Proportion of obstructed diffuse intensity transmitted (42 - 18).	0.43

Obstructed diffuse intensity transmitted (135.8 x 0.43). 58 watts/m^2

This value can be added to the maximum direct intensity transmitted to find the total. An additional component corresponding to the radiation reflected from the ground and from surfaces facing the window should also be added, but it is assumed that this component is equivalent to the radiation that is reflected and retransmitted from the interior to the exterior.

INTERNAL TEMPERATURE VARIATION:

The variation in internal temperature can now be calculated using the admittance method as explained by Burberry (13) or publications of the Building Research Establishment (3). To aid the calculation, a nomogram has been prepared, figure 14.

The first section 'A' in the upper right-hand corner is used to find the swing in radiation intensity above and below the average intensity. The horizontal scale shows the daily average global radiation intensity and the diagonal lines indicate the maximum global intensity. The variation in global intensity is found on the vertical scale, horizontally across from the intersection of the two known values. This variation has been adjusted to take into account the alternating solar gain factor.

Section 'B' is used to find the total gain according to the effective surface area of the glazing, by reading across from the variation found in section 'A' to the diagonal corresponding to the effective surface area. On the horizontal scale directly below the intersection, the swing in the total gain can be found. Before reading vertically down to the next section of the graph, an adjustment should be made for the variation in the internal incidental heat gains. The average internal heat gains were calculated earlier. The variation in these internal gains should be calculated for the time of maximum solar radiation gain. If these are lower than the average, the difference should be subtracted from the solar gains to find the swing in the total gains, while if these are higher the difference should be added.

TABLE 1

THE THERMAL ADMITTANCE OF BUILDING ELEMENTS

Element Construction	Admittance w/m^2 deg C.
Walls:	
Lightweight or hollow block more than 75mm thick.	3.0
Hollow concrete or perforate clay block 75mm thick.	4.0
Brick more than 75mm thick.	5.0
Concrete more than 75mm thick.	6.0
Two fibre board sheets with an air space between them.	2.0
Heavy partitions with an insulated lining.	3.0
Floors:	
Dense concrete.	6.0
Concrete covered with carpet, cork tile or wood block.	3.0
Suspended timber floor.	2.0
Suspended timber floor with carpet.	1.5
Ceilings:	
Plastered concrete.	6.0
Plasterboard, air cavity and a dense concrete slab.	3.0
Plasterboard or traditional plaster ceiling with roof cavity and pitched roof.	2.0
Windows:	
Calculate the heat flow according to the 'U' value and the heat transfer due to ventilation.	

Source B.R.E.

Before using section 'C' of the graph the 'admittance' of the space or building under consideration should be calculated. The admittance can be defined as the rate at which heat enters (or leaves) a unit area of the surface of a building element for a unit difference in temperature between the air and the surface, it is a measure of the ability of a surface to reduce temperature swings. The admittance values of various forms of construction are given in Table 1.

The admittance value from Table 1 for each of the internal surfaces should be multiplied by the internal surface area of that surface. The ventilation gains identical to those calculated earlier should be added to the sum of the products. This total indicates the flow of heat into the building elements and the flow due to ventilation and transmission for a one degree temperature difference. The diagonal corresponding to this total should be found in section 'C' of the figure. The vertical scale horizontally across from the point of intersection shows the maximum variation in temperature above and below the average.

The adjacent scale in section 'D' of the nomogram shows the maximum range of temperature (the difference between maximum and minimum). The horizontal scale shows the average internal temperature calculated earlier. The point of intersection between the range and the average should now be found. If this point lies within the solid triangle, then the thermal conditions are suitable for a living space. If the point lies within the dotted trapezium, then the thermal conditions are suitable for bedrooms or sleeping spaces. Lower average temperatures are acceptable but the temperature range should be lower as large temperature swings will disturb sleep. Finally the lightly dotted triangle defines the range of thermal conditions that are acceptable for circulation spaces, attached greenhouses or sun spaces that are used occasionally for circulation or when comfortable.

If the point lies outside the comfort zone appropriate for the use required, then the nomograms can be used in reverse. Firstly, the

appropriate remedial action should be decided; change the average internal temperature or reduce the range or both. The corresponding design change can now be found using figure 11 of figure 2 (or both). The thermal characteristics of the building can be improved increasing the thermal insulation or the admittance or adjusting the surface areas. The area of the glazed opening can be reduced (to reduce the swing) or increased (to raise the average temperature). The solar radiation intensities can be improved by optimising the orientation or increasing the spacing between buildings. Finally, as a last resort, auxiliary heating may be needed.

REFERENCES:

1. Methods developed by D. Balcomb in the Los Alomos Scientific Laboratories.

2. Beckman, William A. Solar heating design by the 'F' chart method. J. Wiley, New York, 1977.

3. Millback, N.O. and Harrington-Lynn, J. Thermal response and the admittance procedure. Current paper 61/74, Building Research Establishment, 1974.

4. Duffie, J.A. and Beckman, W.A. Solar energy thermal processes. Wiley Interscience, New York, 1974.

5. de Masccaro, L.R. Luminotecnia: luz natural, Ediciones Summa, Buenos Aires, 1977.

6. Evans, J.M. Climat comfort and housing. Architectural Press, London, 1980.

7. Koenigsburger et al. Manual of tropical housing and building. Longmans, London 1973.

8. Markus, T.A. and Morris, E.N. Buildings, climate and energy. Pitman, London 1980.

9. Liu, B.Y.H. and Jordan, R.C. The interrelationship and characteristic distribution of direct, diffuse and total solar radiation. Solar Energy, 4 (3), 1-19, 1960. (quoted in 8).

10. Based on the relationships in the computer programme developed by Page and others in the University of Sheffield.

11. Page, J.K. Geographical variations in the climatic factors influencing solar building design, 1.10 (38-70) Solar Technology for Building Proceedings of the first International conference on solar building technology, London, 1977.

12. Burberry, P. Building for Energy conservation, Architectural Press, London 1979.

CUADRO: 1

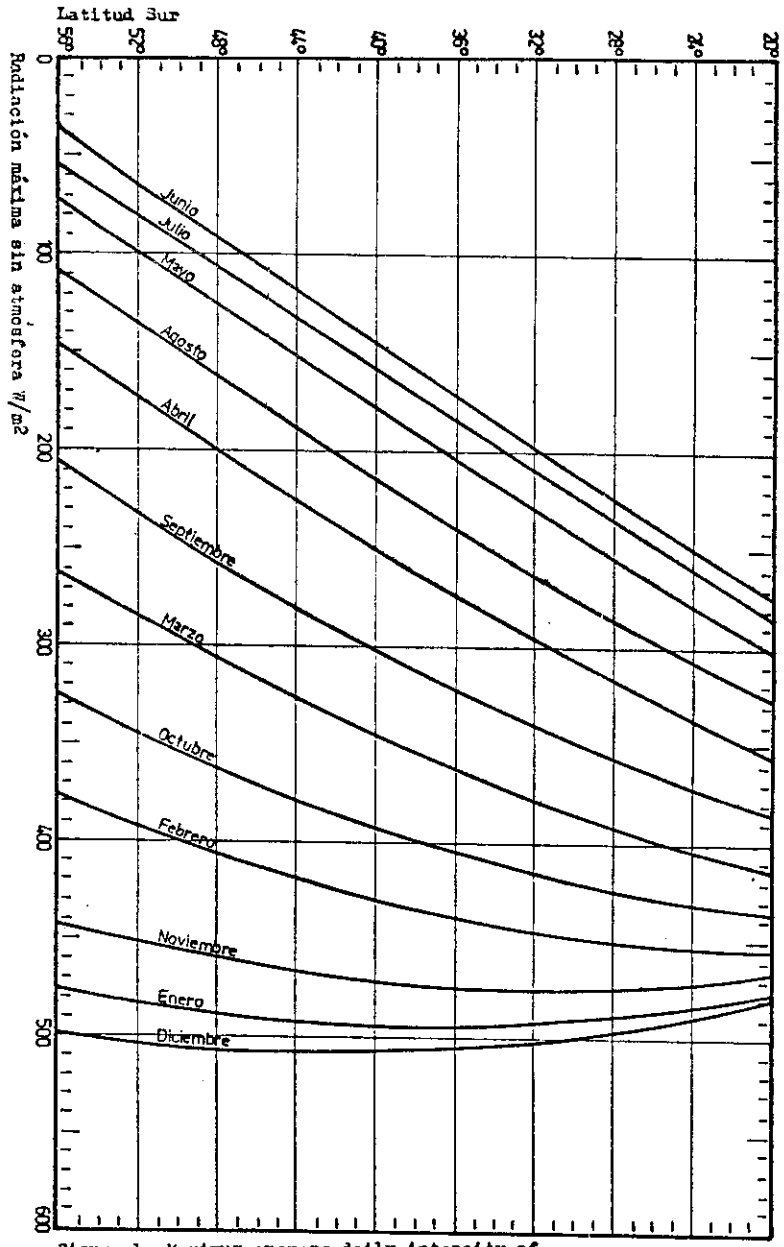

Figure 1. Maximum average daily intensity of solar radiation on a horizontal surface without atmospheric absorpcion.

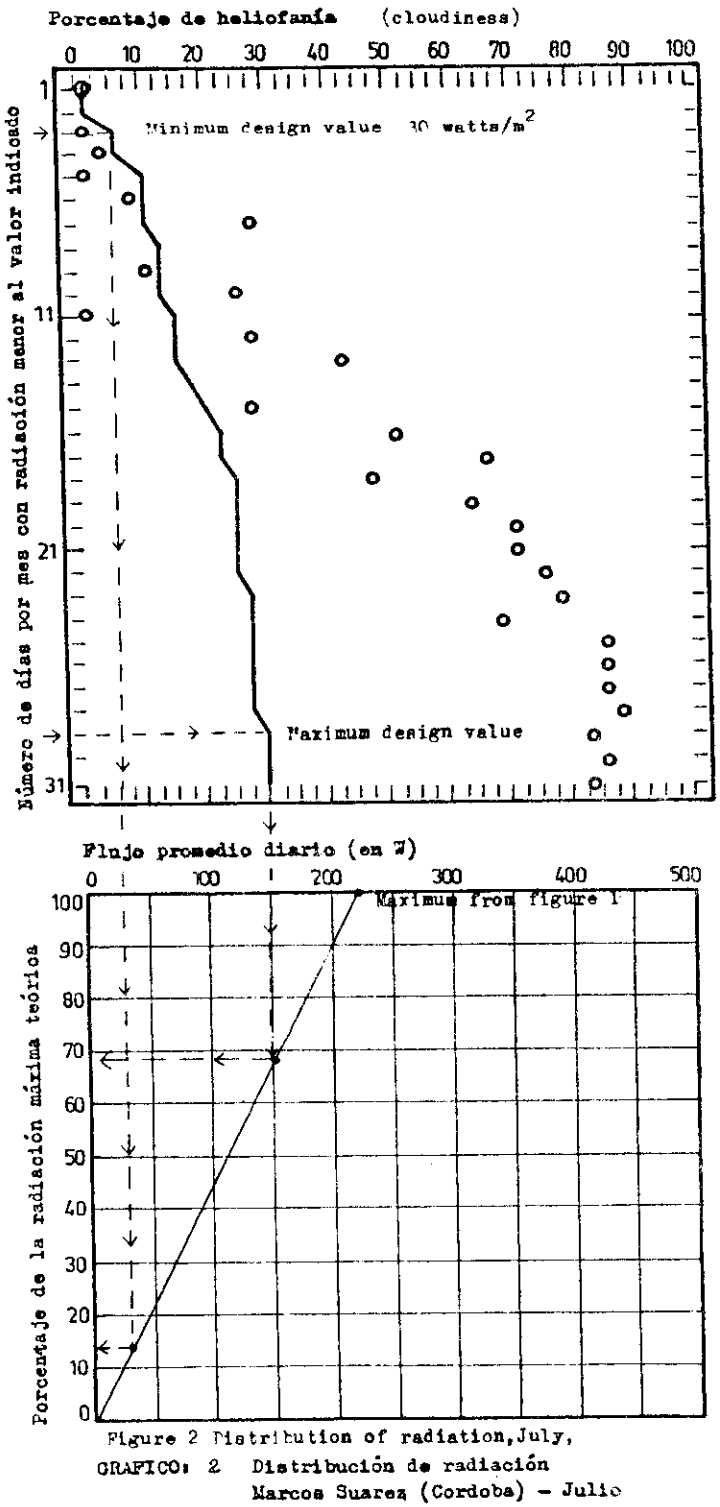

Figure 2 Distribution of radiation, July,

GRAFICO: 2 Distribución de radiación

Marcos Suarez (Cordoba) - Julio

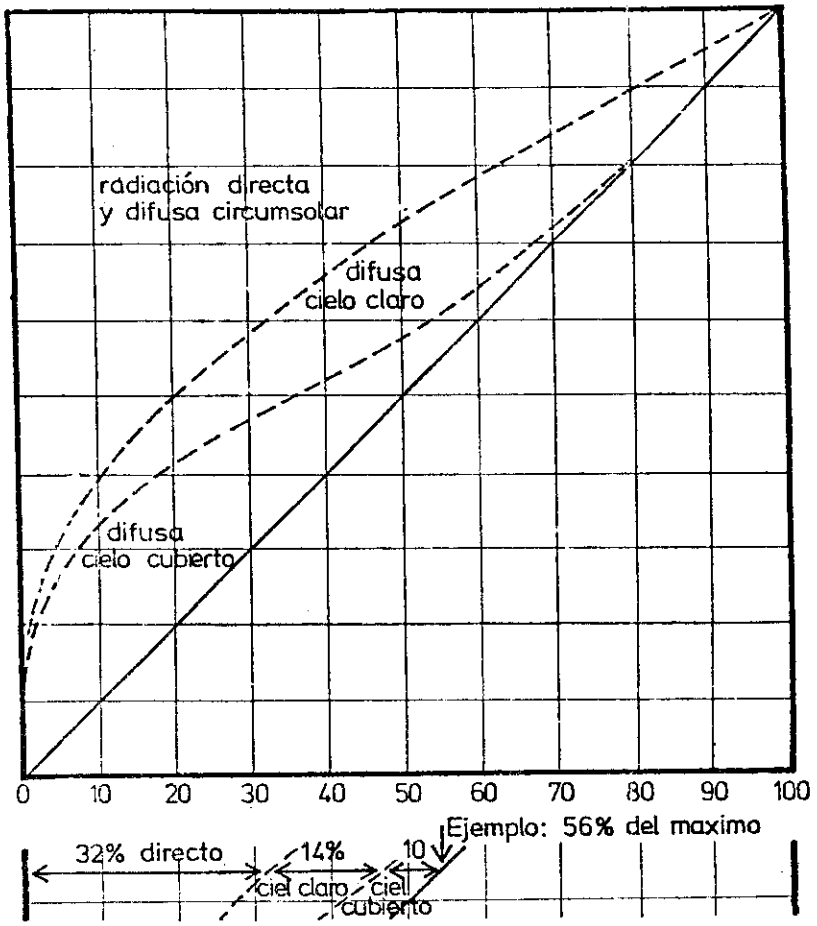

Figure 3 Distribution of direct and diffuse radiation, according to the proportion of the theoretical maximum recieved on a horizontal plane.

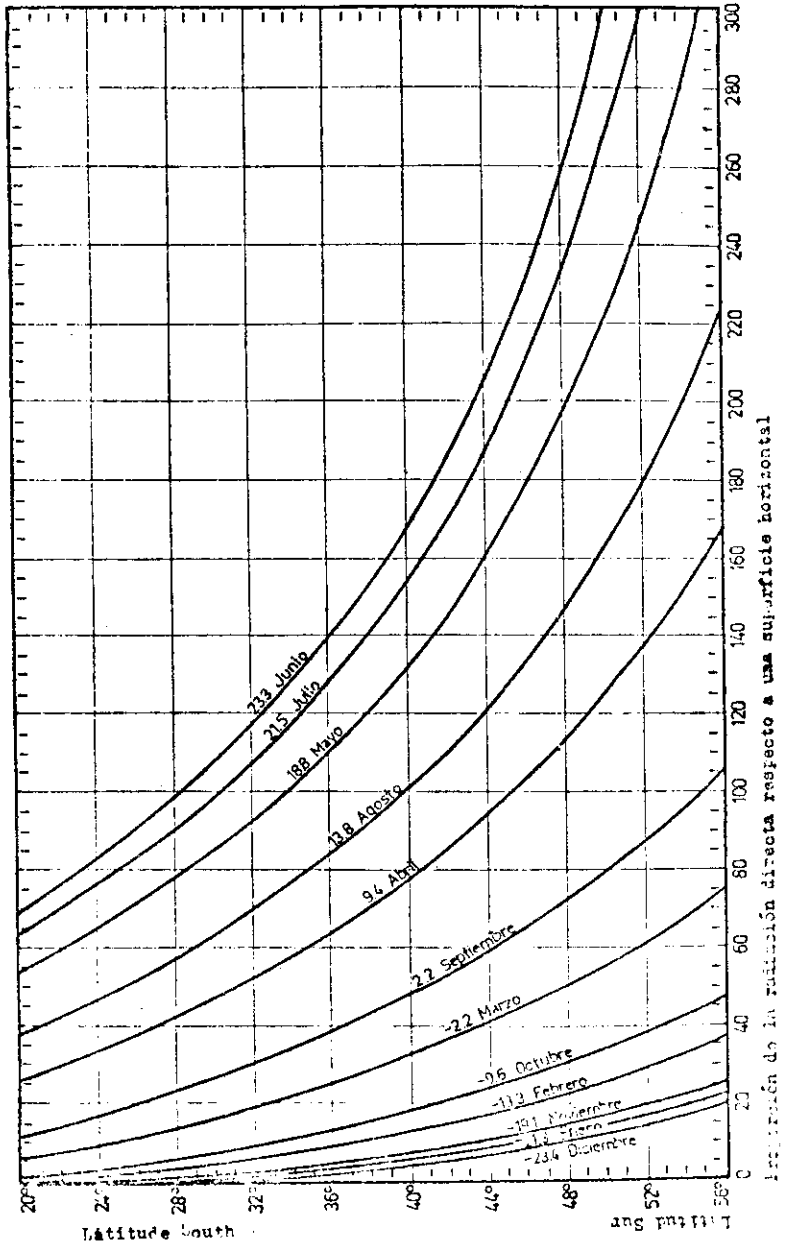

Figure 4 The proportion of the direct radiation recieved on a horizontal plane that is transmitted through a north facing window. (Daily average)

GRÁFICO: 4 Relación directa sobre plano vertical al norte con absorción de vidrio respecto a una superficie horizontal

R directa tras vidrio vert. s/orientación y h edificio en frente
R directa tras vidrio vert. al norte, y ningun edificio en frente

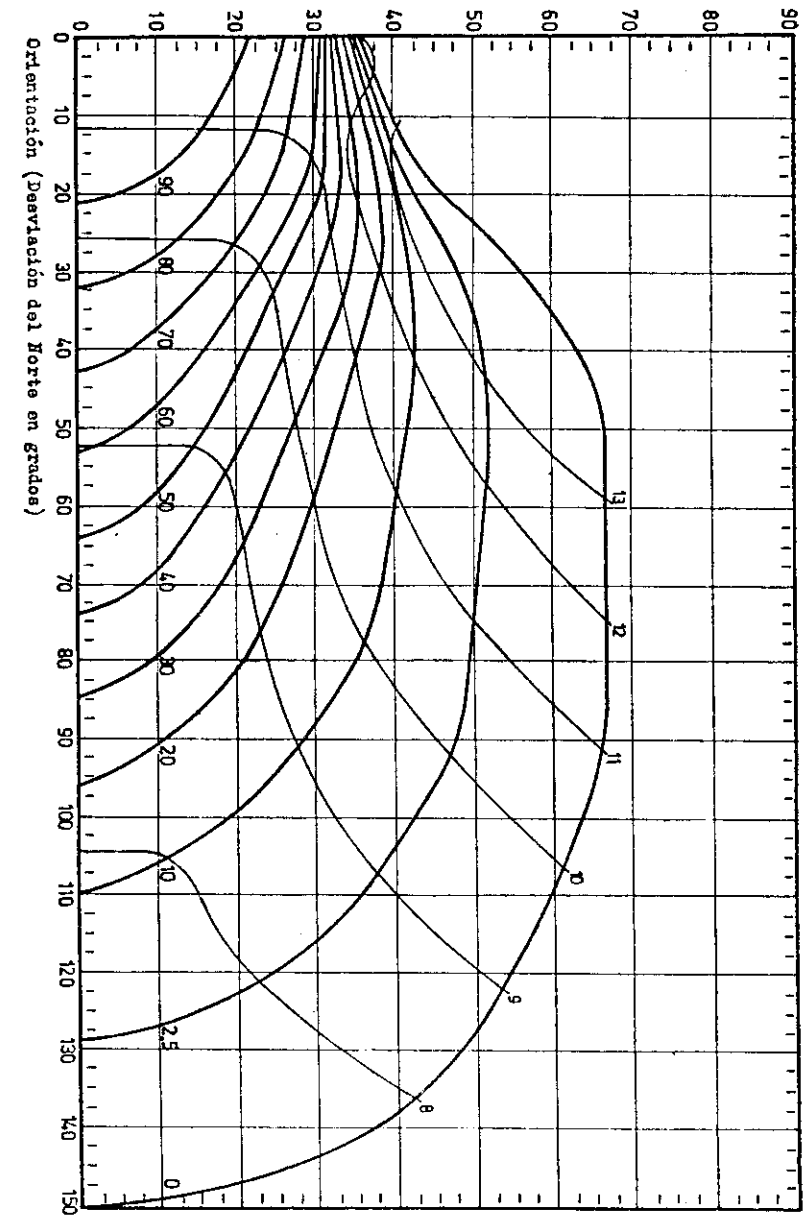

GRÁFICO: 5 Proporción de Radiación Directa Latitud 32° S Declinación 23

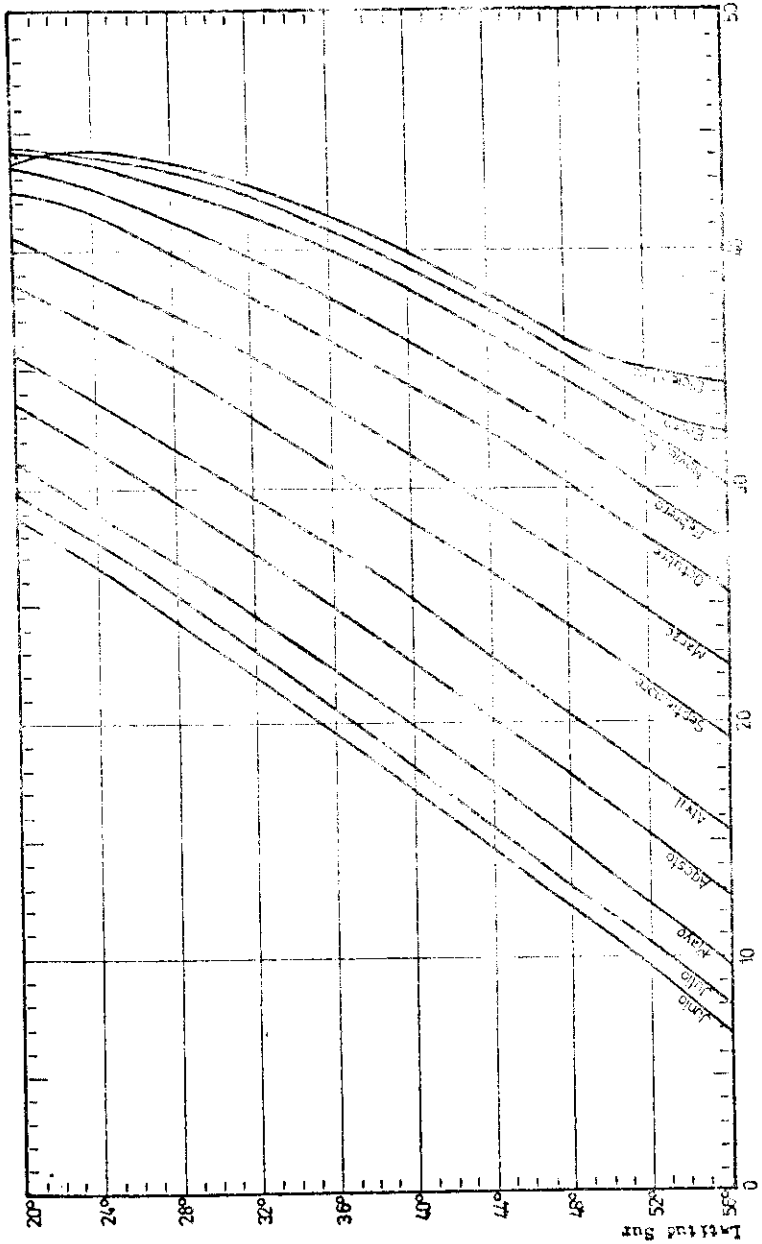

Figure 6. Average solar altitude.

Promedio del Angulo

GRAFICO: 6 Altura promedio del ...

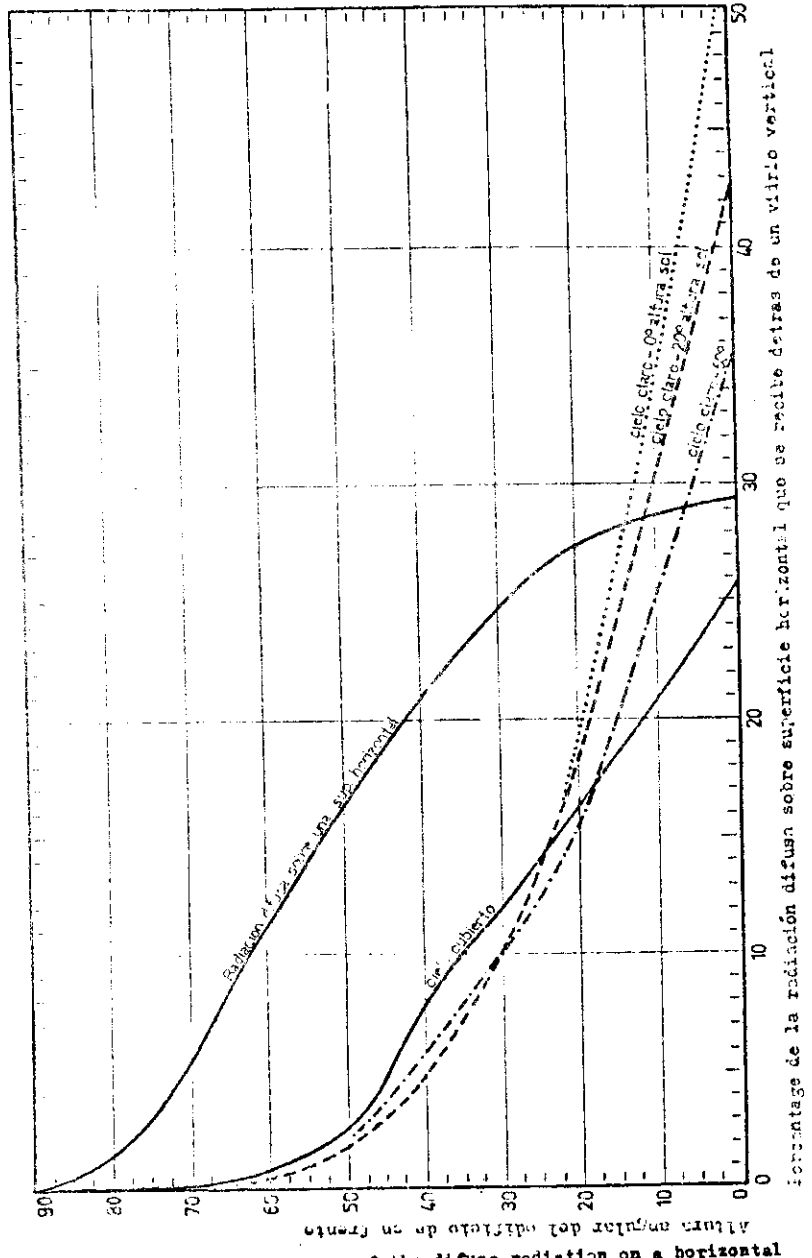

Figure 7. The percentage of the difuse radiation on a horizontal plane that would be transmitted through vertical glazing.

Porcentaje de la radiación difusa sobre superficie horizontal que se recibe detras de un vidrio vertical

GRAFICO: 6

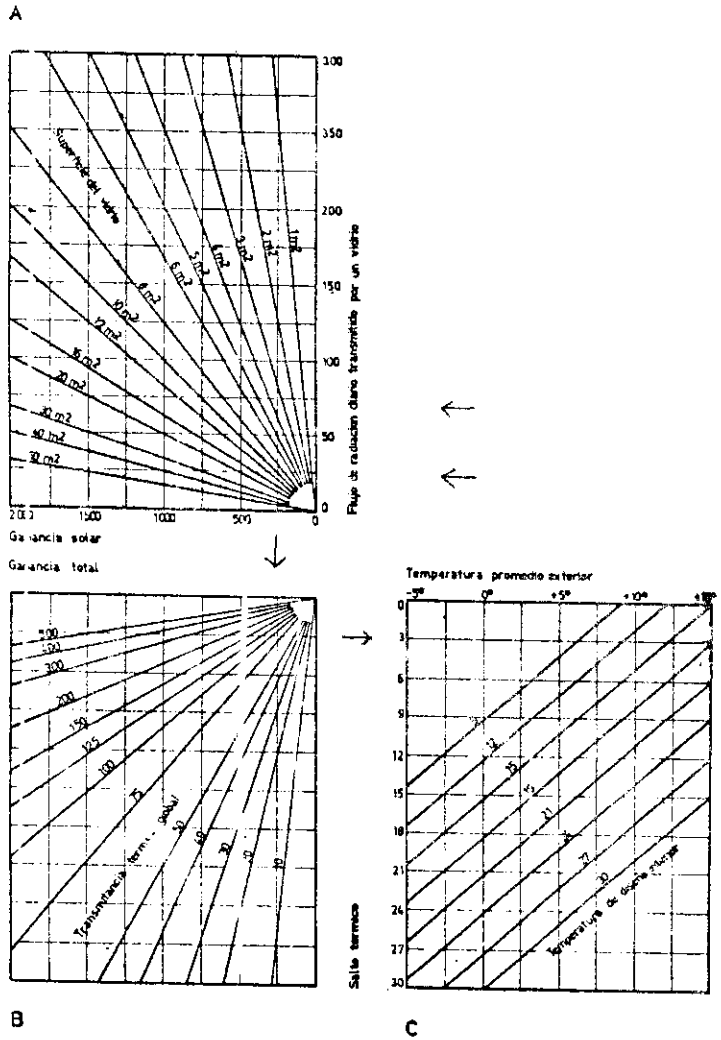

Figure 8. Nomogram to calculate the average internal temperature.

GRAFICO: Abaco para calcular la temperatura interior promedio

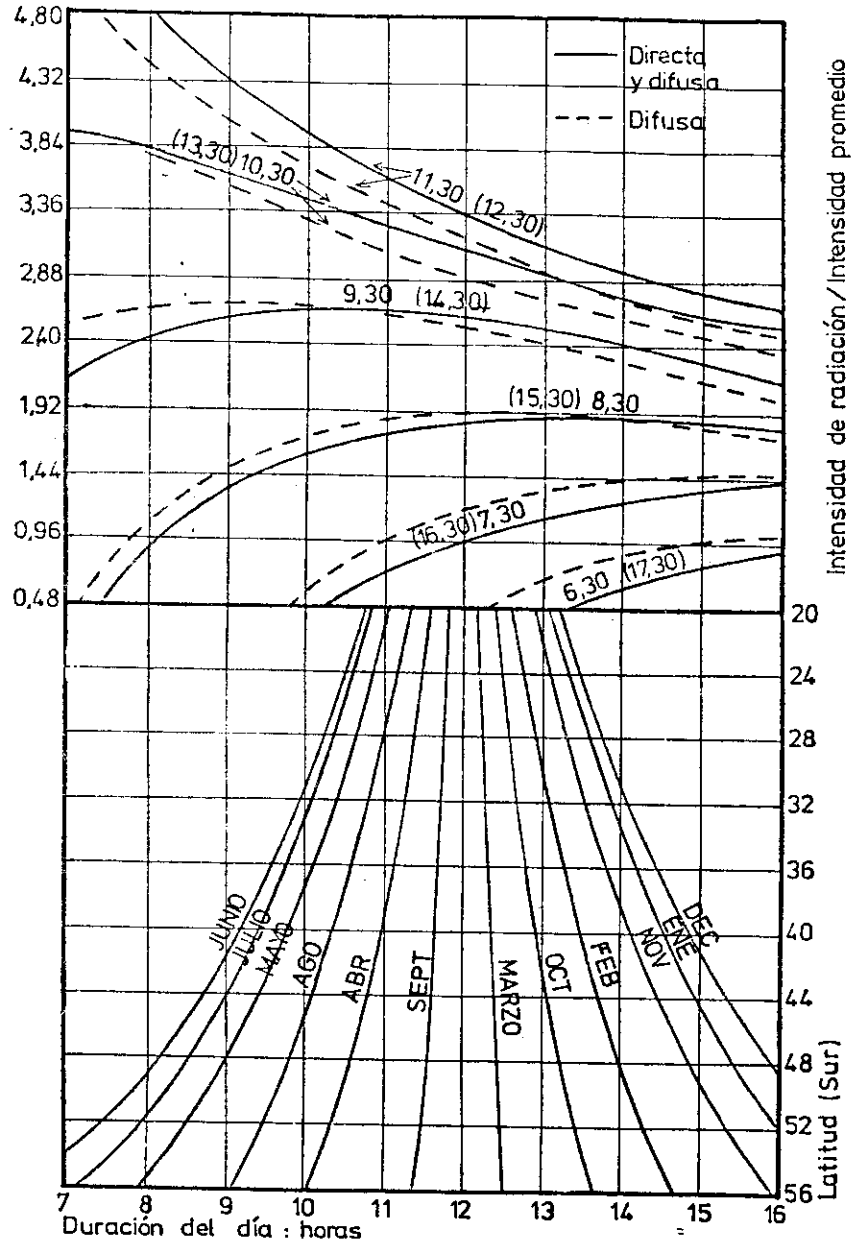

GRAFICO: 9 Intensidad de radiación como proporción del promedio

Figure 9 Average hourly intensity of solar radiation as a proportion of the average daily intensity.

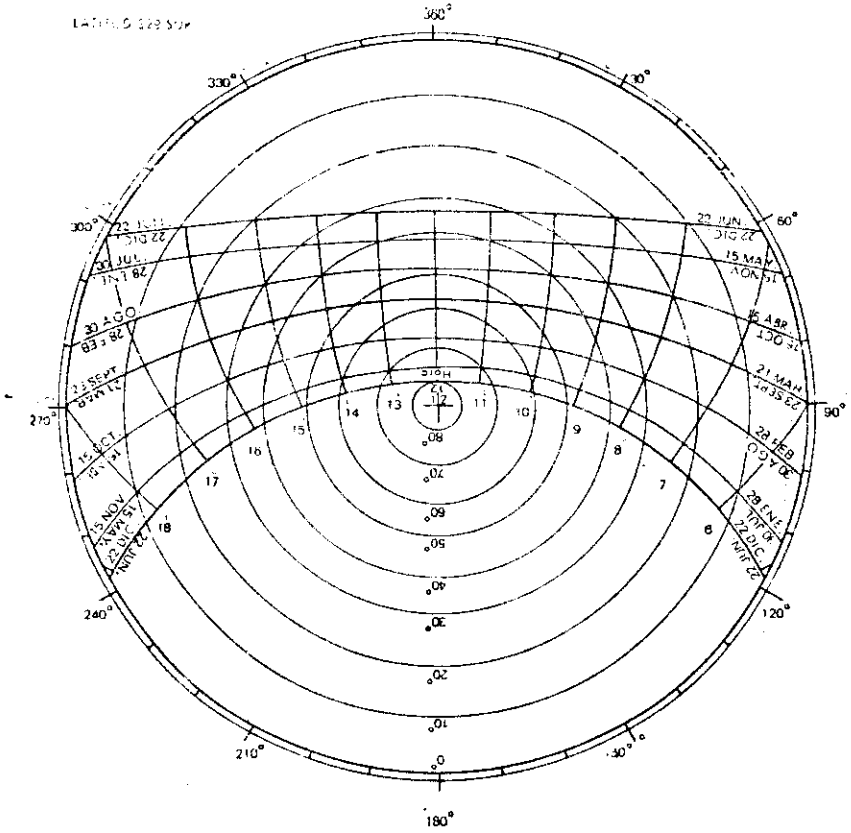

Figure 10 Sun path diagram for 32° south .

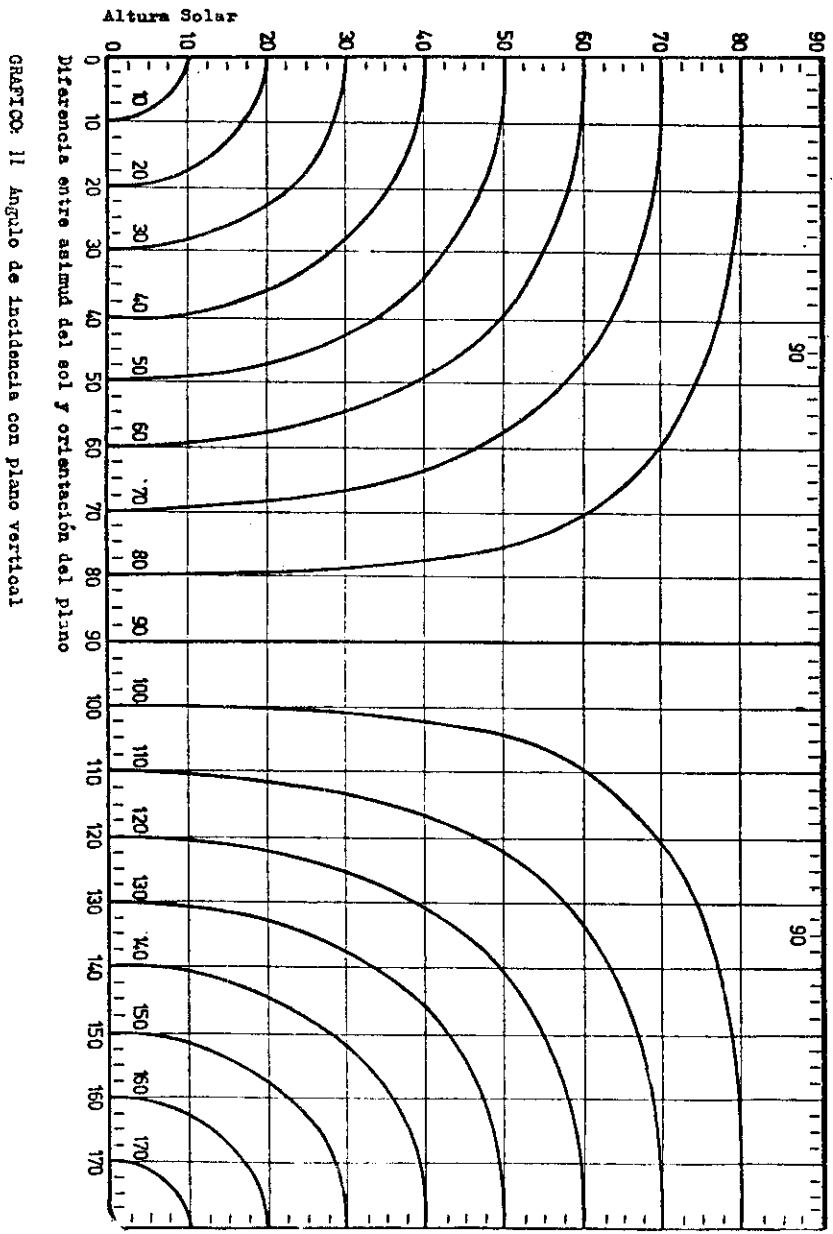

GRAFICO: 11 Angulo de incidencia con plano vertical

Diferencia entre azimut del sol y orientación del plano

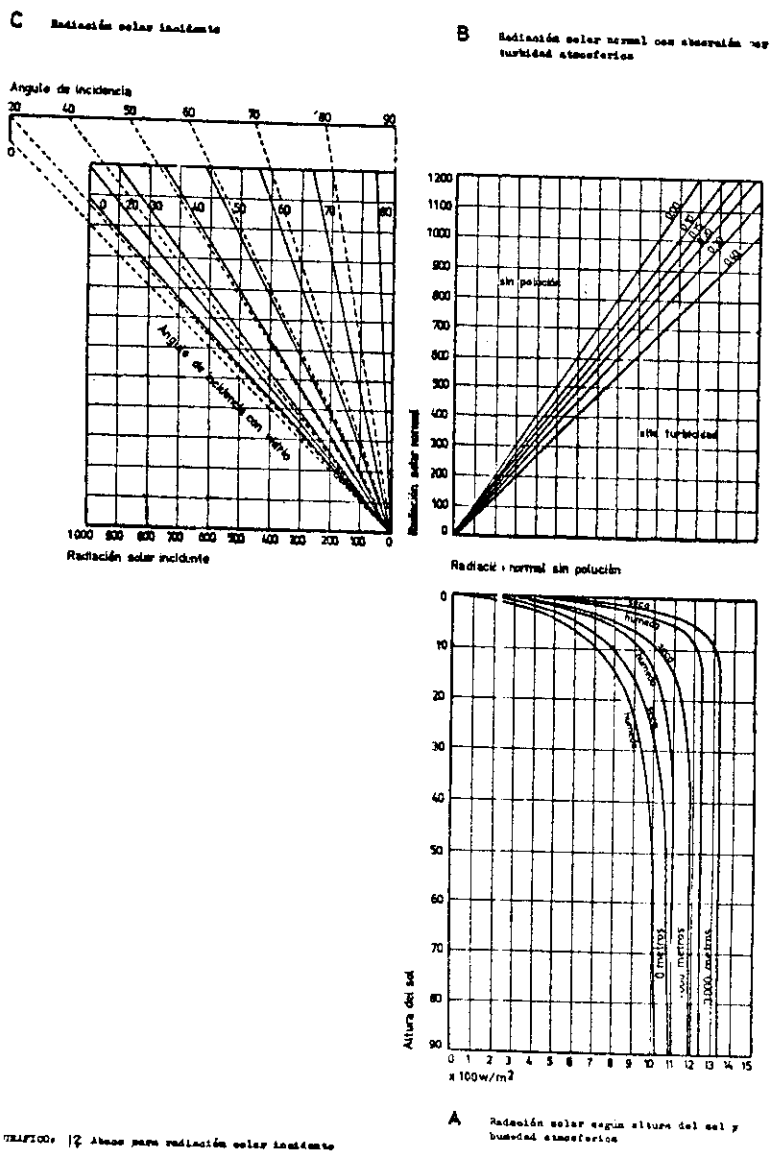

GRAFICO: 12 Abaco para radiación solar incidente

Figure 12 Nomogram for calculating direct radiation intensity.

GRAFICO: 13 Radiación difusa transmitida a través de un vidrio como proporción de la radiación difusa sobre superficie horizontal

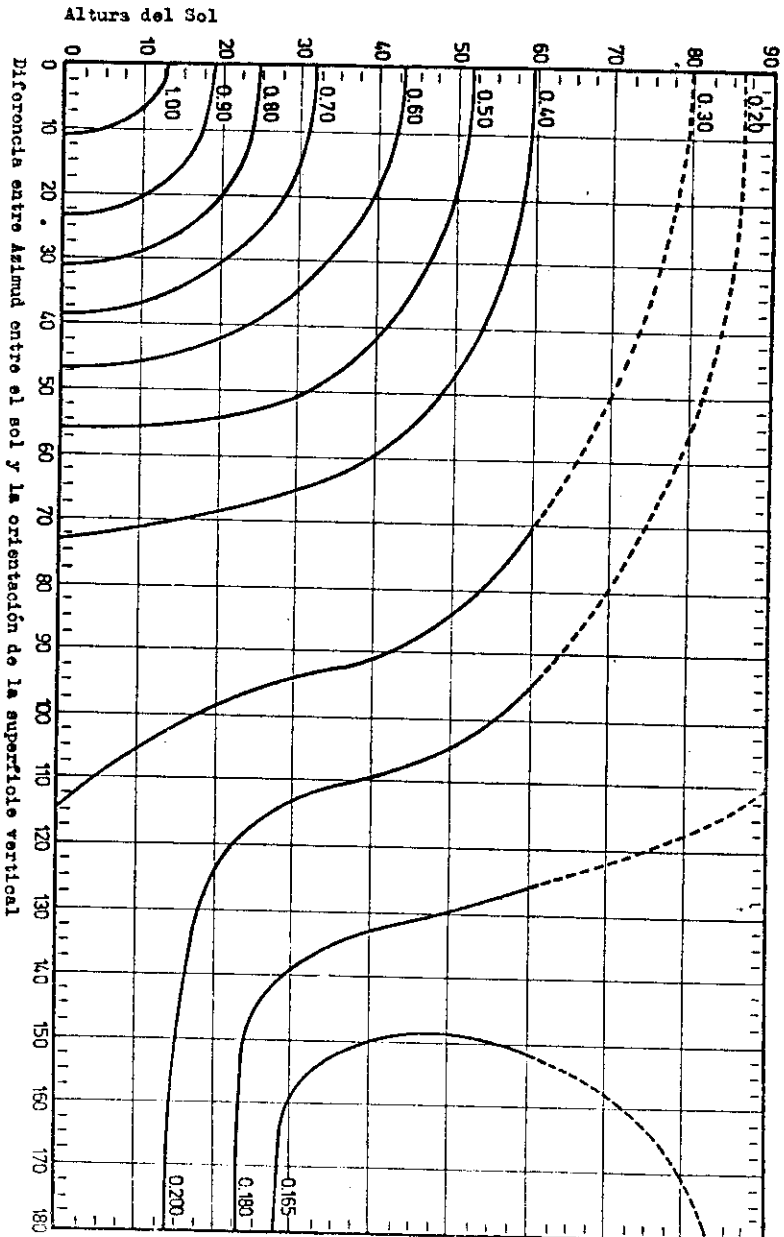

Figure 13. Diffuse radiation transmitted through vertical glazing as a proportion of the diffuse radiation incident on a horizontal surface.

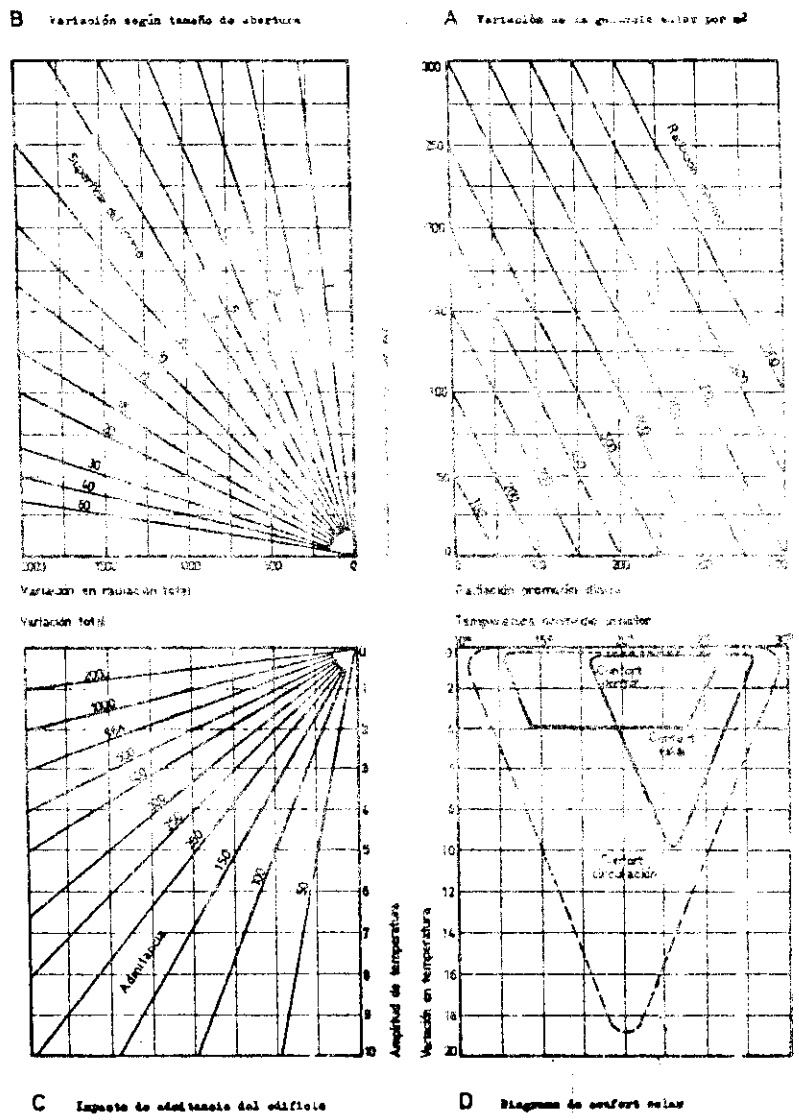

GRAFICO: Abaco para verificar confort térmico
Figure 14. Nomogram to verify thermal comfort.

Dr. M. Sharief Abdelhafiez
Faculty of Engineering, Alexandria University.
Dr. Salah Eldandouch, Dr. Mahmoud Abdelsalam
Faculty of Engineering and Technology,
Helwan University.

ABSTRACT:

The present paper concerns a solar collector for hot air generating at a considerable flow rate and temperature. It may be described as a new design solar air heater, which has a compact size and low cost absorber. This hot air generator is a radial double-pass collector with top-glass cooling by a uniformly distributed air stream at the entrance, which results in a considerable reduction of heat loss. The hot air generator has a packed bed absorber, made from metal aluminium shavings. This material is available in abundance in Europe. The performance of the hot air generator is investigated experimentally and compared with the published data of other designs. The present design gives 5-10% increased efficiency.

INTRODUCTION:

In the past few decades, the solar air heaters have found a wide range of application, namely, space heating, crop drying and industrial dehumidification and have succeeded in most of these applications. The earliest practical use of solar air heaters was for space heating (1). At the present time there are more than 5,000 houses heated by the solar energy air heater technique (2).

Also, the use of solar energy in the field of drying becomes very attractive, and in 1968 alone, Australia exported over 72,000 ton of sun-dried food worth over $27 million (3).

The majority of air heaters used in these applications are conventional hot-box types of adequate size (4,5). The earliest modification of the conventional air heater was done by Lof (6), and was an overlapped glass plate. The feasibility of matrix solar air heater was studied too (7). Both types were recently analysed by Seluck (8,9). Bevil and Brandt (10) have done experimental work on a specularly reflecting, finned-plate air heater (11-14).

The effect of selective surfaces varying heat transfer coefficient (15-16) and the merit of a stagnant air gap between the absorber plate and the cover glazing, have also been investigated (17). Several other designs of solar air heaters have been postulated, constructed and tested over the last years (4,5).

The study of the abovementioned types of solar heaters, show that they may be described as modifications or improvements in heater performance of conventional type. This development while producing the sought for improvements in heater performance, at the same time adds to the cost of the unit. Moreover, the use of special material such as high selectivity black coating, selective non-reflective glass, matrix, overlapped or honeycomb glazing, in the solar air heaters would raise the cost of it to unacceptable levels. From our point of view, the solar devices must be fabricated from materials that are readily available locally. Hence, the improvement in air heater performance must also be sought in other less expensive directions.

Also, the analysis of solar collectors heat balance shows that the rate of heat loss from the top glass cover plays an important part in the collector performance evaluation. This loss amounts to more than 25% of the total input solar radiation (18), and depends on the temperature difference between the glass cover temperature and ambient one.

The author of (18) tries to estimate the reduction of heat loss corresponding to one degree reduction of top glass cover temperature. He

found that with cover temperature 38°C and insolation 630 w/m^2, the expected reduction is 20 w/m^2 for one degree reduction which represents a saving of about 3.17%. This saving, of course, has no meaning unless the medium to be heated is used to cause the reduction in cover glass temperature. These considerations led to the present investigation.

HOT AIR GENERATOR DETAILS:

Some considerations are taken at the design and construction of the hot air generator in order to minimise the troubles existing in the known air heaters. These considerations may be summarised as follows:-

1. The circular shape is chosen for the hot air generator, to avoid the problems associated with the rectangular shape, mainly the non-uniform distribution of the air over the absorber plate. That creates a dead zone, and results in incomplete utilisation of absorber plate leading to a remarkable reduction of efficiency.

2. The air entrance of hot gas generator is made in the centre of the top glass cover to secure the uniform distribution of air to make cooling of the top glass cover to minimise the losses from it which usually amounts to about 25% in conventional rectangular air heaters.

3. The hot air generator absorber consists of a rectangular cross-sectional ring made from shavings of iron and a central iron disc. The absorber cost is cheap and simple in design and construction if compared with the well known absorbers of other constructions. In the frame of these considerations, the hot air generator is designed and constructed as shown in Fig. (1). It consists of a 800mm - 1mm thickness iron disc surrounded by 130 x 100mm rectangular cross-sectional ring of iron shavings. They both represent the solar device absorber, which is coated with black paint. The absorber is covered with a double glass plate. The upper has 1080mm diameter and 3mm thickness. The lower glass plate is 790mm diameter and the same thickness. The

front glass cover contains the air entrance hole at centre which was supplied by air filter (150mm diameter), and is fixed by a rubber ring into a wooden frame. The absorber plate and the glass covers are mounted into a cylindrical metallic vessel having a bottom hole of 150mm, operating as the hot air exit. This vessel is concentric with another metallic vessel representing the outer frame of the hot air generator. The space between the two cylindrical vessels is filled with insulation. The hot air generator is fitted at the bottom with a low power radial blade blower. The hot air generator is fixed to a frame which allows the required inclination angle.

Figure (2) gives two photographs of the apparatus located horizontally (a) and at the optimum angle of inclination (b).

INSTRUMENTATION AND TESTING:

The apparatus is provided with $0.1^{o}C$ mercury thermometer to measure the inlet and exit temperatures of air. The air-flow velocity was determined by standard calibrated pitot-tube. The total incident solar radiation on horizontal surface was evaluated by a portable type solarimeter, calibrated in the organisation of meteorology at Kobry-el-kobba, Cairo. Ten calibrated cu-co thermocouples were attached at suitable points on the glass cover and absorber to measure surface temperatures. All thermocouples were connected to a potentiometer through a multi-point over-change switch.

The effective area of the hot air generator is $0.82m^{2}$. It was oriented N-S, and was tested with 0^{o} angle of tilt (local latitude 30^{o}). The air flow rate was adjusted by air valve at the blower outlet. The hot air generator was tested in June 1981.

RESULTS AND DISCUSSIONS:

The hot air generator performance is given by Fig.3, which shows the variation of air temperature at heater exit, ambient temperature, heater efficiency and insolation received by the heater in horizontal position versus the day time. These curves represent the average values of the given parameters for a one-week test (15.6 - 21.6.1981) of the apparatus.

The performance curves are approximately similar around the noon time. The efficiency curves show values up to 0.78 for the maximum efficiency, which is higher with 5-8% of the efficiency of convential type air heaters.

REFERENCES:

1. Lof, G.O.G. Solar Energy Utilisation for house heating. Office of the Publication Board, PB 25375, May, 154 P. 1946.
2. Double Exposure Solar Air Heater. M.Sc. Cairo University 1965.
3. Lawand, T.A. The Potential of Solar Agricultural Driers in Developing Areas. UNIDO Conference Vienna, Austria, 14-18 February, 1977.
4. Close, D.J. Solar Air Heaters for Low and Moderate Temperature Application. Solar Energy 7, (3), 1963.
5. Whiller, A. Performance of Black Painted Solar Air Heaters of Conventional Design. Solar Energy, 8 (1), 1964.
6. Lof, G.O.G. Solar Energy Collectors of Overlapped Glass Plate Type. Proceeding Space Heating with Solar Energy, M.I.T. pp. 72-86, 1950.
7. Chiou, J.P. et al. A Slit and Expanded Aluminium Foil Matrix Solar Collector, Solar Energy, Vol. 9, No. 2, pp. 73-80, 1965.
8. Sayigh, A.A.M. Solar Energy Engineering. Academic Press 1977. Chapter 8.
9. Selcuk, M.K. Thermal and Economic Analysis of the overlapped Glass Plate Solar Air Heater, Solar Energy 13, No. 2, 165-191, 1971.
10. Bevill, V.D. and Brandt, H. A Solar Energy Collector for Heating Air. Solar Energy 12 (1) 1968.

11. Duffie, J.A. New Materials in Solar Energy Utilisation, Solar Energy 6, (3), 1962.

12. Hottel, H.C. and Unger, T.A. The Properties of a Copper Oxide Aluminium Selective Black Surface Absorber of Solar Energy. Solar Energy 3 (10), 1959.

13. Edwards, E.K., Gier, J.T., Nelson, K.E. and Roddick, R.D. Spectral and Directional Thermal Radiation Characteristics of Selective Surfaces for Solar Collector. Proc. of the U.N. Conference on New Sources of Energy, Rome, 1961.

14. Hollands, K.G.T. Direction Selectivity, Emittance and Absorption of three Corrugated Specular Surfaces, Solar Energy 7, (3), 1963.

15. O'Toole, J.L. and Silveston, P.L. Correlation of Convective Heat Transfer in Confined Horizontal Layers, Chem.Eng.Prog. Symp.Ser.57 (32), 81-86, 1961.

16. Hollands, K.G.T. Conventional Heat Transport between Rigid Horizontal Boundaries after Instability, Phys. Fluids 8, 389-390, 1965.

17. Molhotra, A., Garg, M.P. and Rani, U. Minimizing Convective Heat Losses in Flat Plate Solar Collectors. Solar Energy Vol. 25, pp.521-526, 1980.

18. Satcunanthan, S. and Deonarihe, S. A Two-Pass Solar Air Heater. Solar Energy, Vol.15, pp.41-49, 1973.

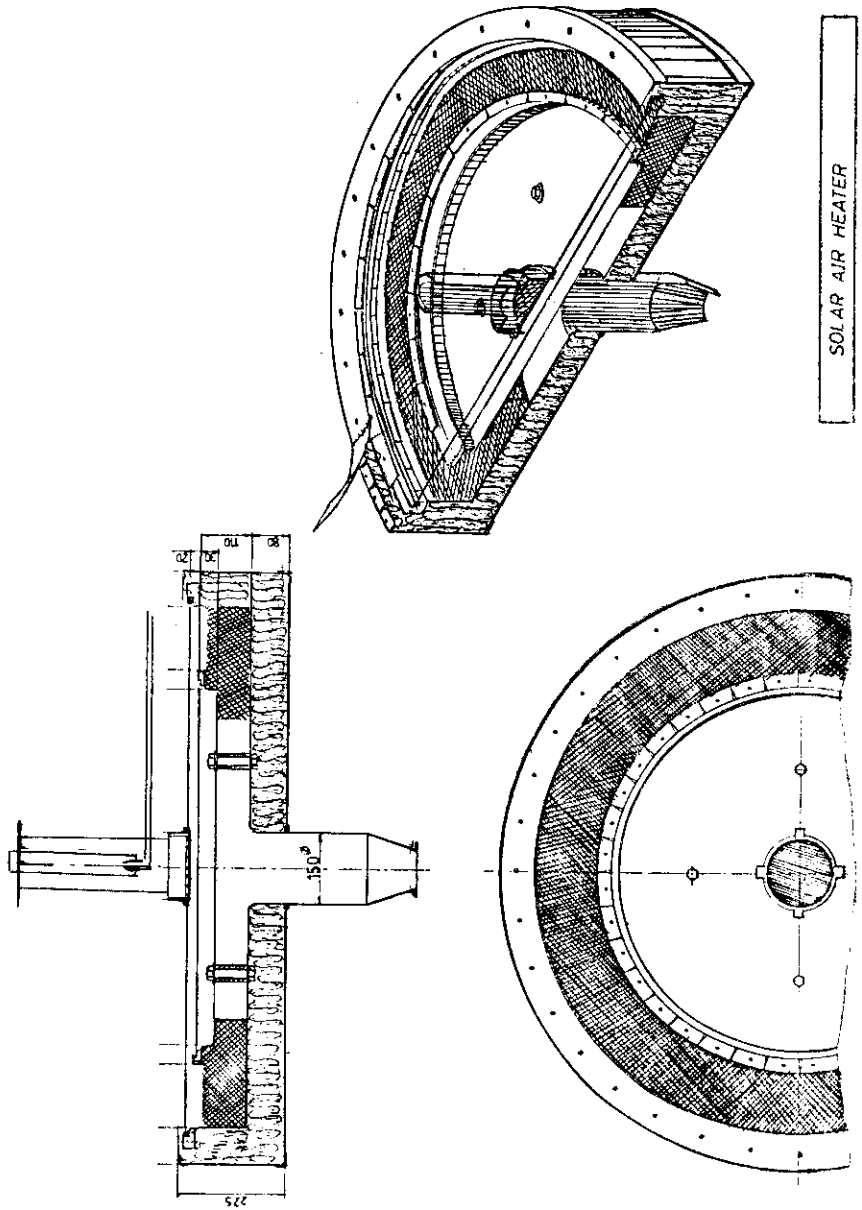

Fig. (I) Construction details of the radial double-pass circular collector

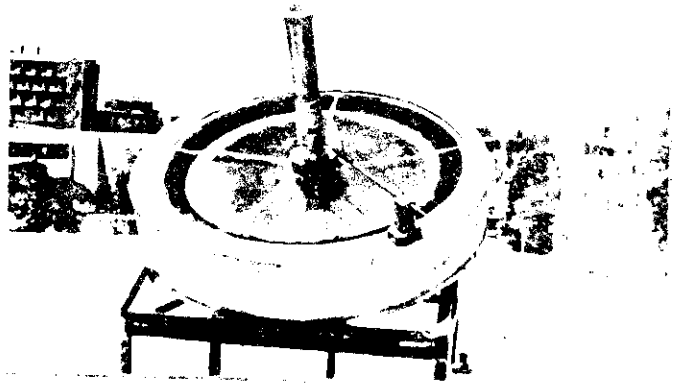

Fig. (2-b) The hot air generator at optimum angle of inclination

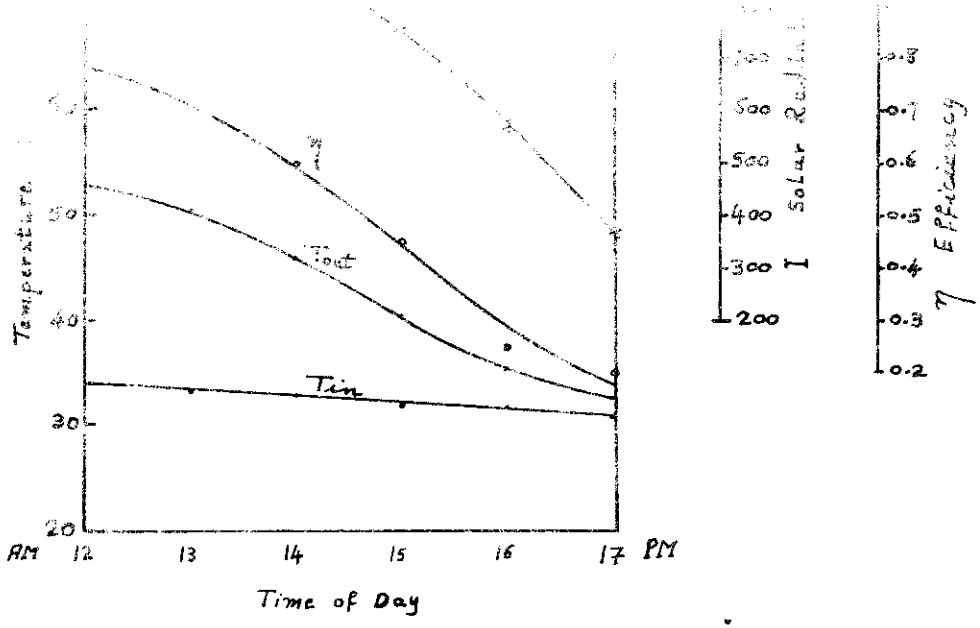

Fig.(3) Variation of Air Temperatures at Heater inlet and exit, Heater Efficiency and Insolation received by the Heater in Horizontal Position versus the Day Time.

THE PERFORMANCE OF AN IMPROVED HIGH TEMPERATURE THERMOELECTRIC MATERIAL

D M Rowe
Department of Physics, Electronics
and Electrical Engineering
UWIST
King Edward VII Avenue
CARDIFF

ABSTRACT

An unconventional method of generating electricity is by the thermoelectric effect. Thermocouples made from semiconductor alloys are employed in a range of specialised applications where combinations of their desirable properties outweigh their relatively high cost and low conversion efficiency - typically less than 10%. Silicon germanium alloy is an established high temperature thermoelectric material and thermocouples fabricated from it are used in thermoelectric generators which provide the onboard power to the Voyager spacecrafts. In this paper the results of the first measurements of the thermoelectric properties of small grained heavily doped silicon germanium alloys are reported. It is concluded that in these materials the lattice thermal conductivity is substantially less than comparable "single crystal" material. This manifests itself in a significant improvement of the materials' figure of merit and hence in its thermoelectric conversion efficiency.

INTRODUCTION

Spacecraft engaged on missions into intense radiative environments such as those encountered in the vicinity of the Sun or Mercury; or on distant missions to the outer planets, are for obvious reasons unable to derive electrical power from solar panels. In these situations, thermoelectric generators are used to provide onboard electrical power to the craft by converting the heat energy derived from nuclear radiation into electrical energy. Silicon germanium alloys are established high temperature thermoelectric materials and have successfully been employed on the Voyager spacecrafts to Jupiter and Saturn. Recently, however, the dominance of silicon germanium has been threatened by the development of a new family of thermoelectric materials - the selenides - and both techniques are competing for selection by NASA/JPL for use on the Galileo (Jupiter orbiter) planetary mission scheduled for August 1985* (1,2,3).

*Since presenting the paper the author has learned that Si-Ge technology has been chosen for use in the Galileo mission.

The basic equations which govern the conversion of heat energy into electrical energy by the thermoelectric effect are well known and it is suffice to state here that once the operating temperature conditions of the thermoelectric device have been decided, the conversion efficiency is dependent upon the so-called figure of merit Z of the materials from which the thermocouples are fabricated. $Z = \frac{\alpha^2\sigma}{K}$ where α is the Seebeck coefficient, σ the electrical conductivity and K, the total thermal conductivity is the sum of the lattice component K_L and the electronic component K_e. Evidently any improvement in Z would result in a corresponding increase in conversion efficiency and an accompanying saving in both weight and expensive nuclear fuel.

One possible method of improving the Z value for silicon germanium alloy, is to reduce the thermal conductivity without reducing the electrical properties by limiting the phonon mean free path through the use of grain-boundary scattering. In practice this may be achieved through the use of very small grain size "compacts" rather than the "single crystal" or the relatively large grain size materials currently employed, (4).

In a paper presented at a previous symposium, the results of calculations of the potential improvement in the thermoelectric figure of merit which would accompany the use of small grain size material was reported and the consequent predicted improvement in the thermoelectric conversion efficiency discussed, (5). In this paper the results of the first measurements of all three parameters occurring in the figure of merit for small grain size silicon germanium alloys are reported. The thermal conductivity is derived from the measured thermal diffusivity data using published specific heat values and the lattice thermal conductivity obtained by subtracting the electronic component. The results confirm that the lattice thermal conductivity decreases with a reduction in grain size while within experimental error (<5%) the electrical properties do not change with grain size. The thermoelectric conversion efficiency of small grain size material is substantially improved compared to equivalent "single crystal" or large grain material and exhibits a figure of merit which is significantly higher than values quoted in the literature for the selenides,(6,7).

EXPERIMENTAL METHOD:

The material used in the investigation was cut from a single crystal ingot of homogeneous, zone levelled $Si_{63.5}$ $Ge_{36.5}$ alloy, doped n-type with phosphorus to about $1 \times 10^{26} m^{-3}$. A disc shaped sample suitable for thermal diffusivity measurement by the laser flash technique (6mm diameter x 1mm thick) and an ingot shaped sample suitable for electrical conductivity and Seebeck coefficient measurement (2mm x 2mm x 8mm) was cut from a slice using an ultrasonic cutter. The remainder of the slice was crushed, sieved, and compacts 10mm in diameter and $\sim$ 3mm thick were prepared from starting powders possessing a grain size L in the range $10 < L < 25\,\mu m$, $5 < L < 10\,\mu m$ and $< 5\,\mu m$ using a previously described pressing procedure. The densities of the compacts were determined by the method of hydrostatic weighing. The error in density determination was less than 0.5% and the density of the three compacts were better than 98% that of the parent ingot,(8).

Electrical conductivity and Seebeck coefficient measurements were carried out in a furnace evacuated to 10^{-5} torr. The samples were instrumented with NiCr/NiAl thermocouples (44SWG) wedged with graphite into two fine holes drilled along one side of the sample. The sample was held in a holder by spring loading between a ceramic heater and a molybdenum heat sink. Current leads to the sample for electrical resistivity measurements were made at the ends of the sample using platinium wire and the alumel

thermocouple wires used to measure resistance voltage. Seebeck coefficient values obtained relative to alumel were converted to absolute values from a calibration of alumel against copper. The transport properties of these materials can change during the period of measurement due to precipitation of dopant. In order to minimise such effects a dip stick sample holder arrangement was employed which allowed the sample to be annealed at 1000°C for 1-2 hours before its insertion into the quartz vacuum furnace. Although the arrangement enabled the sample's temperature environment to be altered rapidly, the samples required 10-20 mins to reach the necessary thermal equilibrium for the commencement of measurement. The experimental error in resistivity measurement was less than $\pm$ 1%. Thermal diffusivity measurements were made on disc shaped samples using a system based upon the laser flash method. Measurements on ARMCO iron indicated that the accuracy of the system was better than $\pm$ 2% at room temperature. Reproductibility of measurements was about the same,(9,10).

RESULTS:

The variations of electrical resistivity, Seebeck coefficient, and thermal resistivity over the temperature range 300K to 1100K are displayed in figures 1 and 2. To all intents the electrical resistivity values do not change with reduction in grain size and any change in the Seebeck coefficient, falls within the experimental error of 5%. The thermal diffusivity decreases with reduction in grain size and in the compact with a grain size of $< 5\,\mu m$ is reduced by $\sim$ 28% compared to the single crystal value. Thermal conductivity is obtained from the measured thermal diffusivity using the relationship $K = C_p a$ where C_p is the specific heat per unit volume at constant pressure and a value of C_p appropriate to the alloy investigated is taken from the literature. The electronic component is given by $K_e = \mathcal{L} (\frac{k}{e})^2 \sigma$. $\mathcal{L}$ depends upon the scattering mechanism of the charge carriers and for the materials under investigation is about 2.9. The lattice thermal diffusivity obtained after subtracts K_e from K is displayed as a function of temperature in figure 3. In figure 4 the figure of merit of the improved silicon germanium alloy is compared with values taken from the literature for 2N and 3N lead telluride and n-type gadolinium selenide,(10,11,12).

DISCUSSION AND CONCLUSION:

The results of measurement of all three transport properties which occur in the figure of merit indicate that in these fine grained materials, a reduction in lattice thermal conductivity is not accompanied by a reduction in electrical conductivity. In the compact with $L < 5\,\mu m$ the thermoelectric figure of merit at 1000K exceeds 1.4×10^{-3} compared with a value of about 1.0×10^{-3} reported for gadolinium selenide. The preparation of fine grained compacts of silicon germanium alloy is tedious but not exceptionally difficult. Providing that there are not any unforeseen thermoelement fabrication problems peculiar to fine grained materials, thermoelectric generators based upon this technology would exhibit a conversion efficiency significantly higher than that of its competitors.

ACKNOWLEDGMENTS:

The author wishes to thank Professor D.J. Harris, Head of the Department of Physics, Electronics and Electrical Engineering at UWIST for use of Departmental facilities and Dr. Robert D. Nasby of The Sandia Laboratories, Albuquerque, New Mexico, for supplying [illegible]

REFERENCES:

1. Raag, V. "Comprehensive thermoelectric properties of n- and p-type 78 a/o Si-22 a/o Ge alloy". Proceedings of Second International Conference on Thermoelectric Energy Conversion, University of Texas at Arlington, 22-24 March, pp 5-10, 1978.

2. Mitchell, W.C. et al, "Transport Theory of 3M High Performance Thermoelectric Materials" Proceedings of 11th IECEC, pp 1539-1545, 1976.

3. Hinderman, J.D. et al, "Selenide Thermoelectric Converter Technology", Proceedings of 13th IECEC, pp 1938-1945, 1978.

4. Goldsmid, H.J. and Penn, A.W. "Boundary Scattering of Phonons in Solid Solutions", Solid State Electronics, 11, pp 523-524, 1968.

5. Rowe, D.M. "Thermoelectricity, - Its Potential as an alternative source of Electricity", Participants contribution to the First International Symposium on Non-Conventional Energy, Paper No. SMR/60-p7, 27 August - 21 September, 1979.

6. Dismukes, J.P. et al, "Thermal and Electrical Properties of Heavily Doped Ge-Si Alloys up to 1300K", J. Appl. Phys. pp.2899-2907, 1964.

7. Bass, J.C. and Elsner, N.B. "Segmented Selenide Thermoelectric Generator", Proceedings of Third International Conference on Thermoelectric Energy Conversion, University of Arlington at Texas, March 12-14, pp 8-13, 1980.

8. Rowe, D.M. "Vacuum Hot-Pressing of Germanium and Silicon Germanium Alloys", Proceedings of the Fourth International Round Table on Sintering, Dubrovnik, Yugoslavia, pp. 307-311, 1979 (1980).

9. Savvides, N. and Rowe, D.M. "Precipitation of Phosphorus from Solid Solutions of Si-Ge alloys and its effect on thermoelectric transport properties", J. Phys D. Appl. Phys. 14, pp 723-732, 1981.

10. Rowe, D.M. and Shukla, V.S. "The Effect of Phonon-Grain Boundary Scattering on the Lattice Thermal Conductivity and Conversion Efficiency of Heavily-doped, Hot-Pressed Silicon German Alloy". Accepted for publication in J. Appl. Phys.

11. Meddins, H.R. and Parrott, J.E. "The Thermal and Thermoelectric Properties of Sintered Germanium-Silicon Alloys". J. Phys. C. Solid State Physics, 9, pp 1263-1276, 1976.

12. Rowe, D.M. and Bhandari, C.M. "Modern Thermoelectricity", Chapter 4, to be published by Holt-Saunders, 1981.

Legends to Figures:

Figure 1. Electrical Resistivity p and Seebeck Coefficient a of $Si_{63.5}$ $Ge_{36.5}$ alloy as a function of temperature.

Figure 2. Thermal Resistivity of $Si_{63.5}$ $Ge_{36.5}$ Alloy as a function of temperature for different grain sizes.

Figure 3. Lattice thermal conductivity of $Si_{63.5}$ $Ge_{36.5}$ Alloy as a function of temperature for different grain sizes.

Figure 4. The figure of merit of improved $Si_{63.5}$ $Ge_{36.5}$ alloy compared with values of its competitors.

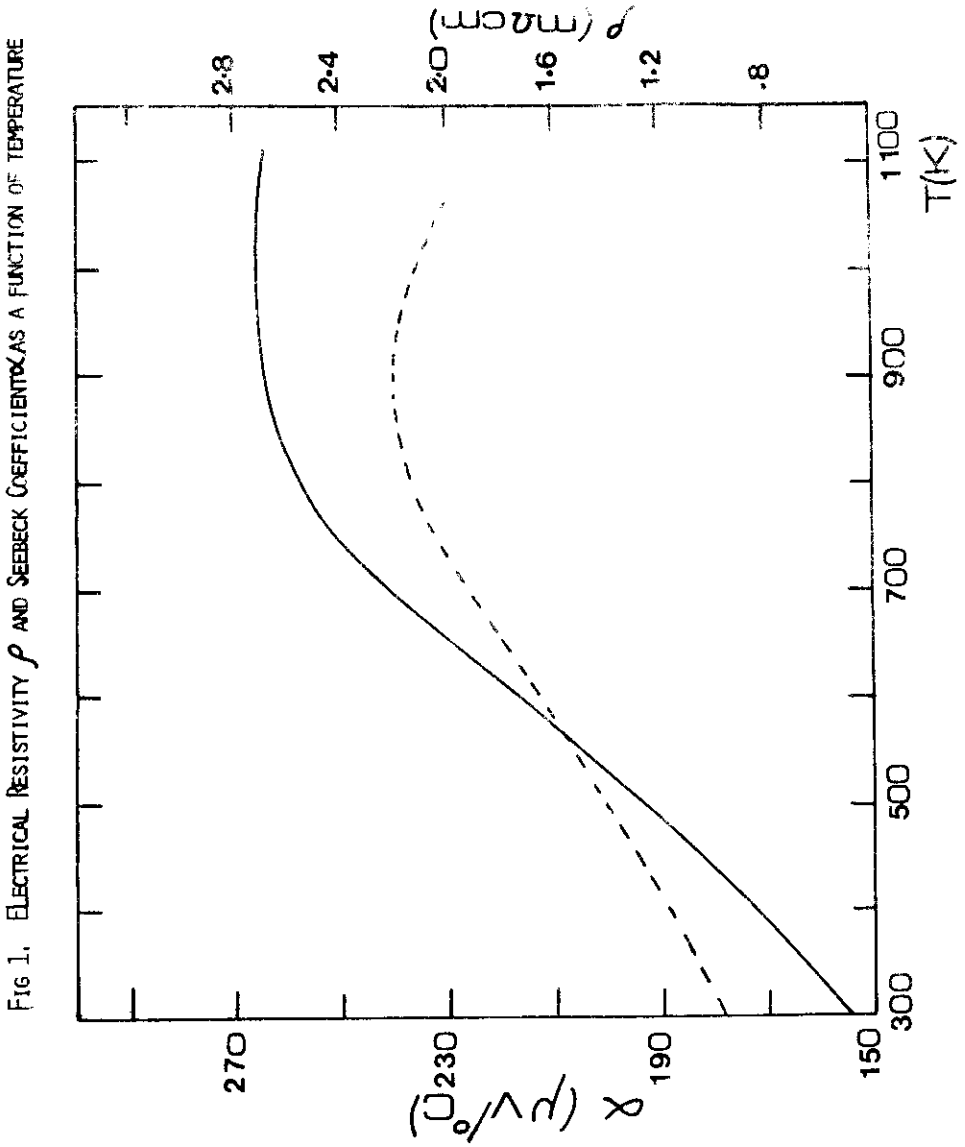

FIG 1. ELECTRICAL RESISTIVITY ρ AND SEEBECK COEFFICIENT α AS A FUNCTION OF TEMPERATURE

FIG 2. THERMAL RESISTIVITY OF $Si_{63.5}Ge_{36.5}$ ALLOY AS A FUNCTION OF TEMPERATURE FOR DIFFERENT GRAIN SIZES.

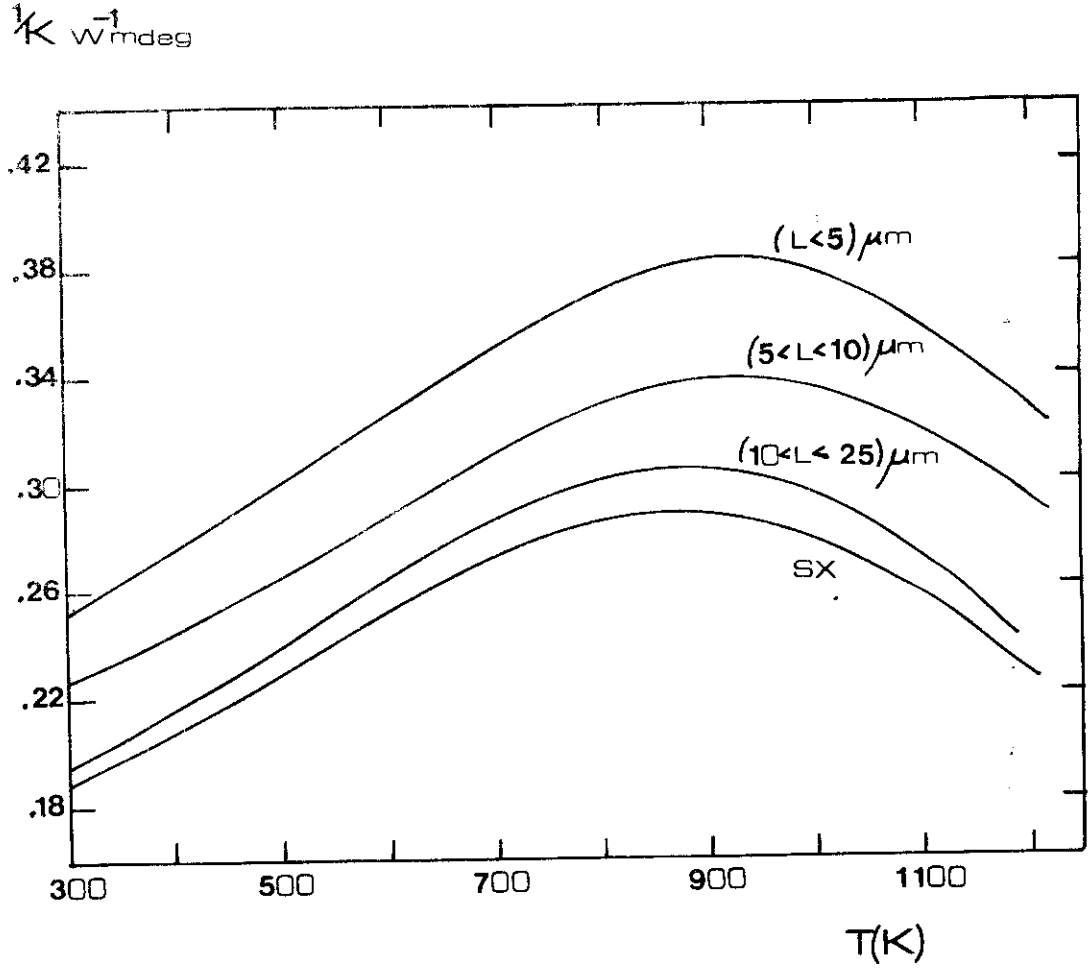

FIG 3. LATTICE THERMAL CONDUCTIVITY OF $Si_{63.5}Ge_{36.5}$ ALLOY AS A FUNCTION OF TEMPERATURE FOR DIFFERENT GRAIN SIZES.

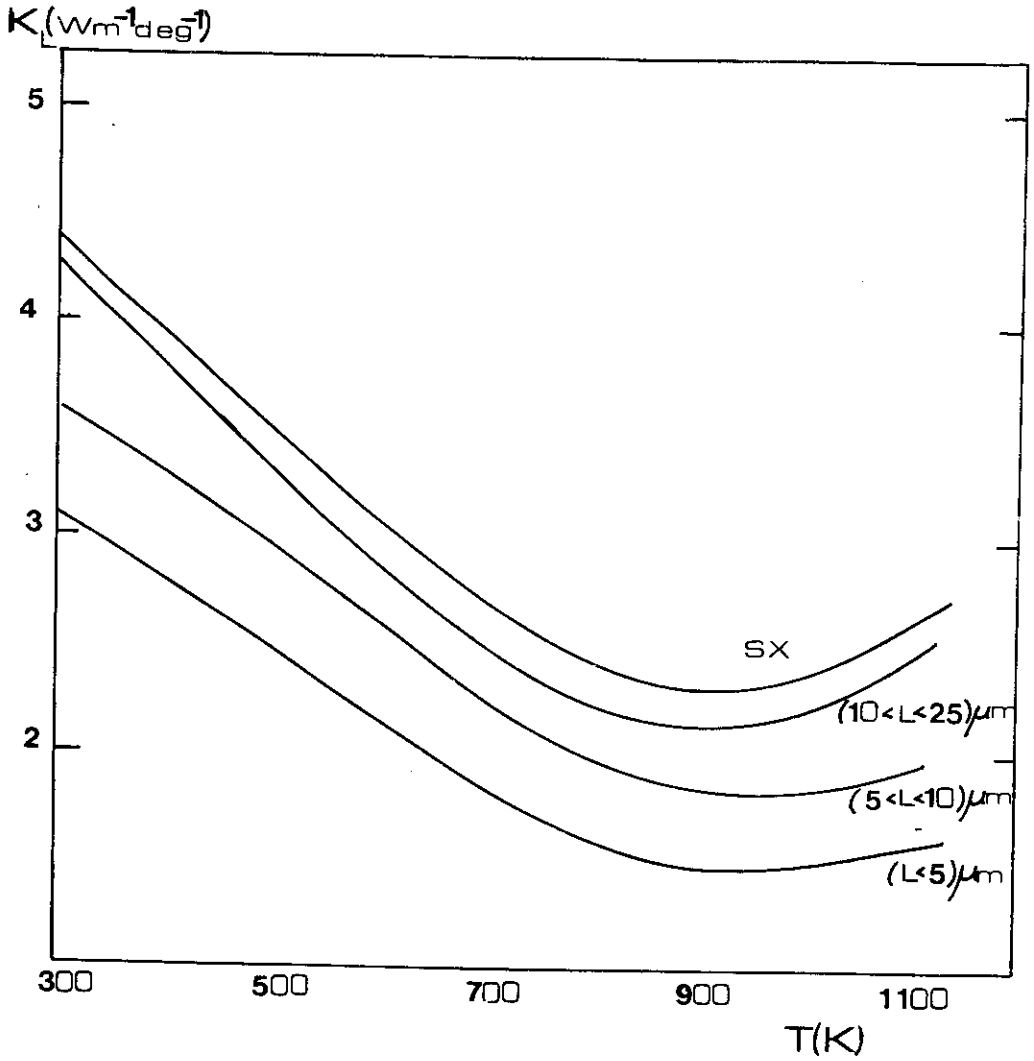

FIG. 4 THE FIGURE OF MERIT OF IMPROVED $Si_{63.5}Ge_{36.5}$ ALLOY COMPARED WITH VALUES OF ITS COMPETITORS.

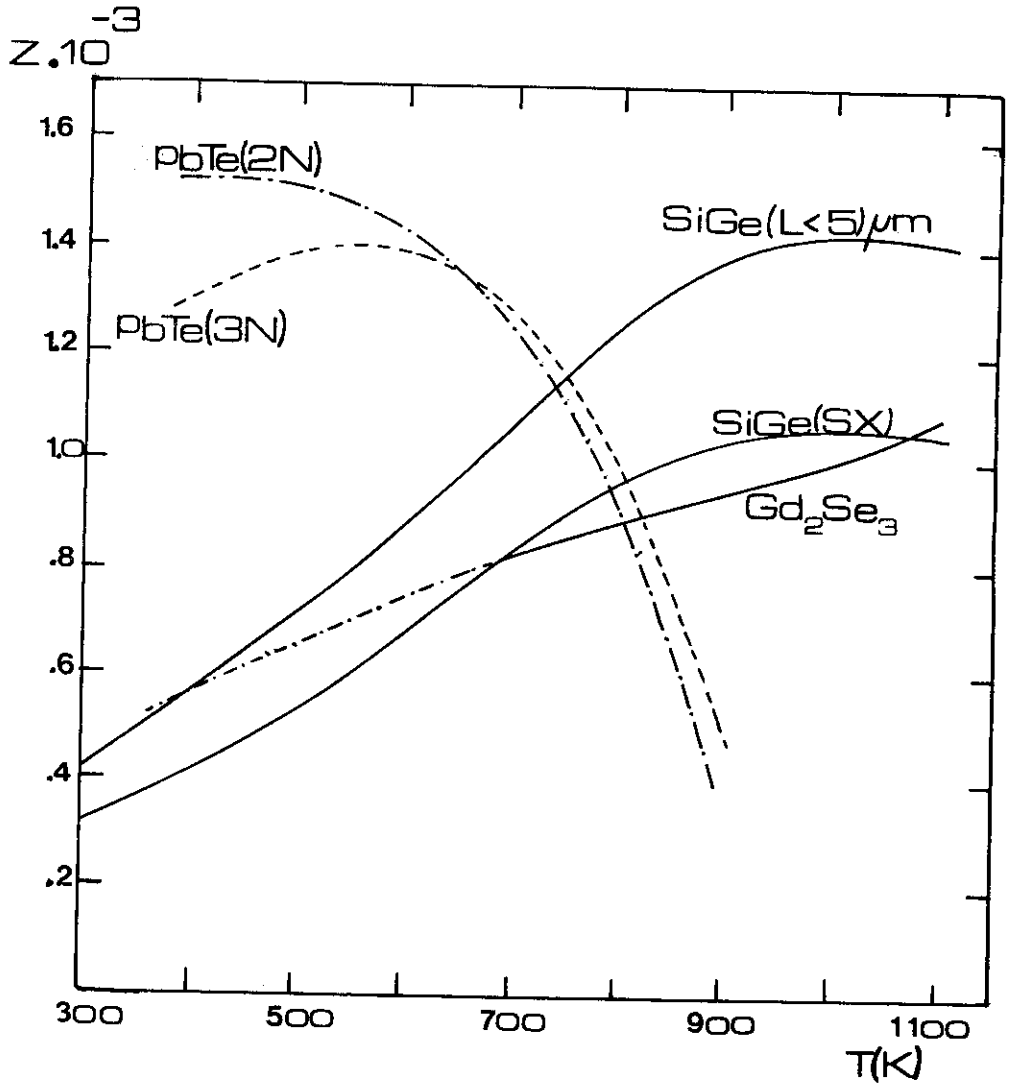

ANALYSIS AND DESIGN OF A DIFFERENTIAL SUNSHINE RECORDER

A. Ayensu

Department of Physics
University of Cape Coast
Cape Coast, Ghana

ABSTRACT

A differential sunshine recorder for measuring solar insolation has been designed and constructed from locally available materials. The device could measure and record the absolute value of the intensity of the sun during any period of the day. The maximum solar intensity measured for the locality (Cape Coast) is 1045 Wm^{-2} and the minimum intensity measured is 547 Wm^{-2}. The variation in solar intensity is due to the diurnal weather changes.

The theory of the diffential sunshine recorder was based on Stefan's radiation law and the mathematical relation for the intensity calculations was derived as

$$I = 16\sigma T_B^3 (T_1 - T_2)$$

where the room temperature $T_B \approx$ 301K, $(T_1 - T_2)$ K is the differential temperature between a shaded and unshaded sphere and σ is Stefan's constant. The equation makes it possible to use a thermocouple as the sensing element. A direct current amplifier with a gain of 100 was used to record the thermocouple output.

From the data obtained, the atmospheric absorption factor was calculated as 25% and the average daily energy received was 30 MJm^{-2}.

INTRODUCTION

The design of any solar system (e.g. a heating system) requires the total value of insolation on the collectors. Unfortunately, most meteorological stations in Ghana have the Campbell-stockes recorder which comprises a glass sphere with a card recording element mounted at its focal surface. The sphere focuses the sun's rays from any direction onto the card and when the intensity exceeds 150 Wm^{-2} a burn is produced. This device only gives a sun or no sun record; it cannot record the intensity variations during the day.

However with the recent construction of dams for irrigation purposes where quantitative analysis of the rate of evaporation is necessary as much more detailed information on solar intensity is needed. Recently, Sayigh[1] has given a compendium of the solar measuring instruments and has remarked on the importance of proper calibration. Since these instruments are not readily available in Ghana, it was decided to design and construct a simple differential sunshine recorder, that will record and measure direct solar radiation but would ignore 'sky' radiation (or diffuse radiation) scattered by the air molecules, water droplets in clouds, aerosols (dust, smoke, pollen) and gases present in the atmosphere (O_3, O_2, CO_2, H_2O).

THEORY OF DIFFERENTIAL SUNSHINE RECORDER

The theory of the differential sunshine recorder is based on Stefan's radiation law. To apply the law to our case, consider a small blackened sphere in a transparent enclosure whose walls are at an absolute temperature T_B. The sphere reaches thermal equilibrium at an absolute temperature of T_1 when its re-radiation rate balances the radiation per second falling on it; that is

$$4\pi r^2 \sigma T_1^4 = 4\pi r^2 \sigma T_B^4 + 4\pi r^2 D + \pi r^2 I \quad \ldots\ldots\ldots \quad (1)$$

where r is the radius of the sphere, D is the sky radiation (in Wm^{-2}) averaged over 4π steradians, I is the direct solar radiation (in Wm^{-2}) and is the Stefan's constant. Eqn. 1 ignores any conduction or convection losses from the small sphere.

If the sphere was shielded from the direct solar radiation then the eqn.(1) would be

$$4\pi r^2 \sigma T_2^4 = 4\pi r^2 \sigma T_B^4 + 4\pi r^2 D \quad \ldots\ldots\ldots\ldots\ldots \quad (2)$$

That is, the sphere would have an equilibrium temperature of T_2 which is less then T_1.

Equations (1) and (2) can be re-arranged into:

$$T_1^4 - T_B^4 = \frac{D}{\sigma} + I/4\sigma \quad \ldots\ldots\ldots\ldots\ldots \quad (3)$$

and

$$T_2^4 - T_B^4 = D/\sigma \quad \ldots\ldots\ldots\ldots\ldots \quad (4)$$

Approximating $T_1 \approx T_B$ and $T_2 \approx T_B$ for a minimum value of I detectable on the recorder,

$$T_1^4 - T_B^4 = (T_1 - T_B)\, 4T_B^3 \quad \ldots\ldots\ldots\ldots\ldots \quad (5)$$

and $$T_2^4 - T_B^4 = (T_2 - T_B)\, 4T_B^3 \quad \ldots\ldots\ldots\ldots\ldots \quad (6)$$

This gives $$(T_1 - T_B)\, 4T_B^3 = \frac{D}{\sigma} + I/4\sigma \quad \ldots\ldots\ldots\ldots\ldots \quad (7)$$

and $$(T_2 - T_B)\, 4T_B^3 = \frac{D}{\sigma} \quad \ldots\ldots\ldots\ldots\ldots \quad (8)$$

Subtracting eqn. (8) from eqn. (7) we obtain

$$(T_1 - T_2) = \frac{I}{16\sigma T_B^3} \quad \ldots\ldots\ldots\ldots\ldots \quad (9)$$

which is the differential result between a shaded and an unshaded sphere. Eqn. (9) makes it possible to use a thermocouple as the sensing element, the hot junction to be imbedded in a small sphere fully exposed and the cold junction in a sphere shaded from direct solar radiation. Since the output of a thermocouple is dependent on the the temperature difference of the junctions the output would be a direct measurement of I and by recording this output the variation of I through the day could be obtained.

CONSTRUCTION OF THE RECORDER

Two cuboids of dimensions 5 x 5 x 5 cm^3 and 2.5 x 2.5 x 2.5 cm^3 were built from sheets of perspex (PmmA). The sheets were glued together with chloroform. Two holes were bored under the small cube through which the two junctions of the thermocouple were passed. The two junctions of the thermocouple were embedded in spheres of black plasticine of 2mm diameter inside the smaller cuble such that they have exactly the same view of the sky. Thin foil of aluminium was used to line the adjacent sides of the smaller cube. The smaller box and its contents were suspended inside the larger box which also had outlets for the thermocouples.

Two holes were bored at the top and bottom of the larger box for water to flow around the hollow space surrounding the smaller box. Rubber tubings were used as inlet and outlets for the circulating water. The side view of the recorder is shown in Fig. 1. A is the totally exposed junction sphere and B is shaded at all times by aluminium foil strips as the rig rotates to follow the sun. A clock driven mechanism was constructed to rotate the recorder so that the sphere A was always directed to the solar radiation. Copper-constantan thermocouples were used as these give a fairly large output for a

given temperature difference. By using fairly thick wires (of 1mm diameter) the junctions were made self-supporting although this would mean appreciable losses down the leads.

TEST PROCEDURES AND RECORDING

The recorder was set up on a high flat roof with a clear view of the sky. The leads were connected to a student potentiometer which was shielded from sunlight. Water was passed into the inlet tube from an ordinary tap. Preliminary data for the potentiometer reading for a given temperature difference was of the order of 1mV. It was therefore decided to construct a direct current (d.c.) amplifier with a gain of 100 to increase the sensitivity of the measurement. Fig. 2 shows the circuit diagram of the d.c. amplifier with the power supply. The amplifier was stable enough that noise, leakage current and voltage drift or fluctuations in the a.c. mains were removed. The amplifier has two outputs, an internal and external which are controlled by a switch. A voltmeter was put at the internal output, while the external output was connected to a chart recorder for continuous monitoring. If X is the output metre reading and the gain is 100, then the e.m.f. in volts generated across the thermocouple junctions is X/100. The calibration graph, for the Copper-Constantan thermocouple is shown in Fig. 3. This gives the temperature difference for a given value of e.m.f. (mV).

The recorder readings were taken at an hourly interval throughout the day. Table 1 shows a typical data for 23 March 1981. Using eqn. (9) and taking $\sigma = 5.7 \times 10^{-8}$ $Wm^{-2} K^{-4}$ and $T_B = 301K$, the values of temperature difference $(T_1 - T_2)$ were converted into values of intensity measurements I. The relationship between $(T_1 - T_2)$ and I represented by eqn. (9) is shown in Fig. 4. A typical diurnal variation of total irradiance (i.e. radiant flux density incident on a surface) is shown in Fig. 5.

ANALYSIS OF RESULTS

The results discussed in this section are based on data obtained on 23 March 1981; and the analysis is applicable to the data for other days (see Appendix for the mean solar intensity data for February, March and April, 1981).

From Table 1, the maximum intensity for the day occurs between 1200-1400 hours local time and there is the usual diurnal variation of solar irradiance. These known results conform the accuracy of the

device as a suitable recorder. Theoretically, the intensity of the sun in a locality under study ought to be a constant (2). The reason is that since the junction of the thermocouple which is exposed to the solar radiation is a sphere it ought to receive $\pi r^2 S W$ at any angle of the elevation of the sun where S ($\sim 1.39 \times 10^3 Wm^{-2}$) is the energy per second per unit area normal to the sun's rays falling on the earth from the sun. Hence it is expected that all values of I on the graph should therefore be the same and equal to the solar constant S. This will be true only in the absence of atmospheric absorption. The atmosphere absorbs and scatters a great deal of the incident solar radiation. The variation of the effective thickness of the atmosphere also affects the solar insolation received. The effective thickness is greatest at dawn and at dusk.

The way in which insolation changes during the day depends in a complex way on changes in water vapour and aerosol content of the atmosphere and the distribution of the cloud. This is also true for the insolation changes during the year. Roughly, a third of the radiation received outside the atmosphere is scattered back to space, a third is absorbed and a third is transmitted to the surface[12].

The absorption factor A is defined as the ratio of the absorbed radiation to the incident radiation, i.e.

$$A = \frac{S - I_{max}}{S} \times 100\% \quad \ldots\ldots\ldots\ldots\ldots\ldots \quad (10)$$

where I_{max} is the maximum intensity received. From the data obtained, the total solar energy absorbed in the atmosphere by water vapour, cloud, dust and smoke is 25%. The flux at the surface is expected to be 25% less than it would be in a perfectly clear atmosphere.

It can be deduced from figure 5 that the diurnal variation of total irradiance is approximately sinusoidal. The flux of total solar radiation I_t at t hours after sunrise can therefore be expressed as

$$I_t \simeq I_{max} \sin (\pi t/N) \ldots\ldots\ldots\ldots\ldots \quad (11)$$

where I_{max} is the maximum irradiance at solar noon and N is the day length in hours. Eqn. 11 can be integrated to give an approximate relation between maximum irradiance and the daily integral of irradiance, conveniently referred to as daily insolation. The integral is

$$\int_0^N I_t \, dt \simeq 2 I_{max} \int_0^{N/2} \sin (\pi t/N) \, dt$$

$$\simeq (2N/\pi) I_{max} \ldots\ldots\ldots\ldots\ldots \quad (12)$$

For Cape Coast, $I_{max} = 1075 \ Wm^{-2}$, N = 12 hours = 43.2×10^3S, so the approximate insolation (i.e. the total direct solar energy received) is 30 MJm^{-2}.

The solar intensity was found to be greatest at 13 hours local time when the effective thickness of the atmosphere is expected to be least. This may be due to the build up of dust and water vapour in the atmosphere during the day as a result of convection currents. There is an appreciable lag between the increase of intensity after dawn and the rise of temperature of the earth's surface so that the dust raising convectional currents to not set in strongly until after mid-day[3].

The maximum and minimum intensity for specific days in the months under consideration differ from one month to another by 5-6%. Even within a particular month, the maximum and minimum intensities for different days varies by ± 2%. The mean intensity for the months studied is $762.04 Wm^{-2}$.

CONCLUSIONS

1. A differential sunshine recorder has been constructed from locally available materials, and the device could measure and record the intensity of the sun during any period of the day.

2. The maximum solar intensity of $1075 Wm^{-2}$ and minimum intensity of $550 Wm^{-2}$ were recorded. The intensity variations depend on the diurnal weather changes.

3. The atmospheric absorption factor in the locality is 25% and the total energy received in a day is $30 MJm^{-2}$.

REFERENCES

1. A.A.M. Sayigh, Solar Energy Engineering, Academic Press, New York 1977; Lectures at 2nd International Symposium on Non-Conventional Energy, ICTP, Trieste, Italy, 14 July–6 August 1981.

2. A.B. Meinel, and M.B. Meinel, Applied Solar Enegy – An Introduction, Addison Wesley Series in Physics, New York, 1976.

3. J.L. Monteih, Principles of Environmental Physics, Edward Arnold (Publishers) Ltd., London, 1975.

4. H.C. Hottel, Residential Users of Solar Energy in 'Proceedings of World Symposium on Applied Solar Energy', Pheonix, Arizona 1955.

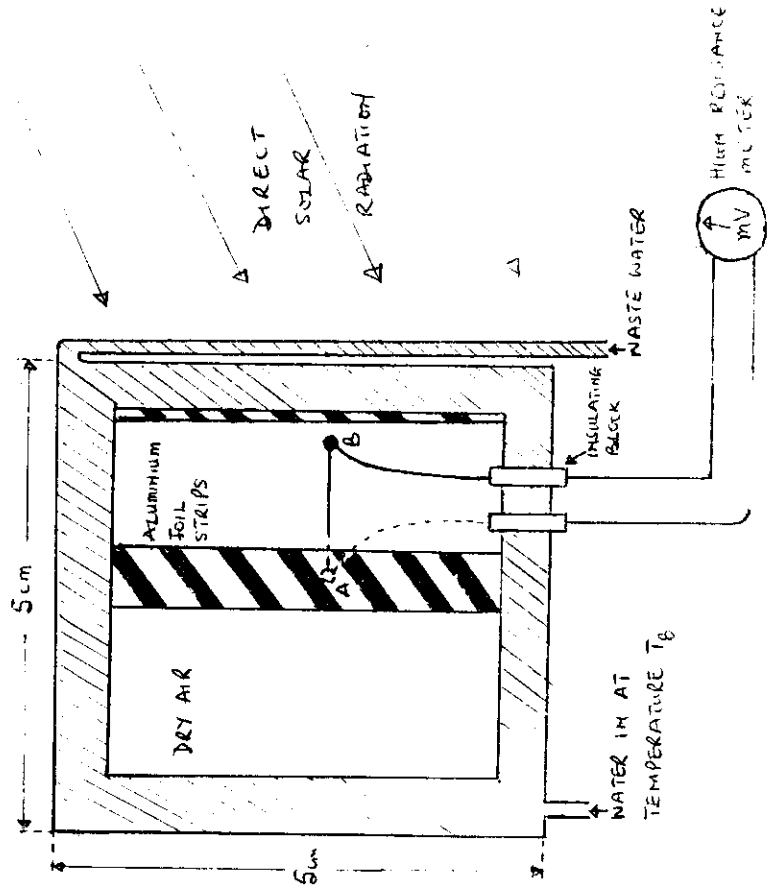

Figure 1. Side view of the differential sunshine recorder (not to scale)

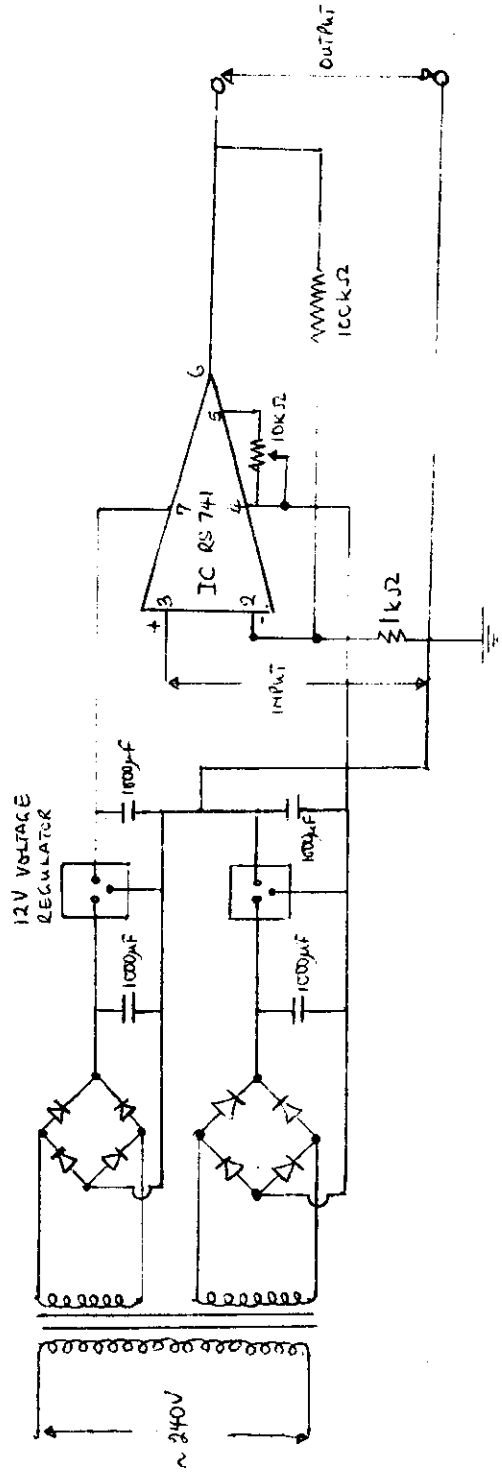

Figure 2. Circuit diagram of a direct current amplifier with a gain of 100.

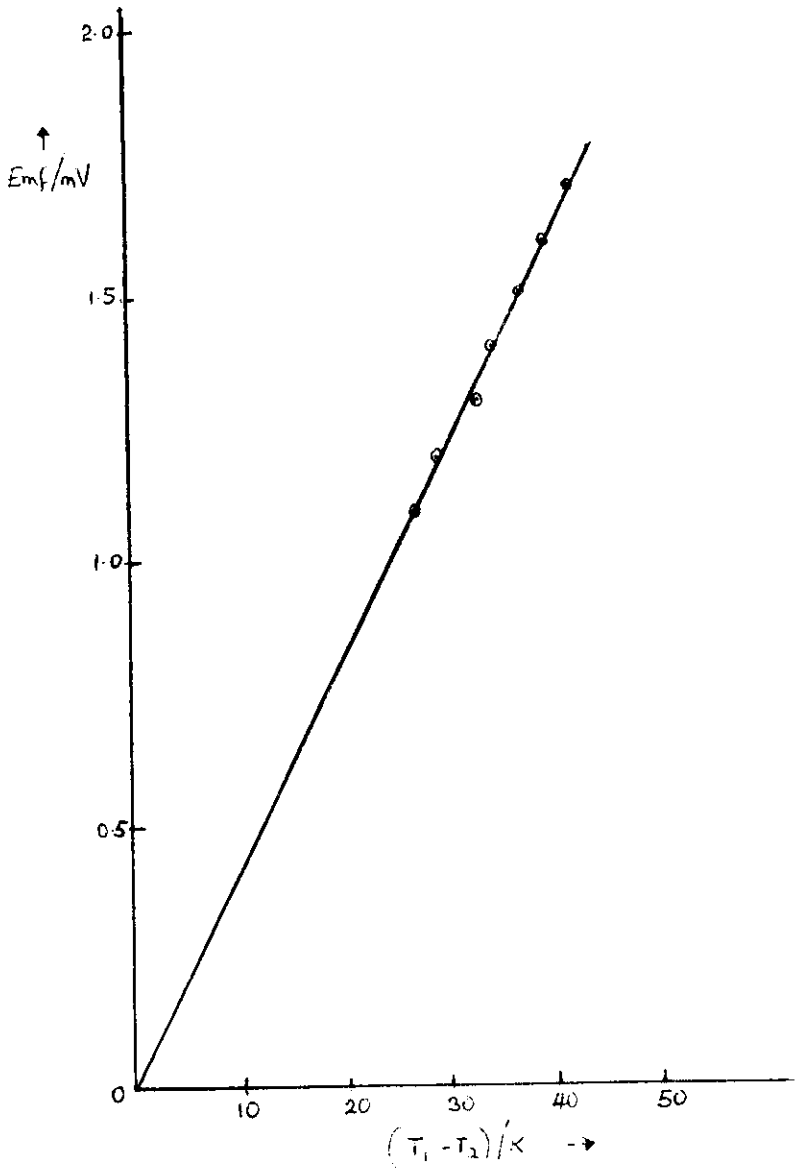

Figure 3. A calibration graph for the Copper-Constantan thermocouple

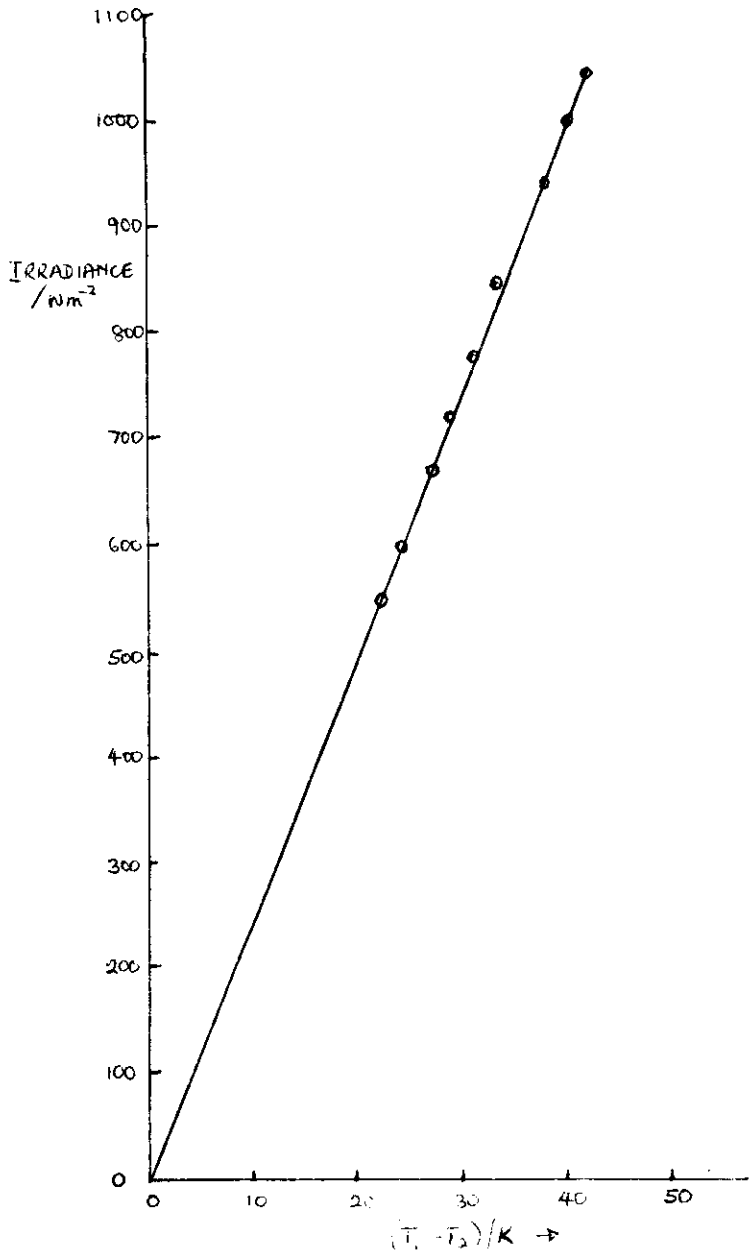

Figure 4. A graph of intensity values against temperature difference

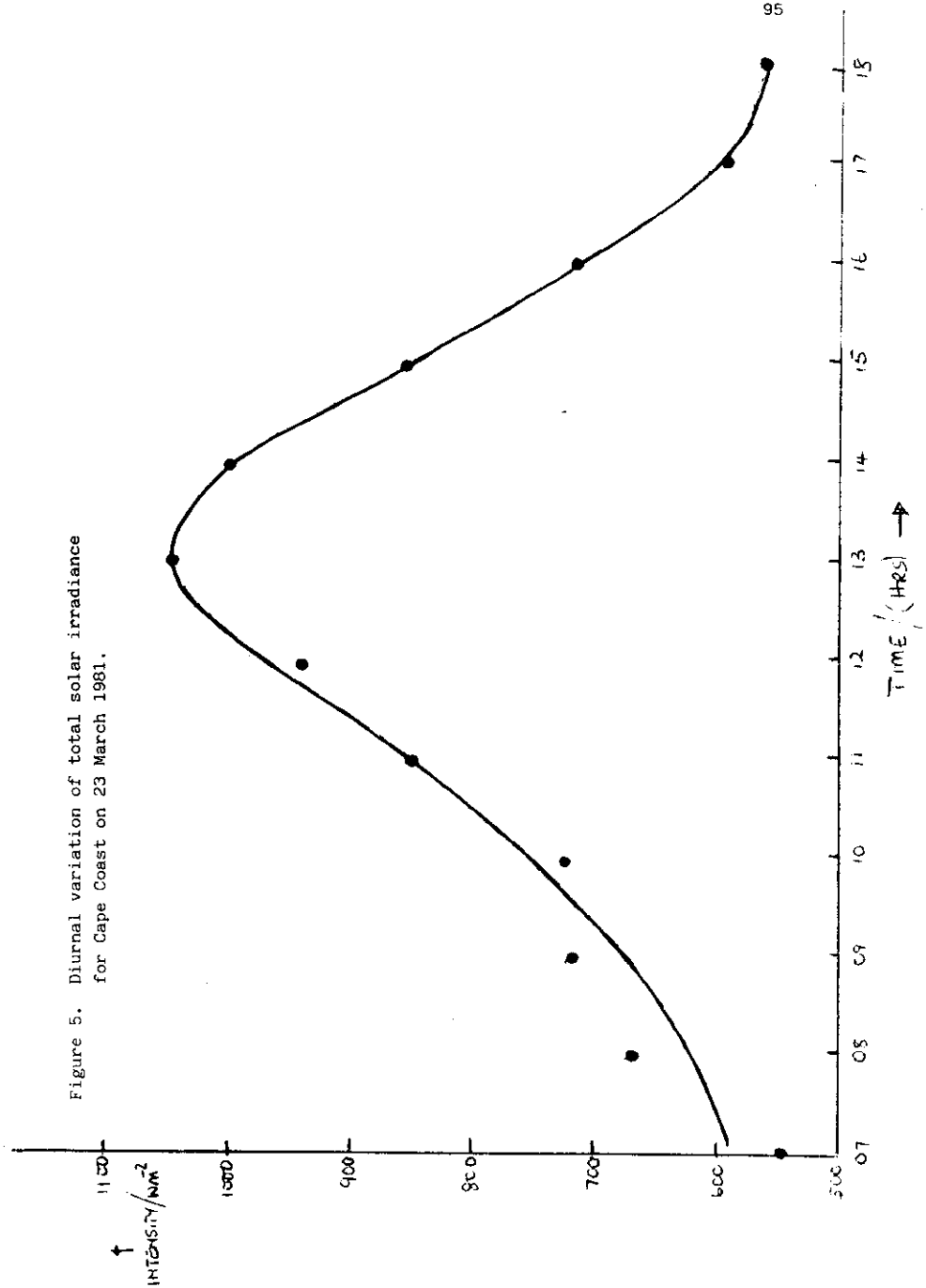

Figure 5. Diurnal variation of total solar irradiance for Cape Coast on 23 March 1981.

Table 1. Solar insolation data for the recorder on 23 March 1981

Local Time /(Hours)	Amplifier Output/(Volts)	Thermocouple Output/(mV)	Temperature difference (T_1-T_2)/K	Intensity /Wm^{-2}
07	9.0	0.90	22.0	547.2
08	11.0	1.10	27.0	671.5
09	12.0	1.20	29.0	721.2
10	12.0	1.20	29.0	721.2
11	13.0	1.30	33.4	848.3
12	15.0	1.50	37.8	940.0
13	17.0	1.70	42.0	1044.5
14	16.0	1.60	40.0	994.8
15	14.0	1.40	34.5	858.0
16	12.0	1.20	29.0	721.2
17	10.0	1.00	24.0	596.9
18	9.5	0.95	23.0	572.0

APPENDIX

Solar Intensity Measurements for February, March and April 1981. Location: Cape Coast, Central Region of Ghana. (Altitude: 33.5m; Average annual rainfall: 1193mm; Relative Humidity: 84%; Ambient temperature: 300K).

February 1981

Local Time/ (Hours)	Mean Intensity/(Wm^{-2})			
	1st Week 1/2-7/2/81	2nd Week 8/2-14/2/81	3rd Week 15/2-21/2/81	4th Week 22/2-28/2/81
0700	600	550	550	575
0800	600	650	550	650
0900	600	700	600	750
1000	650	750	600	800
1100	650	750	750	800
1200	650	850	900	950
1300	750	950	900	950
1400	900	900	850	900
1500	800	850	800	875
1600	750	750	800	900
1700	600	650	750	850
1800	550	625	600	600

March, 1981

Local Time/ (Hours)	Mean Intensity/(Wm^{-2})			
	1st Week	2nd Week	3rd Week	4th Week
0700	550	575	600	575
0800	650	600	650	650
0900	750	650	750	750
1000	800	750	800	800
1100	800	850	850	850
1200	900	950	1000	1000
1300	1000	975	1000	1000
1400	950	950	950	1000
1500	850	900	900	950
1600	750	850	800	850
1700	900	750	750	900
1800	575	600	650	650

INTERNATIONAL ATOMIC ENERGY AGENCY
UNITED NATIONS EDUCATIONAL, SCIENTIFIC AND CULTURAL ORGANIZATION
INTERNATIONAL CENTRE FOR THEORETICAL PHYSICS
34100 TRIESTE (ITALY) - P.O.B. 586 - MIRAMARE - STRADA COSTIERA 11 - TELEPHONE: 224281/2/3/4/5/6
CABLE: CENTRATOM - TELEX 460392-1-ICTP
AND
INTERNATIONAL COLLEGE ON APPLIED PHYSICS - CATANIA

SECOND INTERNATIONAL SYMPOSIUM ON NON-CONVENTIONAL ENERGY

SECOND INTERNATIONAL SYMPOSIUM
ON
NON-CONVENTIONAL ENERGY
(14 July - 6 August 1981)

FINAL LIST OF PARTICIPANTS

	Name and Institute	Member State
	DIRECTORS	
1.	G. FURLAN Istituto di Fisica Teorica Università di Trieste Trieste Italy	Italy
2.	N.A. MANCINI Istituto di Fisica Università di Catania Corso Italia 57 Catania Italy	Italy
3.	I.F. QUERCIA * Istituto Nazionale di Fisica Nucleare Laboratori Nazionali di Frascati Casella Postale 13 Frascati Rome Italy	Italy
4.	A.A.M. SAYIGH Kuwait Institute for Scientific Research Department of Energy P.O. Box 24885 Safat Kuwait	Kuwait/Iraq

* Did not attend Symposium

	Name and Institute	Member State
	LECTURERS	
1.	J. ALLENTUCK Economics and Systems Analysis Div. Brookhaven National Laboratory Associated Universities Inc. Upton, New York 11973 U.S.A.	U.S.A.
2.	C.E. BACKUS College of Engineering and Applied Sciences Arizona State University Tempe, Arizona 85281 U.S.A.	U.S.A.
3.	J.A. BASSHAM Lawrence Berkeley Laboratory Chemical Biodynamics Division University of California Berkeley, CA 94720 U.S.A.	U.S.A.
4.	G. BEGHI Commission of the European Communities Joint Research Centre Ispra Establishment Ispra, Varese Italy	Italy
5.	C. BOFFA Istituto di Fisica Tecnica Politecnico di Torino Corso Duca degli Abruzzi 24 10129 Torino Italy	Italy
6.	R. BONAIUTI C.N.R. Piazziale Rodolfo Morandi 2 20121 Milan Italy	Italy
7.	E. BRODA Institut f. Physikalische Chemie der Universität Wien Wahringerstrasse 42 Vienna Austria	Austria

	Name and Institute	Member State
8.	P. DA COL Via Larga 38 Udine Italy	Italy
9.	S. DEB Photovoltaic Division Solar Energy Research Institute Golden, Colorado 80401 U.S.A.	U.S.A.
10.	S. DEL GIUDICE Istituto di Fisica Tecnica e Tecnologie Industriale Viale Ungheria 43 Udine Italy	Italy
11.	G. ELIAS Progetto Finalizzato Energetica Consiglio Nazionale delle Ricerche Via Nizza 128 Rome Italy	Italy
12.	G. FANINGER Austrian Solar and Space Agency Garnisongasse 7 Vienna Austria	Austria
13.	H. GERISCHER Fritz-Haber-Institut der Max-Planck Gesellschaft Faradayweg 4-6 1000 Berlin 33/Dahlem Federal Republic of Germany	Fed. Rep. Germany
14.	R. GIBSON University of Dundee Department of Physics Faculty of Science Dundee DD1 4HN Scotland U.K.	U.K.

	Name and Institute	Member State
15.	B. GIVONI The Jacob Blaustein Institute for Desert Research Ben-Gurion University of the Negev Sede Boqer Campus Israel	Israel
16.	M.C. GUPTA Solar Energy Division Indian Institute of Technology Madras - 600 036 India	India
17.	R. MATERASSI Istituto di Microbiologia Agraria e Tecnica Università di Firenze Piazziale Cascine 27 Firenze Italy	Italy
18.	H. MATTAR Instituto de Pesquisas Tecnologicas Cidade Universitaria 05508 Sao Paulo S.P. Brazil	Brazil
19.	D. NOBILI LAMEL - Laboratori del CNR Via Castagnoli 2 Bologna Italy	Italy
20.	P. PEISER E.N.E.L. Via Giovanbattista Martini 3 Rome Italy	Italy
21.	E. RIMINI Istituto di Fisica Università di Catania Corso Italia 57 Catania Italy	Italy

	Name and Institute	Member State
22.	M. SAVELLI Université des Sciences et Techniques du Languedoc Centre d'Etudes d'Electronique des Solides Groupe d'Etudes Matériaux, Composants et Systems Place E. Bataillon Montpellier Cedex France	France
23.	B.O. SERAPHIN Optical Science Center University of Arizona Tucson, Arizona 85721 U.S.A.	U.S.A.
24.	H.D. TALAREK Solar Energy Branch/IKP Kernforschungsanlage Jülich Postfach 1913 Jülich Federal Republic of Germany	Fed. Rep. of Germany
25.	T.N. VEZIROGLU Clean Energy Research Institute School of Engineering and Architecture University of Miami P.O. Box 248294 Coral Gables, Florida 33124 U.S.A.	U.S.A./Turkey
26.	Z.-I. YOSHIDA Department of Synthetic Chemistry Faculty of Engineering Kyoto University Yoshida, Kyoto Japan	Japan

	Name and Institute	Member State
	PARTICIPANTS	
1.	M. ABD EL AAL Ain Shams University Faculty of Women Cairo Egypt	Egypt
2.	A.G. ABDEL GAWAD El-Fateh University P.O. Box 13292 Tripoli Libya	Libya/Egypt
3.	M.A. ABDEL SALAM Faculty of Engineering and Technology Mataria Cairo Egypt	Egypt
4.	H.M.H. ABOU-LEILA Qatar University P.O. Box 2713 Doha Qatar	Qatar/Egypt
5.	K.G. ADANU University of Ghana Department of Physics Legon Ghana	Ghana
6.	G.A. ADEGBOYEGA Department of Electronic & Electrical Engineering University of Ife Ile-Ife Nigeria	Nigeria
7.	A.M. AJLOUNI Royal Scientific Society P.O. Box 6945 Amman Jordan	Jordan
8.	B.G. AKINOGLU Department of Physics Middle East Technical University Ankara Turkey	Turkey

	Name and Institute	Member State
9.	L.I. AL-HOUTY Qatar University P.O. Box 2713 Doha Qatar	Qatar
10.	T.A.A. AL-KHALED National Housing Authority Kuwait	Kuwait
11.	G.F. AL-NOAIMI Department of Physics University of Qatar P.O. Box 2713 Doha Qatar	Qatar
12.	A.A. AL-RASHID National Housing Authority Kuwait	Kuwait
13.	H.R. AL-SHAMI Kuwait Institute for Scientific Research P.O. Box 24885 Safat Kuwait	Kuwait/Jordan
14.	M. AL-ZARIEY Department of Physics Sana'a University Sana'a Yemen Arab Republic	Yemen Arab Rep.
15.	K.A.S. ALLAF Lebanese University Faculty of Science "El-Hadeth" Lebanon	Lebanon
16.	A.M. AMIENSITURU Laboratoire de Thermodynamique et Energetique Université de Perpignan Avenue de Villeneuve Perpignan France	France/Indonesia

	Name and Institute	Member State
17.	M.R. ARELLANO Instituto de Investigaciones Fisicas Laboratorio de Fisica Cosmica Universidad Boliviana La Paz Bolivia	Bolivia
18.	M.R. ARIAS Institut f. Allgemeine Physik Technische Universität Wien Karlsplatz 13 Vienna Austria	Austria/ Ecuador
19.	O.A. ARPESELLA Facultad de Ingenieria Quimica Universidad Nacional del Litoral Santiago del Estero 2654 Santa Fe Argentina	Argentina
20.	S.Y. AYYASH Kuwait Institute for Scientific Research Department of Energy P.O. Box 24885 Safat Kuwait	Kuwait/Jordan
21.	A. AYENSU Department of Physics University of Cape Coast Cape Coast Ghana	Ghana
22.	M.R. BAH Institut National de Recherche et Documentation B.P. 561 Conakry Guinea	Guinea
23.	A.A. BAIMBA Department of Physics Njala University College Private Mail Bag Freetown Sierra Leone	Sierra Leone
24.	M.M. BANERJEE A.C. College Jalpaiguri 735101 West Bengal India	India

	Name and Institute	Member State
25.	M.W. BASSEY Department of Mechanical Engineering Fourah Bay College University of Sierra Leone Freetown Sierra Leone	Sierra Leone
26.	M.O. BECK Faculty of Engineering University of Aleppo Aleppo Syria	Syria
27.	A.S. BHUIYAN Department of Physics University of Chittagong Chittagong Bangladesh	Bangladesh
28.	P. BISWAS P.D. College Jalpaiguri 735101 West Bengal India	India
29.	E. BOLLIN University of Karlsruhe Akademiestrasse 21 Karlsruhe 1 Fed. Rep. Germany	Fed. Rep. Germany
30.	M.D. BOSANAC Faculty of Electrical Engineering Rudjera Boskovića bb Split Yugoslavia	Yugoslavia
31.	A. BOWEN Fundacion Nacional Aquileo Parra Calle 7, No. 4-60 Bogotà Colombia	Colombia
32.	A.J. CEPPI Rawson 2643 1640 Martinez (S. Isidro) Prov. de Buenos Aires Argentina	Argentina

	Name and Institute	Member State
33.	L. CHARRY Departamento de Fisica Universidad de Antioquia Medellin Colombia	Colombia
34.	M.A. CHENDO Department of Physics University of Lagos Yaba - Lagos Nigeria	Nigeria
35.	O.D. CORBELLA PPGEMM/UFRGS Av. Osvaldo Aranha 99/6 Porto Alegre Brazil	Brazil/Argentina
36.	J.L. DE ANDRADE Universidade dos Asores Dept.o Geociencias Ponta Delgada Codex Azores Portugal	Portugal
37.	A.O. DEMUREN Universität Karlsruhe Kaiserstrasse 12 Karlsruhe Fed. Republic of Germany	Fed.Rep. Germany/Nigeria
38.	M.I. DE SOUSA TELES Departamento de Engenharia Electrotécnica Facultade de Ciencias e Tecnologia Universidade Coimbra Coimbra Codex Portugal	Portugal
39.	M.A. DURAN Departamento de Matematicas y Fisica Universidad de Huamanga Ayacucho Peru	Peru
40.	A. ECEVIT Department of Physics Middle East Technical University Ankara Turkey	Turkey

	Name and Institute	Member State
41.	A. EGAN Department of Physics Faculty of Science University of Khartoum PO Box 321 Khartoum Sudan	Sudan/U.K.
42.	M.Y. EL-ASHRY Suez Canal University Faculty of Science Ismailia Egypt	Egypt
43.	S.M. EL-GAMMAL Department of Physics Assiut University Assiut Egypt	Egypt
44.	M.K. EL-MOUSLY Department of Physics Faculty of Science Ain Shams University Cairo Egypt	Egypt
45.	D. EROL-KANSU Department of Physics Middle East Technical University Ankara Turkey	Turkey
46.	R.O. FAGBENLE Mechanical Engineering Department The Polytechnic Ibadan Nigeria	Nigeria
47.	A. FERNANDEZ Instituto de Investigaciones en Materiales Universidad Nacional Autonoma de Mexico Apartado Postal 70 360 Mexico	Mexico
48.	F. FRANDOLI C.T.A.-Studio Associato Via delle Erbe 9 Udine Italy	Italy

	Name and Institute	Member State
49.	I.A. GABER Faculty of Electronic Engineering Menoufia University Menoufia Egypt	Egypt
50.	H.P. GARG Centre of Energy Studies Indian Institute of Technology Hauz Khas, New Delhi India	India
51.	R. GOPALAKRISHNAN Sri Venkateswara University College of Engineering Tirupati 511502 India	India
52.	J.R. GUERRA-FERNANDOIS Instituto de Investigaciones Fisicas Universidad Major de San Andrés La Paz Bolivia	Bolivia
53.	H. HASNAIN Directorate General of Energy Resources M/o Petroleum and Natural Resources House No. 3 Street 88, G-6/3 Islamabad Pakistan	Pakistan
54.	A.R. HASSAN Department of Physics Faculty of Science King Abdulaziz University P.O. Box 1540 Jeddah Saudi Arabia	Saudi Arabia/Egypt
55.	P. HORACEK Czechoslovak Atomic Energy Commission Slezska 9 120 29 Prague 2 Czechoslovakia	Czechoslovakia
56.	M. HORN Universidad Nacional de Ingenieria Av. Tupao Amaru S/N Apartado 1301 Lima Peru	Peru/Fed.Rep. Germany

	Name and Institute	Member State
57.	S.D. HURRY School of Industrial Technology University of Mauritius Reduit Mauritius	Mauritius
58.	M. HUSSAIN Department of Physics University of Dacca Dacca - 2 Bangladesh	Bangladesh
59.	P.C. JAIN Department of Physics University of Zambia P.O. Box 32379 Lusaka Zambia	Zambia/India
60.	A. JOYCE Centro de Fisica da Materia Condensada Av. Do Prof. Gama Pinto 2 Lisboa 2 Portugal	Portugal
61.	D. KALACHE Station d'Energie Solaire Route de l'observatoire Bouzareah Algeria	Algeria
62.	A.R. KAMAL Kuwait Institute for Scientific Research Department of Energy P.O. Box 24885 Safat Kuwait	Kuwait
63.	L. KEITA Ecole Normale Supérieure B.P. 241 Bamako Mali	Mali
64.	M.E. KENAWY Department of Physics Ain-Shams University Cairo Egypt	Egypt

	Name and Institute	Member State
65.	A.M. KHAN Applied Systems Analysis Group Pakistan Atomic Energy Commission P.O. Box No. 1114 Islamabad Pakistan	Pakistan
66.	O. KHARIZANOV Central Laboratory for Solar Energy & New Energy Sources 72 Boul Lenin 113 Sofia Bulgaria	Bulgaria
67.	D. KIRIN Institut "Ruder Boskovic" Bijenicka C. 54 P.O.B. 1016 Zagreb Yugoslavia	Yugoslavia
68.	J. KLAINSEK Universidad Politecnica di Madrid Av. Juan de Herrera 4 Cuidad Universitaria Madrid 3 Spain	Spain
69.	P. KULISIC Elektrotehnicki Fakultet Unska 3 Zagreb Yugoslavia	Yugoslavia
70.	H. KULUNK D.M.M. Akademisi Ogretim Görevlisi Zonguldak Turkey	Turkey
71.	E.M. LUSHIKU Department of Physics University of Dar Es Salaam P.O. Box 35063 Dar Es Salaam Tanzania	Tanzania
72.	M.R. MAHMOUD Chemistry Department Faculty of Science Assiut University Assiut Egypt	Egypt

	Name and Institute	Member State
73.	S.Q.G. MAHTABOALLY Department of Physics University of Rajshahi Rajshahi Bangladesh	Bangladesh
74.	S.H. MAKARIOUS Applied Mathematics Department Faculty of Science Ain Shams University Abbassia, Cairo Egypt	Egypt
75.	M. MAURETTE Laboratoire René Bernas B.P. 1 Batiment 108 Orsay France	France
76.	C.M. MBOW Laboratoire des Semi Conducteurs et Energie Solaire Université de Dakar Dakar Senegal	Senegal
77.	M. MEBARKI Université d'Oran Institut des Sciences Exactes Oran Algeria	Algeria
78.	S. MELINTE Catedra de Fizica Institutul Politehnic Iasi Spali Bahlui Stg. 63 Iasi Romania	Romania
79.	M. MIKI Centre d'Etudes Nucléaires de Grenoble Avenue des Maryres Grenoble France	France/Peru
80.	P. MOSCONI Institute of Architecture Faculty of Architecture Rosario Argentina	Argentina

	Name and Institute	Member State
81.	A. MOSTAVAN Heliotechnology Laboratory Department of Engineering Science Institute of Technology of Bandung Jalan Ganesha 10 Bandung Indonesia	Indonesia
82.	C. MOYA Instituto de Investigaciones en Materiales Universidad Nacional Autonoma de Mexico Apartado Postal 70 360 Mexico D.F.	Mexico
83.	P. MPAWENAYO National University of Rwanda Centre for Studies and Energy Applications B.P. 117 Butare Rwanda	Rwanda/Burundi
84.	M.A. MUNOZ Departamento Geofisica Blanco Encalada 2085 Casilla 2777 Santiago Chile	Chile
85.	M.T.S. NAIR Department of Physics University of Jos PMB 208A, Jos Nigeria	Nigeria/India
86.	P.K. NAIR Department of Physics University of Jos PMB 208A, Jos Nigeria	Nigeria/India
87.	O.A. OMAR Faculty of Engineering Ain Shams University Cairo Egypt	Egypt
88.	F.N. ONYANGO Department of Physics University of Nairobi P.O. Box 30197 Nairobi Kenya	Kenya

	Name and Institute	Member State
89.	M.B. OUAIDA Centre National de la Recherche Scientifique B.P. 5 Odeillo Font-Romeu France	France/Lebanon
90.	G. PANTIS Department of Physics University of Ioannina Ioannina Greece	Greece/Canada
91.	S. PANYAKEOW Semiconductor Research Laboratory Faculty of Engineering Chulalongkorn University Bangkok Thailand	Thailand
92.	S. PARANGTOPO University of Indonesia Jl. Salembaraya no. 4 Jakarta Indonesia	Indonesia
93.	J.K. PATNAIK Department of Meteorology & Oceanography Andhra University Visakhapatnam 3 India	India
94.	C. PATUWATHAVITHANE University of Moratuwa Katubedda Moratuwa Sri Lanka	Sri Lanka
95.	M.A. PEER Department of Physics University of Kashmir Srinagar 190006 India	India
96.	G. PIANI (Private) Via Spina 27 40139 Bologna Italy	Italy

	Name and Institute	Member State
97.	J. PRAKASH Department of Physics Ramjas College University of Delhi Delhi 110007 India	India
98.	I. PRIETO Universidad Politecnica di Madrid Escuela Tecnica Superior de Arcitectura Av. Juan de Herrera 4 Madrid 3 Spain	Spain
99.	K.S. RABBANI Department of Physics University of Dacca Dacca -2 Bangladesh	Bangladesh
100.	S. RAJANARONK Faculty of Science Ramkhamhaeng University Bangkok 24 Thailand	Thailand
101.	R.N. RAY Department of Physics Indian Institute of Science Bangalore India	India
102.	J.A. RETAMOZO Centre d'Etudes Nucléaires de Grenoble Avenue des Martyres Grenoble France	France/Peru
103.	C. RIVASPLATA National University of Tacna Av. Bolognesi s.n Casilla 316 Tacna Peru	Peru

	Name and Institute	Member State
104.	H. RODRIGUEZ Solar Energy Research Group Department of Physics National University Ap. Aereo 100102 Bogotà 10 Colombia	Colombia
105.	R.L. ROMAN Department of Mechanical Engineering University of Chile Casilla 2777 Santiago Chile	Chile
106.	D.M. ROWE Department of Physics UWIST King Edward VII Avenue Cardiff CF1 3NU South Wales U.K.	U.K.
107.	A.O. ROJO UPIICSA - Instituto Politécnico Nacional Té 950 Mexico D.F.	Mexico/Venezuela
108.	M. SADEGHI Institut f. Experimentalphysik II Universität Linz Linz-Auhof Austria	Austria/Iran
109.	A.M. SALAU Department of Physics University of Ife Ile-Ife Nigeria	Nigeria
110.	T. SAMUEL Faculty of Engineering University of Peradeniya Peradeniya Sri Lanka	Sri Lanka
111.	E. SCABAR A.S.E.S. Viale XX Settembre 67/B Trieste Italy	Italy

	Name and Institute	Member State
112.	T.P. SHARMA Department of Physics Institute of Advanced Studies Meerut University Meerut 250 001 India	India
113.	M.A. SHAUKAT Department of Physics Punjab University New Campus Lahore Pakistan	Pakistan
114.	V.M. SHRESTHA Department of Physics Kirtipur Campus Kathmandu Nepal	Nepal
115.	D. SIDDIQUE Department of Physics University of Dacca Dacca - 2 Bangladesh	Bangladesh
116.	A. SKRINJAR C.T.A.-Studio Associato Via delle Erbe 9 Udine Italy	Italy
117.	E. SPINADEL Facultad de Ingenieria Departamento Electrotecnica Paseo Colon 850 Buenos Aires Argentina	Argentina/Austria
118.	P.D. STEPHENS Department of Physics University of the West Indies Mona, Kingston 7 Jamaica	Jamaica
119.	D.K. SUBRAMANIAN Indian Institute of Science Bangalore 560012 India	India

	Name and Institute	Member State
120.	S.K. SURI University of Garyounis Faculty of Science Department of Physics P.O. Box 9480 Benghazi Libya	Libya/India
121.	K. TANER E.D.M.M. Akademisi Makina Fakültesi Eskisehir Turkey	Turkey
122.	V. THIRUVENGADAM Technical University of Budapest Faculty of Civil Engineering Department of Mechanics Müegytetem Budapest Hungary	Hungary/India
123.	M.S. TOMAR Universidad Simon Bolivar Departamento de Fisica Apartado 80659 Caracas Venezuela	Venezuela/India
124.	J.W. VASQUEZ Departamento Académico de Fisica Universidad Nacional Mayor de San Marcos Av. Venezuela s/n Lima Peru	Peru
125.	I. VILICIC Tehnicki Fakultet Rijeka N. Ustanka 58 Rijeka Yugoslavia	Yugoslavia
126.	J. VULETIN Faculty of Engineering Rudjera Boskovica bb Split Yugoslavia	Yugoslavia
127.	R.O. WESTMAAS Department of Architecture Faculty of Technology University of Guyana Turkeyen Guyana	Guyana

	Name and Institute	Member State
128.	K.K. WONG Department of Environmental Sciences Faculty of Science and Environmental Studies University Pertanian Malaysia Serdang Selangor Malaysia	Malaysia
129.	K.L. YAU Higher Petroleum Institute P.O. Box 201 Tobruk Libya	Libya/U.K.
130.	P.E. YIANOULIS Physics Laboratory II University of Patras Patras Greece	Greece
131.	S. YIN International School for Advanced Studies Trieste Italy	Italy/Burma
132.	M.I. YOUSSEF Department of Physics Faculty of Science Mansoura University Mansoura Egypt	Egypt
133.	A. ZAOUK Ecole National Supérieure de Chimie 118 Route de Narbonne 31077 Toulouse Cedex France	France/Lebanon
134.	I.L. ZULIM Faculty of Electrical Engineering Rudjera Boskovića bb Split Yugoslavia	Yugoslavia